

## REFERENCES

1. MINDLIN, R.D.  
"Influence of rotatory inertia and shear or flexural motions of isotropic elastic plates", J. Appl. Mech., 37, 1031-1036, 1951.
2. TIMOSHENKO, S.P. and WOINOWSKY-KRIEGER, S.  
"Theory of plates and shells", 2nd ed., McGraw-Hill, New York, 1961.
3. DOBYNS, A.L.  
"Analysis of simply-supported orthotropic plates subject to static and dynamic loads", J.AIAA, 19, 642-650, 1982.
4. PLANTEMA, F.J.  
"Sandwich Construction", John Wiley, New York, 1966.
5. VINSON, J. R. and CHOU, T. W.  
"Composite materials and their use in structures", Applied Science Publishers, London, 1975.
6. BASU, A. K. and DAWSON, J. M.  
"Orthotropic sandwich plates", Proc. Instn. Civ. Engrs., Supplement, 87-115, 1970.
7. FREDERICK, D.  
"Thick rectangular plates on an elastic foundation", Trans. A.S.C.E., 122, 1069-1085, 1957  
[See also discussion by Lorsch, H.G., Trans. A.S.C.E., 122, 1086-1087, 1957].
8. ARIMAN, T.  
"On orthotropic thick elastic plates on an elastic foundation", Die Bautechnik, 7, 230-234, 1968.
9. HUSSAINY, S.A. and SRINIVAS, S.  
"Flexure of rectangular composite plates", Fibre Science and Technology, 8, 59-76, 1975.
10. SRINIVAS, S. and RAO, A. K.  
"Bending, vibration and buckling of simply supported thick orthotropic rectangular plates and laminates", Int. J. Solids Structures, 6, 1463-1481, 1970.

## CHAPTER 2

MINDLIN FINITE STRIP AND AXISYMMETRIC FINITE  
ELEMENT SHELL ANALYSIS

E. Oñate\*, B. Suarez\* and E. Hinton†

\* Universidad Politecnica de Cataluña, Spain

+ University College of Swansea, U.K.

## 1. INTRODUCTION

Many engineering structures have constant geometrical properties along a particular direction. Such prismatic structures are very common in plate and folded plate problems, where the transverse cross-section of the structure often remains constant in the longitudinal direction. In axisymmetric shell problems, the cross-section of the shell does not change in the circumferential direction (see Figure 1). If the material properties of the structures are also constant in the same direction, the analysis can be simplified by the combined use of finite elements and Fourier expansions to model the transverse and longitudinal behaviour.

The combination of finite elements and Fourier series is not new and it has for some years been used in the study of un-symmetrically loaded axisymmetric shells and solids by Grafton and Strone[1], Ahmad et al[2], and Wilson[3].

The extension to plate and shell analysis was first developed by Cheung[4] and termed the finite strip method. Since then, further refinements in the method have been made and some of the main contributions are listed in references [5] - [18].

In this chapter the basis of the Mindlin finite strip formulation will be presented for a wide range of prismatic

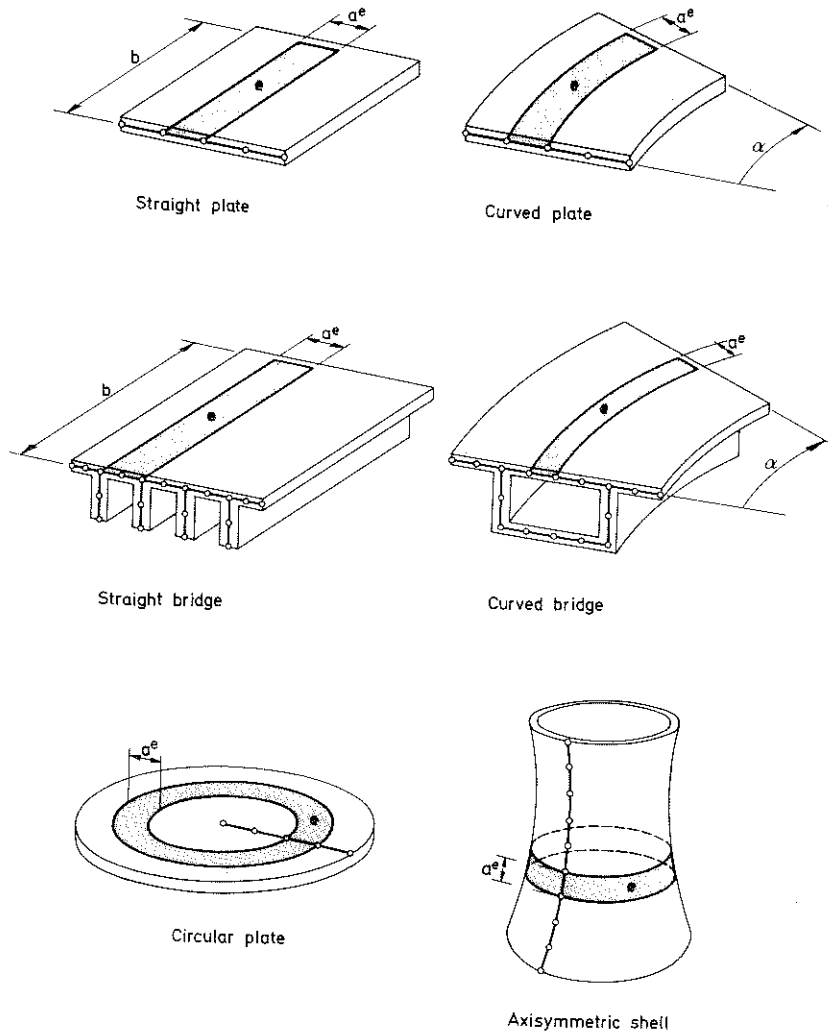


Fig.1 Different structures which can be analyzed with the finite strip method.

structures. Rectangular plates will be considered first as an introduction to more complex problems and details of the general finite strip formulation will be given. The second part of the chapter deals with folded plate shell type structures. It will be shown that the finite strip formulation for right folded plates and axisymmetric shells can be simply derived as a special case of the more general formulation for folded plates with curved planforms which will be presented first. The last part of the chapter deals with the computer implementation of the finite strip method and full details of a finite strip computer program for the analysis of rectangular and curved plates will be given.

Before discussing the basis of the finite strip method, it is interesting to introduce the reader to the basic concepts of the use of Fourier series for structural analysis. This is done in the next section for the simple case of a beam.

## 2. ANALYSIS OF A SIMPLY-SUPPORTED BEAM BY FOURIER SERIES

Consider the beam shown in Figure 2 under an arbitrary loading  $q(y)$ . The Total Potential Energy for a beam in bending can be written as

$$\pi(w) = \frac{EI}{2} \int_0^b \left( \frac{d^2 w}{dy^2} \right)^2 dy - \int_0^b q w dy \quad (1)$$

where  $E$  and  $I$  are the Young's modulus and the modulus of inertia of the beam transverse cross-section, resp., and  $w$  is the lateral beam deflection at each point, which must satisfy the following boundary conditions

$$w = \frac{d^2 w}{dy^2} = 0 \text{ at } y = 0 \text{ and } y = b \quad (2)$$

The above conditions are satisfied by the following Fourier series

$$w = \sum_{\ell=1}^{\infty} w^{\ell} \sin \ell \frac{\pi y}{b} \quad (3)$$

where  $b$  is the beam length and  $\ell$  refers to a particular term, i.e.  $\ell = 1, 2, 3$ , etc. and  $w^\ell$  is the undetermined deflection amplitude for the  $\ell$ th harmonic.

The loading  $q(y)$  is defined by Fourier series as

$$q(y) = \sum_{\ell=1}^{\infty} q^\ell \sin \ell \frac{\pi y}{b} \quad (4)$$

where  $q^\ell$  is the loading amplitude for the  $\ell$ th harmonic, which can be obtained using Euler's formula for Fourier series, i.e.

$$q^\ell = \frac{\int_{b_0}^{b_1} q(y) \sin \ell \frac{\pi y}{b} dy}{\int_0^b \sin^2 \ell \frac{\pi y}{b} dy} = \frac{2}{b} \int_{b_0}^{b_1} q(y) \sin \ell \frac{\pi y}{b} dy \quad (5)$$

where the load is applied in the zone from  $y = b_0$  to  $y = b_1$ , as shown in Figure 2.

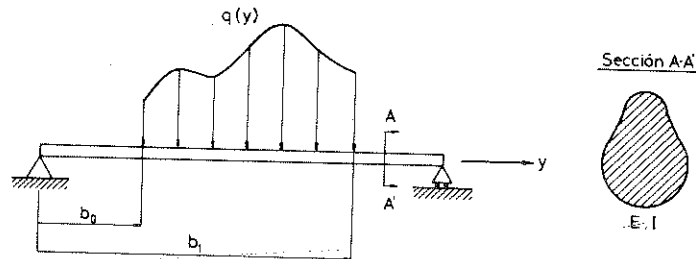


Figure 2 Simple supported beam of constant cross-section under arbitrary distributed loading  $q(y)$

The value of  $q^\ell$  is easily obtained provided that the product  $q(y) \sin \frac{\ell \pi y}{b}$  is integrable. Therefore, for a given load harmonic the problem is one of finding the unknown amplitude  $w^\ell$  which uniquely describes the deflected beam profile for that harmonic. Substituting (3) and (4) into (1) it is possible to write

$$\pi(w) = \sum_{\ell=1}^{\infty} \left( \frac{EI}{4} (w^\ell)^2 \frac{\ell^4 \pi^4}{b^3} - \frac{b}{2} q^\ell w^\ell \right) \quad (6)$$

The value of  $w^\ell$  is obtained by minimising the Total Potential Energy with respect to  $w^\ell$ , i.e.

$$\frac{\partial \pi(w)}{\partial w^\ell} = 0 \quad \text{which leads to} \quad w^\ell = \frac{q^\ell b^4}{EI \ell^4 \pi^4} \quad (7)$$

The first deflected profile is obtained if the summation in (3) is performed and from the deformed shape of the beam the curvatures and hence, the bending moments may be calculated.

As an example of application the beam shown in Figure 3 is subjected to two loading cases: a uniformly distributed loading of intensity  $q$  acting along the whole beam length; and a vertical point load,  $P$ , acting at midspan. The Fourier coefficient,  $q^\ell$ , for each loading can be obtained using (5) as

$$q^\ell = \frac{2q}{\ell \pi} (1 - \cos \ell \pi) \quad \text{for the uniform load} \quad (8)$$

$$q^\ell = \frac{2P}{b} \sin \frac{\ell \pi}{2} \quad \text{for the point load}$$

Thus the vertical deflection for each load case is obtained from (7) and (3) as

$$w = \frac{2qb^4}{EI \pi^5} \sum_{\ell=1}^{\infty} \frac{1 - \cos \ell \pi}{\ell^5} \sin \frac{\ell \pi y}{b} \quad \text{for the uniform load} \quad (9)$$

$$w = \frac{2Pb^3}{EI \pi^4} \sum_{\ell=1}^{\infty} \frac{1}{\ell^4} \sin \frac{\ell \pi}{2} \sin \frac{\ell \pi y}{b} \quad \text{for the point load}$$

The bending moments are obtained by the expression

$$M = -EI \frac{d^2 w}{dy^2} \quad (10)$$

Thus for each loading case the bending moment can be written as

$$M = \frac{2qb^2}{\pi^3} \sum_{\ell=1}^{\infty} \frac{1}{\ell^3} (1 - \cos \ell \pi) \sin \frac{\ell \pi y}{b} \quad \text{for the uniform load} \quad (11)$$

$$M = \frac{2Pb}{\pi^2} \sum_{\ell=1}^{\infty} \frac{1}{\ell^2} \sin \frac{\ell \pi}{2} \sin \frac{\ell \pi y}{b} \quad \text{for the point load}$$

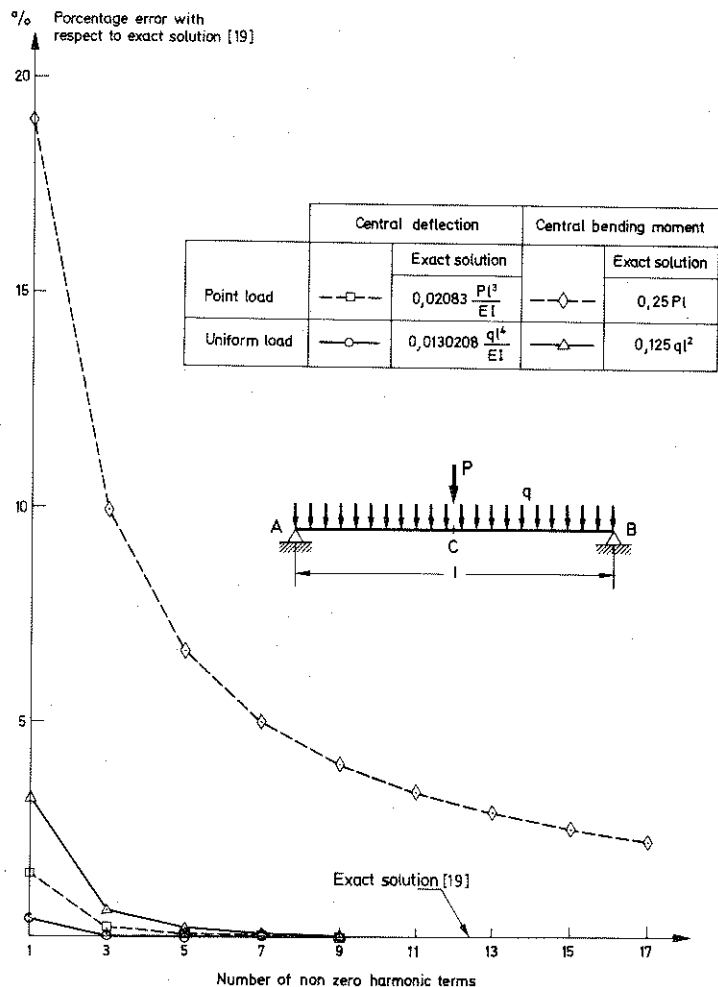


Fig. 3 Simple supported beam analyzed by Fourier series. Convergence study of central deflection and central bending moment for a point load and an uniform load.

Note that in (9) and (11) the even harmonic terms are zero. This is due to the symmetry of the loading about the centre of the beam.

Numerical results for the vertical deflection and bending moment at midspan, taking nine non-zero harmonics for the two load cases, are shown in Figure 3, from which the following conclusions can be drawn:

- Convergence to the theoretical value [19] for the deflection and bending moment is much faster for the uniform loading than for the point load case.
- In both load cases the convergence of the bending moment is slower than that of the vertical deflection.

The convergence of the solution is therefore loading dependent. As a rule, solutions for uniform loads converge much more rapidly than those for point loads. Also, the number of harmonic terms needed to achieve a given degree of accuracy for the solution is greater for the bending moments than for the displacements.

These practical rules, deduced from a simple case, apply for the general finite strip formulation.

### 3. FINITE STRIP FORMULATION FOR THE ANALYSIS OF RECTANGULAR MINDLIN PLATES

In this section the Mindlin finite strip formulation for rectangular plate bending analysis will be derived in detail as an introduction to more complex structural problems, e.g. folded plates, shells, which can also be treated with the strip formulation in a similar manner.

#### 3.1 Basic theory for Mindlin plates

Mindlin's assumptions for plate bending can be stated simply as follows:

- The lateral deflections of the plate,  $w$ , are small.
- Normals to be mid-plane of the plate before deformation

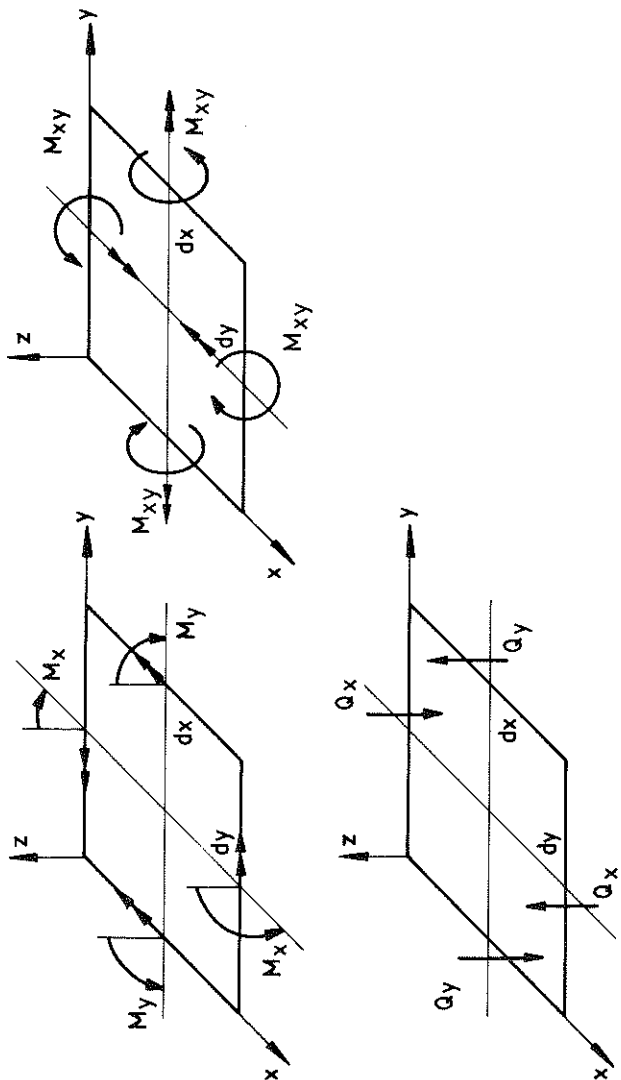


Fig. 5 Sign convention for moments and shear forces.

where for an isotropic plate

$$\underline{D} = \begin{bmatrix} \underline{D}_b & 0 \\ 0 & \underline{D}_s \end{bmatrix} \quad (18)$$

in which

$$\underline{D}_b = \frac{Et^3}{12(1-\nu^2)} \begin{bmatrix} 1 & \nu & 0 \\ \nu & 1 & 0 \\ 0 & 0 & \frac{(1-\nu)}{2} \end{bmatrix}; \quad \underline{D}_s = \frac{Et}{2(1+\nu)} \begin{bmatrix} \gamma & 0 \\ 0 & \gamma \end{bmatrix} \quad (19)$$

are resp. the bending and shear contributions to the elasticity matrix  $\underline{D}$ ;  $E$  and  $\nu$  are the Young's modulus and Poisson's ratio resp.,  $t$  is the plate thickness, and  $\gamma$  is a shear modification coefficient to take into account the warping of the section [19]. (Note that  $\gamma = \frac{5}{6}$  for rectangular sections.)

### 3.2 Finite strip formulation for Mindlin plates

The finite strip formulation for the analysis of Mindlin plates follows similar steps to those involved in the simple beam problem of Section 2. Thus, the displacements are now expanded in terms of truncated Fourier series along direction,  $y$ , in which both the material and geometrical properties of the plate are taken to be constant, i.e.

$$\begin{aligned} w(x,y) &= \sum_{\ell=1}^{\infty} w^{\ell}(x) \sin \frac{\ell\pi}{b} y \\ \theta_x(x,y) &= \sum_{\ell=1}^n \theta_x^{\ell}(x) \sin \frac{\ell\pi}{b} y \\ \theta_y(x,y) &= \sum_{\ell=1}^n \theta_y^{\ell}(x) \cos \frac{\ell\pi}{b} y \end{aligned} \quad (20)$$

where  $b$  is the plate length,  $w^{\ell}$ ,  $\theta_x^{\ell}$  and  $\theta_y^{\ell}$  are the displacement amplitudes for the  $\ell$ th harmonic term and  $n$  is the number of harmonic terms used in the analysis.

The next step is to discretise the displacement amplitudes (which are a function of the  $x$  coordinate only) using a standard finite element representation [20] along the transverse

direction of the plate. Thus, within an element  $e$  the displacement amplitudes can be written as

$$\begin{aligned} w^{\ell}(\mathbf{x}) &= \sum_{i=1}^{n_e} N_i(\mathbf{x}) w_i^{\ell} \\ \theta_x^{\ell}(\mathbf{x}) &= \sum_{i=1}^{n_e} N_i(\mathbf{x}) \theta_{xi}^{\ell} \\ \theta_y^{\ell}(\mathbf{x}) &= \sum_{i=1}^{n_e} N_i(\mathbf{x}) \theta_{yi}^{\ell} \end{aligned} \quad (21)$$

where  $w_i^{\ell}$ ,  $\theta_{xi}^{\ell}$  and  $\theta_{yi}^{\ell}$  are the nodal amplitudes of the  $i$ th node of element  $e$ ,  $N_i(\mathbf{x})$  is the (one-dimensional) shape function of node  $i$  of element  $e$ , and  $n_e$  is the number of nodes in element  $e$ .

Thus, the process is equivalent to dividing the plate into longitudinal elements (or strips) so that each strip has a certain number of nodes (or more accurately, nodal lines) associated with its transverse direction. The displacement field is defined longitudinally by the Fourier expansion of (21) and transversely by the finite element discretisation of (22). (See Figure 4.)

Substituting (21) into (20) it is possible to write

$$\tilde{\mathbf{u}} = \sum_{\ell=1}^n \sum_{i=1}^{n_e} N_i^{\ell} \tilde{\mathbf{a}}_i^{\ell} \quad (22)$$

where  $\tilde{\mathbf{u}} = [w, \theta_x, \theta_y]^T$

$$\tilde{\mathbf{a}}_i^{\ell} = \begin{bmatrix} N_i S_{\ell} & 0 & 0 \\ 0 & N_i S_{\ell} & 0 \\ 0 & 0 & N_i C_{\ell} \end{bmatrix}$$

and  $\tilde{\mathbf{a}}_i^{\ell} = [w_i^{\ell}, \theta_{xi}^{\ell}, \theta_{yi}^{\ell}]^T \quad (23)$

with  $S_{\ell} = \sin \frac{\ell\pi}{b} y$  and  $C_{\ell} = \cos \frac{\ell\pi}{b} y$

The harmonic expansions chosen satisfy the following boundary conditions

$$\left. \begin{aligned} w = \theta_x = 0 \\ \frac{\partial w}{\partial x} = \frac{\partial \theta_x}{\partial x} = \frac{\partial \theta_y}{\partial y} = 0 \end{aligned} \right\} \text{ for } y = 0 \text{ and } y = b$$

which imply that the plate is simply supported at the two opposite ends. Other boundary conditions can be reproduced by an appropriate selection of the Fourier-like expansions of (20). However, the expansions chosen here are the most simple and usual in practice for economy reasons as will be explained later.

The discretised expressions for the strains and stresses within a strip can be simply obtained by substituting (22) into (14) and (18) resp. Thus, after substitution, the following expressions are obtained

$$\tilde{\boldsymbol{\varepsilon}} = \sum_{\ell=1}^n \sum_{i=1}^{n_e} \tilde{\mathbf{B}}_i^{\ell} \tilde{\mathbf{a}}_i^{\ell} \quad (24)$$

and

$$\tilde{\boldsymbol{\sigma}} = \sum_{\ell=1}^n \sum_{i=1}^{n_e} \tilde{\mathbf{D}} \tilde{\mathbf{B}}_i^{\ell} \tilde{\mathbf{a}}_i^{\ell} \quad (25)$$

where  $\tilde{\mathbf{B}}_i^{\ell}$  is the strain-displacement matrix of the  $i$ th node of strip  $e$  for the  $\ell$ th harmonic term, which is written as

$$\tilde{\mathbf{B}}_i^{\ell} = \begin{Bmatrix} \tilde{\mathbf{B}}_{bi}^{\ell} \\ \tilde{\mathbf{B}}_{si}^{\ell} \end{Bmatrix} \quad (26)$$

where

$$\tilde{\mathbf{B}}_{bi}^{\ell} = \begin{bmatrix} 0 & \frac{\partial N_i}{\partial x} S_{\ell} & 0 \\ 0 & 0 & -N_i \frac{\ell\pi}{b} S_{\ell} \\ 0 & N_i \frac{\ell\pi}{b} C_{\ell} & \frac{\partial N_i}{\partial x} C_{\ell} \end{bmatrix} \quad (27)$$

and

$$\tilde{B}_{si}^{\ell} = \begin{bmatrix} \frac{\partial N_i}{\partial x} S_{\ell} & N_i S_{\ell} & 0 \\ N_i \frac{\ell \pi}{b} C_{\ell} & 0 & N_i C_{\ell} \end{bmatrix}$$

in which  $\tilde{B}_{bi}^{\ell}$  and  $\tilde{B}_{si}^{\ell}$  are the contributions to the strain matrix of node  $i$  due to bending and shear, resp. for the  $\ell$ th harmonic term.

Expanding the forces in the same way as the displacements, the distributed vertical load can be represented by the expression

$$q = \sum_{\ell=1}^n q^{\ell} \sin \frac{\ell \pi}{b} y \quad (28)$$

Thus, substituting (25) and (26) and using (21) and (28) the expression for the Total Potential Energy of the plate can be expressed as the sum of the contributions  $\pi^e$  from each strip

$$\begin{aligned} \pi = \sum_e \pi^e = \sum_e \left\{ \frac{1}{2} \right\} & \int_{A_e} \left( \sum_{\ell=1}^n \sum_{i=1}^{n_e} \tilde{B}_{-i}^{\ell} \tilde{a}_i^{\ell} \right)^T \underline{D} \left( \sum_{m=1}^m \sum_{j=1}^{n_e} \tilde{B}_j^m \tilde{a}_j^m \right) dA \\ & - \int_{A_e} \left( \sum_{\ell=1}^n \sum_{i=1}^{n_e} N_i S_{\ell} w^{\ell} \right) \left( \sum_{m=1}^m q^m S_m \right) dA \end{aligned} \quad (29)$$

where  $A^e$  is the area of the transverse cross-section of strip  $e$ . Taking into account the orthogonal properties of the functions  $S_{\ell}$  and  $C_{\ell}$ , i.e.

$$\left. \begin{aligned} \int_0^b S_{\ell} S_m dy &= \frac{b}{2} \quad \text{if } \ell = m \\ \int_0^b C_{\ell} C_m dy &= 0 \quad \text{if } \ell \neq m \end{aligned} \right\} \quad (30)$$

The expression for the Total Potential Energy of the strip,  $\pi^e$ , of (29) can be written as

$$\begin{aligned} \pi^e = \frac{1}{2} & \sum_{\ell=1}^n \sum_{m=1}^n \sum_{i=1}^{n_e} \sum_{j=1}^{n_e} (\tilde{a}_i^{\ell})^T [\tilde{K}_{ij}^{\ell m}]^e \tilde{a}_j^m - \\ & - \sum_{\ell=1}^n \sum_{i=1}^{n_e} (\tilde{a}_i^{\ell})^T [\tilde{f}_i^{\ell}]^e \end{aligned} \quad (31)$$

in which

$$[\tilde{K}_{ij}^{\ell m}]^e \begin{cases} = \frac{b}{2} \int_0^{a^e} (\tilde{B}_{-i}^{\ell})^T \underline{D} \tilde{B}_j^m dx \quad \text{for } \ell = m \\ = 0 \quad \text{for } \ell \neq m \end{cases} \quad (32)$$

is the stiffness matrix of the strip  $e$  of width  $a^e$  connecting nodes  $i$  and  $j$  for the  $\ell$ th harmonic term, and

$$[\tilde{f}_i^{\ell}]^e = \frac{b}{2} \int_0^{a^e} [0, N_i q^{\ell}, 0]^T dx \quad (33)$$

is the vector of forces of node  $i$  of element  $e$  for the  $\ell$ th harmonic term.

Matrix  $\tilde{B}_{-i}^{\ell}$  of (32) is obtained from (27) by simply making  $S_{\ell} = C_{\ell} = 1$ .

From (32) and (33) it can be seen that there is no coupling between the different harmonic terms and, therefore, the stiffness matrix and load vectors of the strip can be computed separately for each harmonic.

The discretised equilibrium equations can be easily obtained by minimising the Total Potential Energy of the plate,  $\pi$ , with respect to all the nodal amplitudes, i.e.

$$\frac{\partial \pi}{\partial \tilde{a}_i^{\ell}} = 0 \quad (34)$$

Equation (34) leads to a system of linear equations of the form

$$\begin{bmatrix} \tilde{K}^{11} & & & & 0 \\ & \tilde{K}^{22} & & & \\ & & \ddots & & \\ & & & \tilde{K}^{nn} & \\ 0 & & & & \end{bmatrix} \begin{Bmatrix} \tilde{a}^1 \\ \tilde{a}^2 \\ \vdots \\ \tilde{a}^n \end{Bmatrix} = \begin{Bmatrix} \tilde{f}^1 \\ \tilde{f}^2 \\ \vdots \\ \tilde{f}^n \end{Bmatrix} \quad (35)$$

Therefore the global stiffness  $\tilde{K}^{\ell\ell}$  and the load vector  $\tilde{f}^{\ell}$  can be computed separately for each harmonic by assembling the contributions from the different strip matrices in the standard manner [20]. The system of equations for the  $\ell$ th harmonic term can then be solved independently for the nodal amplitudes  $\tilde{a}^{\ell}$ . By repeating this process for all the harmonics, the different nodal amplitude parameters can be obtained. Subsequently, the displacements at each point in the structure can be computed by (22), whereas the strains and stresses can be evaluated using (24) and (25) resp.

It is worth pointing out here that the decoupling of the stiffness and load matrices for each harmonic term is a direct consequence of the Fourier expansions chosen for the displacement field in (20). If any other expansion is used to reproduce a different type of boundary condition at the plate ends, then decoupling does not occur due to the appearance of products  $S_{\ell} C_m$  which do not satisfy the orthogonality condition [12]. In such cases the stiffness matrix is a full matrix and special iterative techniques have to be used in order to make the finite strip method competitive by comparison with the more general finite element procedures [12].

### 3.3 Numerical evaluation of the integrals

In the present implementation all integrals in the transverse direction, such as those of (33) and (34), are evaluated numerically using one-dimensional Gauss-Legendre quadrature [20]. Thus, each integral is evaluated as follows

$$\int_0^a f(x) dx = \int_{-1}^{+1} g(\xi) d\xi = \sum_{i=1}^{n_g} g(\xi_i) W_i \quad (36)$$

where  $\xi_i$  and  $W_i$  are the coordinate and weight factor of the  $i$ th Gaussian point, resp. and  $n_g$  is the number of integration points used. A table with the values of the Gaussian coordinates and weights can be found in reference [20].

### 3.4 The reduced integration family of Mindlin finite strips

Mindlin finite strips must be used with caution when dealing with very thin plates. The problem is similar to that experienced with Mindlin plate finite elements. As the plate thickness becomes small, the influence of the shear terms tends to dominate the numerical solution and unrealistic over stiff results (locking) can be obtained unless some precautions are taken.

The stiffness matrix associated with the  $\ell$ th harmonic can be written in terms of bending and shear contribution  $\tilde{K}_b^{\ell\ell}$  and  $\tilde{K}_s^{\ell\ell}$  resp. as

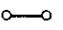
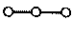
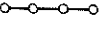
$$\tilde{K}^{\ell\ell} = \tilde{K}_b^{\ell\ell} + \tilde{K}_s^{\ell\ell} \quad (37)$$

One of the simplest ways to ensure the singularity of matrix  $\tilde{K}_s^{\ell\ell}$  and hence avoid locking is to relax the constraint imposed by the shear terms by under-integrating the coefficients of  $\tilde{K}_s^{\ell\ell}$  in the numerical integration of the integrals which appear in the stiffness matrix  $\tilde{K}^{\ell\ell}$ . The rest of the stiffness matrix can be exactly integrated and thus the process is called "selective integration", or else it can also be under-integrated which is usually termed "reduced integration".

The number of integrating points to exactly integrate the strip matrices, obviously depends on the degree of the shape function polynomials of each particular strip. Figure 4 shows the shape functions for the linear, quadratic and cubic Mindlin strip elements. Table 1 gives the number of Gaussian



TABLE 1: Gaussian integration rules for matrices  $\underline{K}_b^{II}$  and  $\underline{K}_s^{II}$  for various Mindlin strip elements.

GAUSSIAN INTEGRATION RULES						
STRIP ELEMENT	FULL (F)		SELECTIVE (S)		REDUCED (R)	
	$\underline{K}_b^{II}$	$\underline{K}_s^{II}$	$\underline{K}_b^{II}$	$\underline{K}_s^{II}$	$\underline{K}_b^{II}$	$\underline{K}_s^{II}$
	2	2	2	1	1	1
	3	3	3	2	2	2
	4	4	3	3	3	3
NUMBER OF INTEGRATION POINTS						

integrating points [20] needed for the full, reduced and selective integration of  $\underline{K}_b^{II}$  and  $\underline{K}_s^{II}$ .

It has been shown by Oñate and Suarez [18] that singularity of matrix  $\underline{K}_s^{II}$  for the linear, quadratic and cubic strips is ensured for most practical cases if reduced or selective integration is used. The linear strip with full integration behaves badly and it gives over stiff, unrealistic results even for the case of moderately thick plates. The quadratic strip with full integration is somewhat unreliable. Although deflections and bending moments agree in most cases with theoretical values, the shear forces oscillate and smoothing is recommended. The cubic strip, however, performs well with full integration. Nevertheless, reduced integration can be recommended for economy reasons.

Some of the properties mentioned above will be shown in the examples which are now presented.

### 3.5 Numerical examples

#### 3.5.1 Example 1: Convergence with number of harmonics

Figure 6 shows the convergence of the central deflection and central bending moment,  $M_x$ , for a simply supported square thick plate under uniform loading. Numerical results have been obtained for the meshes of linear, quadratic and cubic elements shown in the same figure. The convergence rate for reduced, selective or full integration is the same for all strip elements. Five non-zero harmonics (the even harmonic terms are zero due to the symmetry of loading) are required to obtain an error of less than 0.3% in both deflection and bending moment compared with the converged solution.

#### 3.5.2 Example 2: Convergence with number of strips

Figure 7 shows the convergence of the central deflection and central bending moment,  $M_x$ , with the number of strips for the plate considered in Section 3.5.1 for two different thickness/span ratios of  $t/L = 0.1$  and  $0.01$  resp. The percentage error with respect to the theoretical "exact" solution [21] is shown for the linear, quadratic and cubic strip elements with full, selective and reduced integration.

It can be seen that results for the linear element with selective and reduced integration are extremely good in both cases when compared with the quadratic or cubic strips.

#### 3.5.3 Example 3: Thin plate behaviour study

Figure 8 shows the value of the central deflection of the square plate of Figure 6 for a wide range of thickness/span ratios. It can be seen that all elements behave well with reduced or selective integration and give the correct solution for thick, thin and very thin plates.

It is interesting to look at the distribution of shear forces along the centre line of the plate for different thicknesses. The shear forces have been plotted in Figure 9 for

CONVERGENCE FOR ALL ELEMENTS IS THE SAME

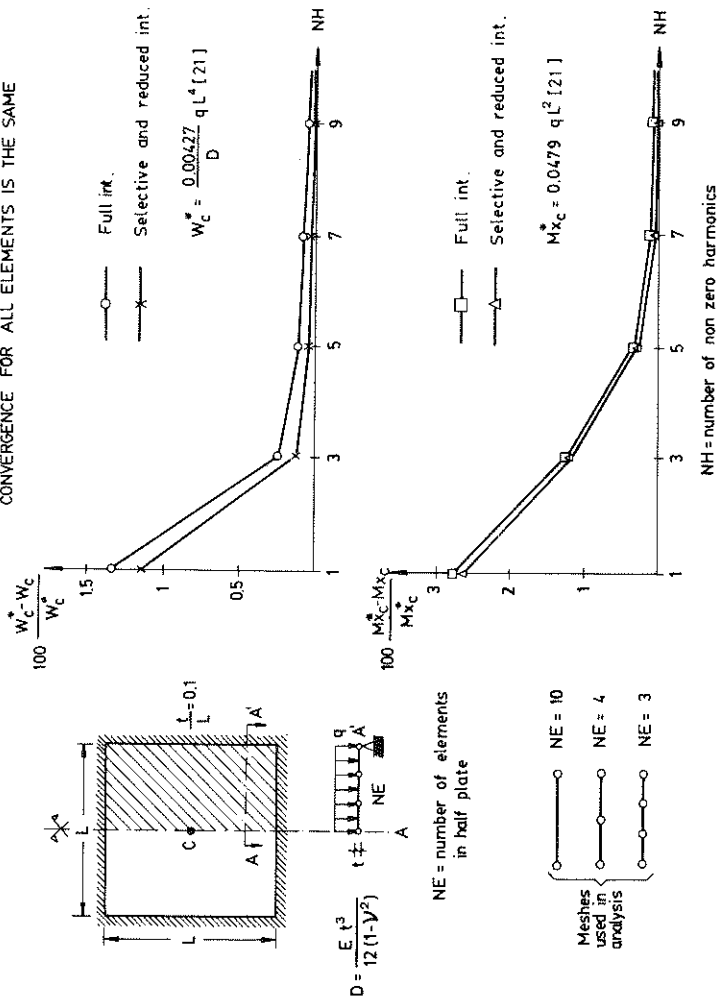


Fig 6 Simply supported square under uniform loading. Convergence of central deflection,  $W_c$  and central bending moment,  $M_{xc}$ , with number of harmonics for the linear, quadratic and cubic strip elements.

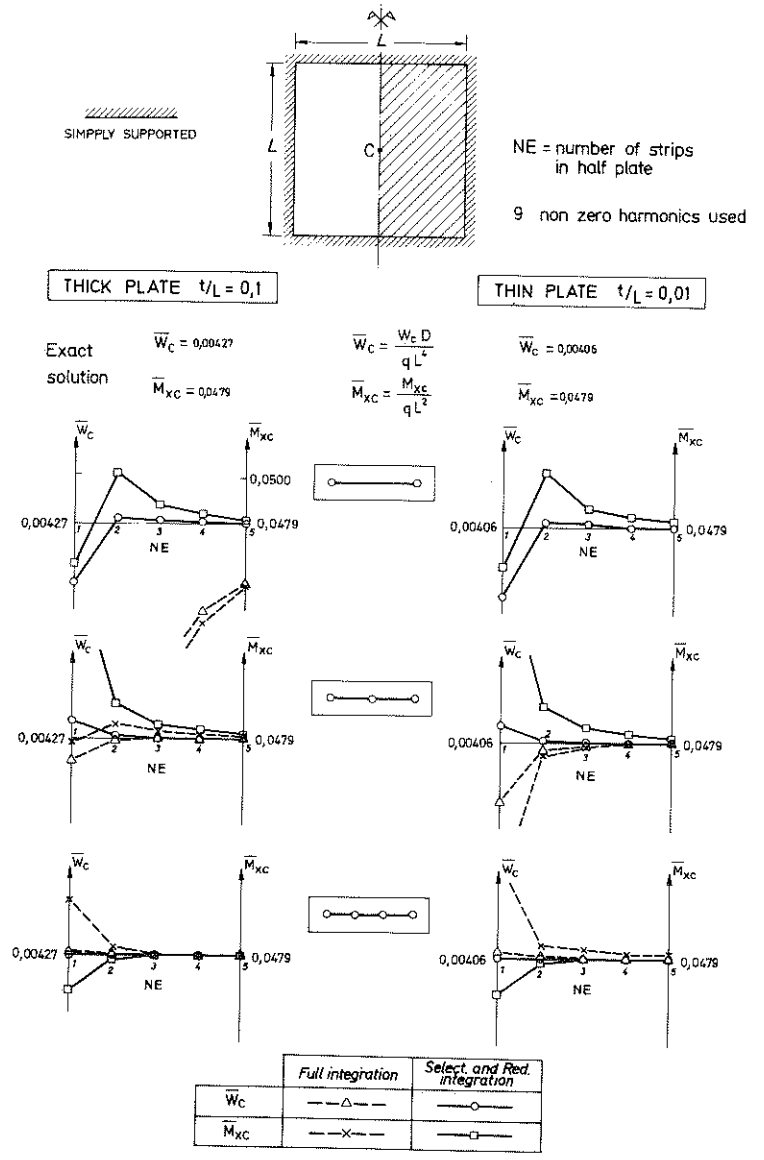


Fig. 7 Square plate under uniform loading. Convergence study of the deflection and bending moment,  $M_x$ , at the plate center for the linear, quadratic and cubic strip elements with full, reduced and selective integration.

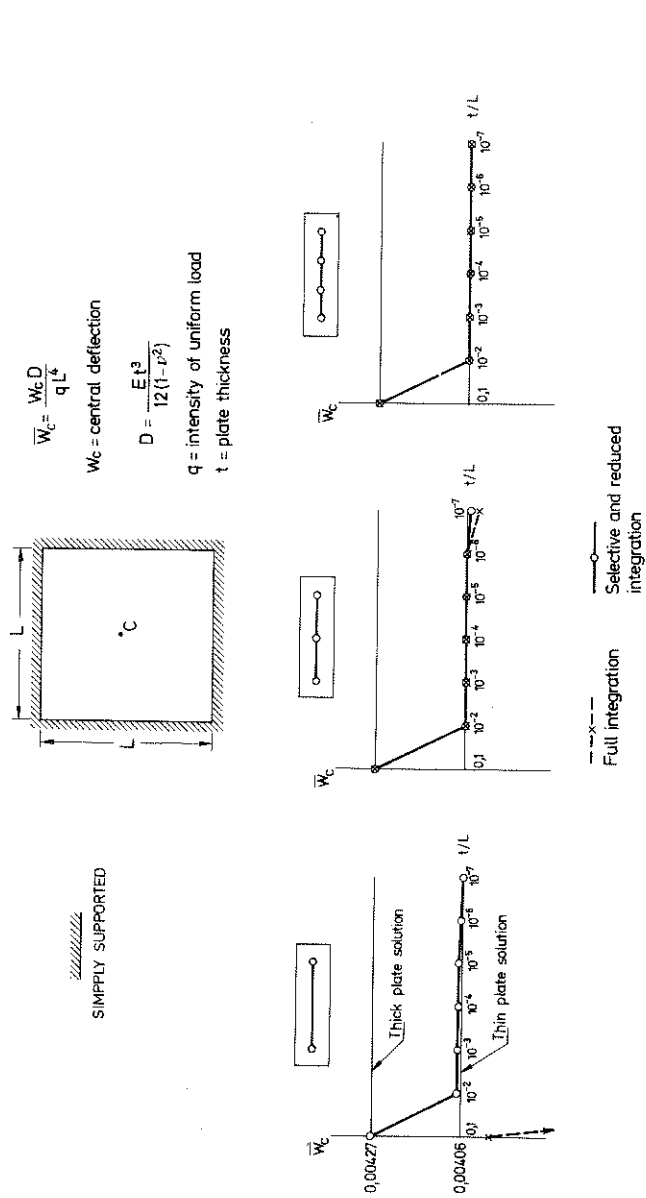


Fig. 8 Square plate under uniformly distributed load. Central deflection versus  $t/L$  for the linear, quadratic and cubic strip elements with full, reduced and selective integration.

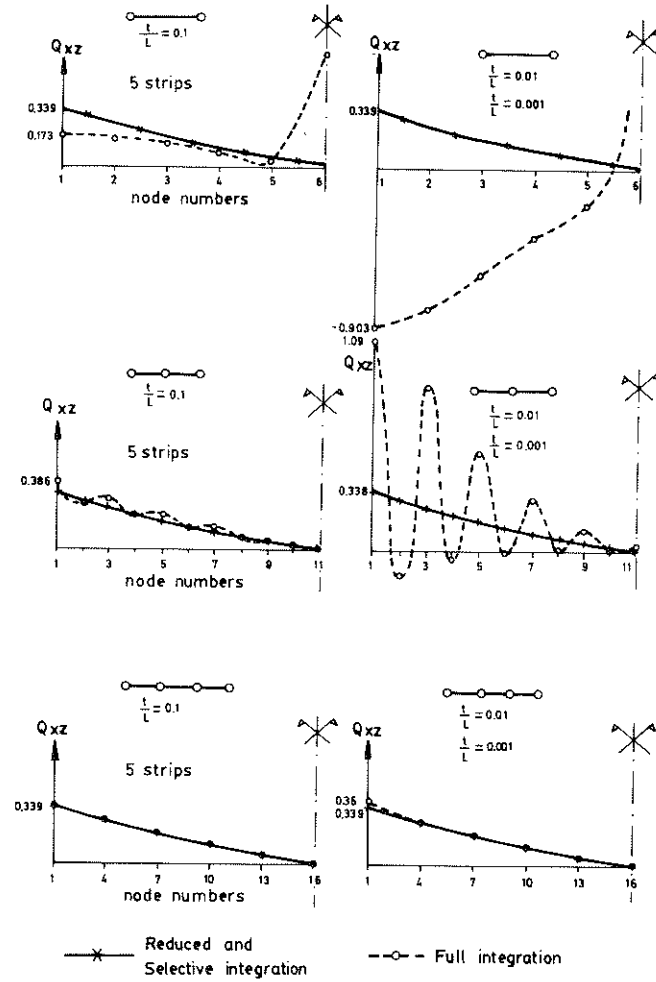


Fig. 9 Distribution of shear forces along the center of the plate for different strip elements and integration rules.

two thickness/span ratios of  $t/L = 0.1$  and  $0.01$ . We can see that wrong results are obtained with the linear element and full integration for the two cases, whereas selective and reduced integration give the correct results. Results for the quadratic element with full integration oscillate, as already mentioned. These oscillations are eliminated if selective or reduced integration is used. More information about this example can be found in reference [18].

#### 3.5.4 Example 4: Square plate subjected to localised edge load

This square plate is simply supported on two opposite edges, clamped on one edge and free on the remaining edge. The centre of the free edge is subjected to a line load of varying intensity, as shown in Figure 10. In the vicinity of the load, the transverse stresses are large compared to the in-plane stresses with the result that shear deformation, in these regions, contributes significantly to the total deformation. The results obtained with the linear, quadratic and cubic Mindlin strips with reduced integration are compared with solutions based on classical plate theory [21] and with results of the work of Alwar and Ramachandran in which Reissner's theory is compared with experimental results [22]. Figure 10 clearly shows the importance of allowing for shear deformation. As the intensity of the line load increases, the numerical results obtained with classical plate theory, seriously overestimate the maximum tensile stress at the centre of the free edge. This situation worsens for thicker plates. The numerical results obtained for all three Mindlin strip elements are in good agreement with the experimental results. Figure 11 shows the localised nature of this overestimate and how thin plate theory is satisfactory in regions not too distant from the load.

#### 3.5.5 Conclusions

For economical solutions which do not exhibit locking

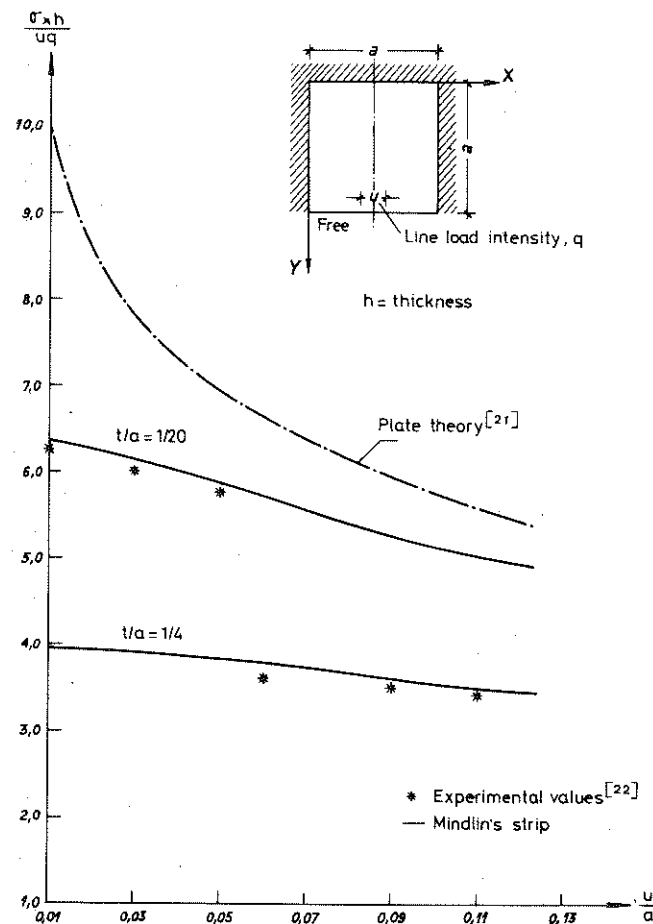


Fig.10 Square plate simply supported at three edges under localised line load acting at free edge. Maximum tensile stress.

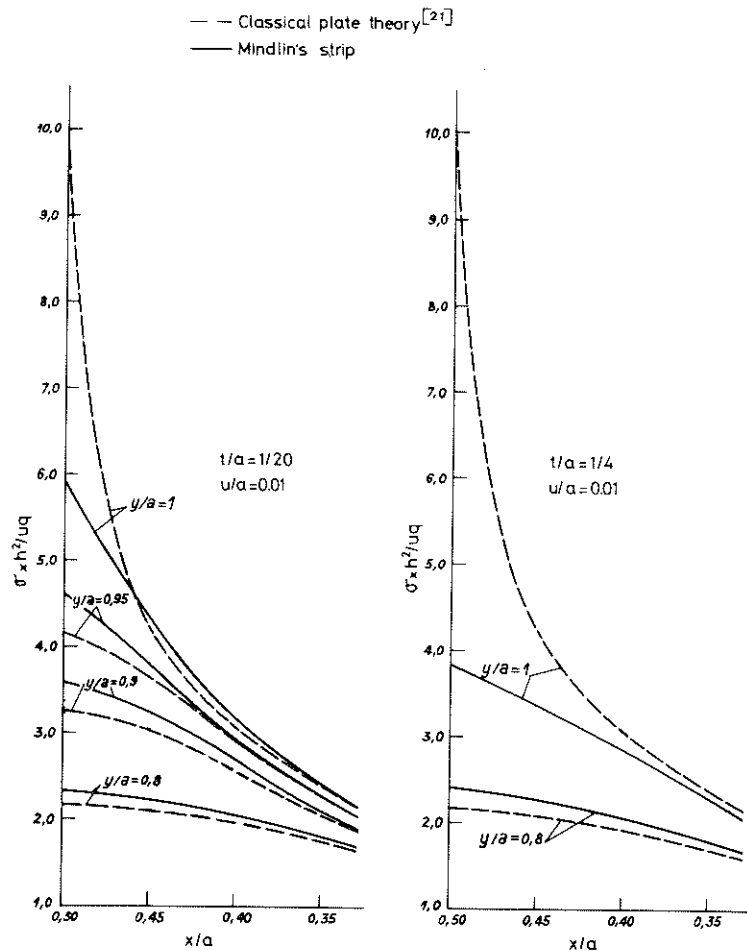


Fig. 11 Square plate simply supported at three edges under localised line load acting at free edge. Maximum tensile stress at various points.

reduced integration should be used in all strip elements for practical plate problems. In addition, the linear strip with reduced integration seems to be the best value element due to its excellent behaviour for thick and thin plate analysis and its simplicity. Moreover, an explicit form of the element matrices is simply obtained by evaluating the integrals at the strip mid-point [18].

#### 4. ANALYSIS OF FOLDED PLATES WITH CURVED PLANFORMS

The Mindlin finite strip formulation for folded plate analysis closely follows the pattern presented for the analysis of plates in the previous sections.

The most general case of curved folded plates with circular plan shape is considered. It will also be shown later that the formulations for folded plates with rectangular planforms and axisymmetric shells can be obtained as particular cases of the formulation for curved folded plates presented in the next sections.

##### 4.1 Basic theory

###### 4.1.1 Displacement field

In the shell element shown in Figure 12, the three displacements,  $u$ ,  $v$ ,  $w$ , of a typical point can be expressed in terms of the three mid-plane displacements  $u_0$ ,  $v_0$  and  $w_0$  and the two normal rotations  $\theta_s$  and  $\theta_t$  as

$$\begin{aligned} u(s, \theta, n) &= u_0(s, \theta) + n \theta_s(s, \theta) \\ v(s, \theta, n) &= v_0(s, \theta) + n \theta_t(s, \theta) \\ w(s, \theta, n) &= w_0(s, \theta) \end{aligned} \quad (38)$$

In (38)  $\theta_s$  and  $\theta_t$  are the normal rotations contained in planes  $sn$  and  $tn$  resp. These rotations can be expressed as the sum of the change in slope of the middle surface and an extra average rotation due to shear, so that

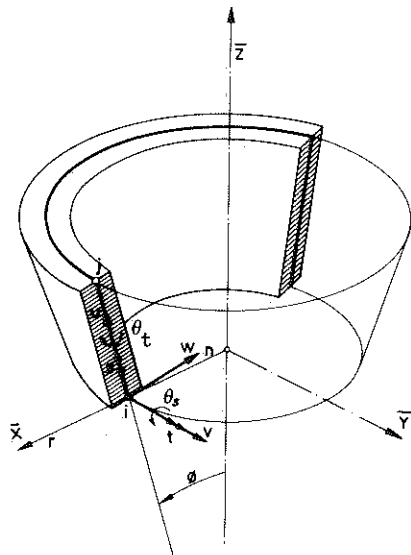


Fig. 12 Sign convention for displacements in a troncoconical shell.

$$\begin{aligned}\theta_s &= -\frac{\partial w_o}{\partial s} + \phi_s \\ \theta_t &= -\frac{1}{r} \frac{\partial w_o}{\partial \theta} + \phi_t\end{aligned}\quad (39)$$

The displacement vector at a typical point may now be defined as

$$\underline{u} = [u_o, v_o, w_o, \theta_s, \theta_t]^T \quad (40)$$

#### 4.1.2 Strains

The relevant strains in the local system (s, t, n) which is illustrated in Figure 12, are defined as

$$\underline{\epsilon} = \begin{Bmatrix} \epsilon_s \\ \epsilon_t \\ \gamma_{st} \\ \gamma_{sn} \\ \gamma_{tn} \end{Bmatrix} = \begin{bmatrix} \frac{\partial u}{\partial s} \\ \frac{1}{r} \frac{\partial v}{\partial \theta} + \frac{u}{r} \sin \phi - \frac{w}{R_t} \\ \frac{1}{r} \frac{\partial u}{\partial \theta} + \frac{\partial v}{\partial s} - \frac{v}{r} \sin \phi - \frac{n}{R_t} \frac{\partial v}{\partial s} \\ \theta_s + \frac{\partial w}{\partial s} \\ \theta_t + \frac{1}{r} \frac{\partial w}{\partial \theta} + \frac{v}{R_t} \end{bmatrix} \quad (41)$$

Upon substitution of (38) into (41) the strain vector can be written as

$$\underline{\epsilon} = \underline{\epsilon}_m + \begin{Bmatrix} n \epsilon_b \\ \epsilon_s \end{Bmatrix} \quad (42)$$

where

$$\underline{\epsilon}_m = \begin{bmatrix} \frac{\partial u_o}{\partial s} \\ \frac{1}{r} \frac{\partial v_o}{\partial \theta} + \frac{u_o}{r} \sin \phi - \frac{w_o}{r} \cos \phi \\ \frac{\partial v_o}{\partial s} + \frac{1}{r} \frac{\partial u_o}{\partial \theta} - \frac{v_o}{r} \sin \phi \\ 0 \\ 0 \end{bmatrix};$$

$$\epsilon_b = \begin{bmatrix} \frac{\partial \theta_s}{\partial s} \\ \frac{1}{r} \frac{\partial \theta_t}{\partial \theta} + \frac{\theta_s}{r} \sin \phi \\ \frac{\partial \theta_t}{\partial s} + \frac{1}{r} \frac{\partial \theta_s}{\partial \theta} - \frac{\theta_t}{r} \sin \phi - \frac{\cos \phi}{r} \frac{\partial v_o}{\partial s} \end{bmatrix}$$

$$\text{and } \underline{\varepsilon}_s = \begin{bmatrix} \theta_s + \frac{\partial w_o}{\partial s} \\ \frac{1}{r} \frac{\partial w_o}{\partial \theta} + \frac{v_o}{r} \cos \phi \end{bmatrix} \quad (43)$$

are the generalised strain vectors due to membrane, bending and shear effects, resp. In obtaining (43) the following assumptions have been made

$$\left(1 + \frac{n}{R_t}\right) = 1, \quad \frac{n^2}{R_t} \frac{\partial \theta}{\partial s} = 0 \quad (44)$$

and  $r = R_t \cos \phi$ .

The generalised strain vector is now defined as

$$\underline{\varepsilon} = [\underline{\varepsilon}_m^T, \underline{\varepsilon}_b^T, \underline{\varepsilon}_s^T]^T \quad (45)$$

#### 4.1.3 Stresses

The vector of stress resultants corresponding to the generalised strain vector of (45) can be written as

$$\underline{\sigma} = [\underline{\sigma}_m^T, \underline{\sigma}_b^T, \underline{\sigma}_s^T]^T \quad (46)$$

where

$$\begin{aligned} \underline{\sigma}_m &= [N_s, N_t, N_{st}]^T \\ \underline{\sigma}_b &= [M_s, M_t, M_{st}]^T \\ \underline{\sigma}_s &= [Q_s, Q_t]^T \end{aligned} \quad (47)$$

are the stress resultant vectors due to membrane, bending and shear effects, resp. For the sign convention see Figure 13.

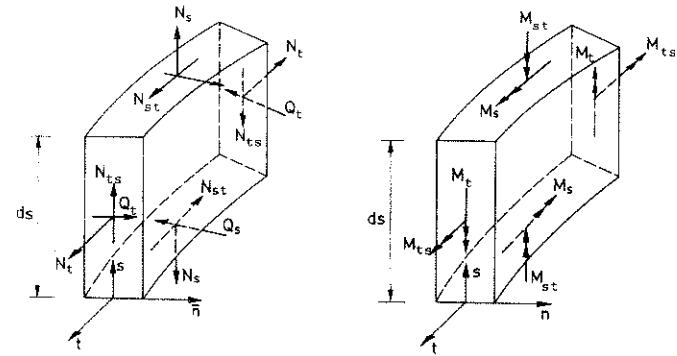


Fig.13 Sign convention for displacements and resultant stresses in a troncoconical shell.

#### 4.1.4 Stress-strain relationship

For an elastic material the relationship between generalised strains and stress resultants can be written as

$$\underline{\sigma} = \underline{D} \underline{\varepsilon} \quad (48)$$

with

$$\underline{D} = \begin{bmatrix} \underline{D}_m & \underline{0} & \underline{0} \\ \underline{0} & \underline{D}_b & \underline{0} \\ \underline{0} & \underline{0} & \underline{D}_s \end{bmatrix} \quad (49)$$

where for an isotropic material the membrane elasticity matrix may be written as

$$\underline{D}_m = \frac{Et}{1-\nu^2} \begin{bmatrix} 1 & \nu & 0 \\ 0 & 1 & 0 \\ 0 & 0 & \frac{1-\nu}{2} \end{bmatrix} \quad (50)$$

and  $\underline{D}_b$  and  $\underline{D}_s$  have the same meaning as those in (19).

#### 4.1.5 Total Potential Energy of the shell

It can be shown [25] that the Total Potential Energy of the shell can be written in a form equivalent to that for a plate in (13) as

$$\pi = \frac{1}{2} \iint_A \underline{\varepsilon}^T \underline{\sigma} dA - \iint_A \underline{u}^T \underline{b} dA - \iint_A \underline{u}^T \underline{t} dA - \int_{\Gamma} \underline{u}^T \underline{P} d\Gamma \quad (51)$$

where  $\underline{u}$  is the displacement vector,  $\underline{b}$  and  $\underline{t}$  are the body force and distributed loading vectors acting per unit area,  $\underline{P}$  is the vector of point loads acting along a line  $\Gamma$ , and  $A$  the area of the shell mid-surface.

#### 4.2 Finite strip formulation for curved folded plates

The folded plate is divided into longitudinal strips as shown in Figure 14.

If  $k$  is the number of nodes within a particular strip  $e$ , the displacement field within the strip is expressed as

$$\underline{u} = \sum_{\ell=1}^n \sum_{i=1}^k N_i^{\ell} a_i^{\ell} \quad (52)$$

where  $N_i^{\ell}$  and  $a_i^{\ell}$  are resp. the generalised shape function matrix and the vector of nodal displacement amplitudes associated with node  $i$  for the  $\ell$ th harmonic term. These matrices have the following form

$$N_i^{\ell} = \begin{bmatrix} N_i S_{\ell} & 0 & 0 & 0 & 0 \\ 0 & N_i C_{\ell} & 0 & 0 & 0 \\ 0 & 0 & N_i S_{\ell} & 0 & 0 \\ 0 & 0 & 0 & N_i S_{\ell} & 0 \\ 0 & 0 & 0 & 0 & N_i C_{\ell} \end{bmatrix} \quad (53)$$

$$a_i^{\ell} = [u_{oi}^{\ell}, v_{oi}^{\ell}, w_{oi}^{\ell}, \theta_{si}^{\ell}, \theta_{ti}^{\ell}]^T \quad (54)$$

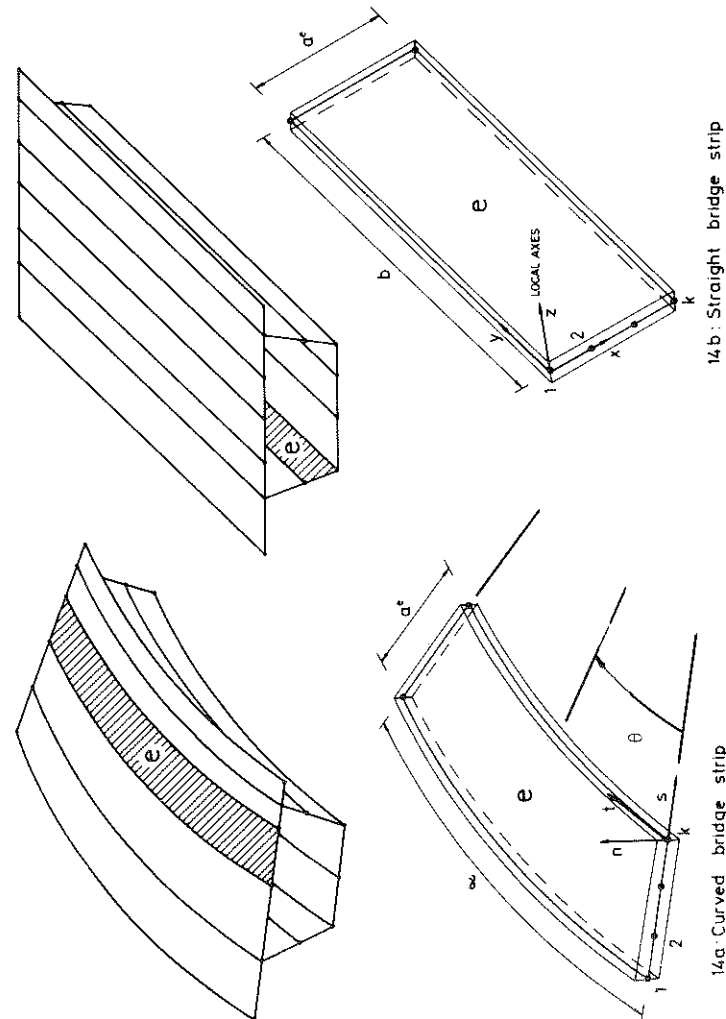


FIG. 14. Curved and straight bridges. Finite strip discretisations and local element coordinate axes.



where  $S_\ell = \sin \frac{\ell\pi}{\alpha} \theta$ ,  $C_\ell = \cos \frac{\ell\pi}{\alpha} \theta$  and the angle  $\alpha$  is defined in Figure 14.

It is easy to check that the chosen harmonic expansions satisfy the simple support conditions at  $\theta = 0$  and  $\theta = \alpha$ . This formulation is thus valid for simply supported folded plates with rigid diaphragms at the two ends.

The generalised strain vector  $\underline{\varepsilon}$  of (41) can be simply obtained at any point within the strip in terms of the nodal displacement amplitudes by substituting (52) into (41) to give

$$\underline{\varepsilon} = \sum_{\ell=1}^n \sum_{i=1}^k \underline{B}_i^\ell \underline{a}_i^\ell \quad (55)$$

where  $\underline{B}_i^\ell$  can now be written as

$$\underline{B}_i^\ell = [\underline{B}_{mi}^\ell, \underline{B}_{bi}^\ell, \underline{B}_{si}^\ell]^T \quad (56)$$

with

$$\underline{B}_{mi}^\ell = \begin{bmatrix} \frac{\partial N_i}{\partial s} S_\ell & 0 & 0 & 0 & 0 \\ \frac{N_i}{r} \sin \phi S_\ell & -\frac{N_i \ell \pi}{b'} S_\ell & -\frac{N_i}{r} \cos \phi S_\ell & 0 & 0 \\ \frac{N_i \ell \pi}{b'} C_\ell & \left( \frac{\partial N_i}{\partial s} - \frac{N_i}{r} \sin \phi \right) C_\ell & 0 & 0 & 0 \end{bmatrix}$$

$$\underline{B}_{bi}^\ell = \begin{bmatrix} 0 & 0 & 0 & \frac{\partial N_i}{\partial s} S_\ell & 0 \\ 0 & 0 & 0 & \frac{N_i}{r} \sin \phi S_\ell & -\frac{N_i \ell \pi}{b'} S_\ell \\ 0 & -\frac{\partial N_i}{\partial s} \frac{\cos \phi}{r} C_\ell & 0 & \frac{N_i \ell \pi}{b'} C_\ell & \left( \frac{\partial N_i}{\partial s} - \frac{N_i}{r} \sin \phi \right) C_\ell \end{bmatrix}$$

$$\underline{B}_{si}^\ell = \begin{bmatrix} 0 & 0 & \frac{\partial N_i}{\partial s} S_\ell & N_i S_\ell & 0 \\ 0 & \frac{N_i}{r} \cos \phi C_\ell & \frac{N_i \ell \pi}{b'} C_\ell & 0 & N_i C_\ell \end{bmatrix} \quad (57)$$

where  $b' = r\alpha$  and  $\underline{B}_{mi}^\ell$ ,  $\underline{B}_{bi}^\ell$  and  $\underline{B}_{si}^\ell$  are resp. the generalised strain matrices due to membrane, bending and shear effects for node  $i$  and the  $\ell$ th harmonic term.

If the force vectors are represented by the same kind of expansion as the one used for the displacement field, then it is possible to write

$$[\underline{b}, \underline{t}, \underline{p}] = \sum_{\ell=1}^n [\underline{S}_\ell \underline{b}^\ell, \underline{S}_\ell \underline{t}^\ell, \underline{S}_\ell \underline{p}^\ell] \quad (58)$$

where

$$\underline{S}_\ell = \begin{bmatrix} S_\ell & 0 & 0 & 0 & 0 \\ 0 & C_\ell & 0 & 0 & 0 \\ 0 & 0 & S_\ell & 0 & 0 \\ 0 & 0 & 0 & S_\ell & 0 \\ 0 & 0 & 0 & 0 & C_\ell \end{bmatrix} \quad (59)$$

and  $\underline{b}^\ell$ ,  $\underline{t}^\ell$  and  $\underline{p}^\ell$  are the force amplitude vectors for the  $\ell$ th term of the series.

Upon substitution of (52), (56) and (48) into the Total Potential Energy expression of (51) and by taking into account the orthogonal properties of functions  $S_\ell$  and  $C_m$  it is possible to obtain, after an identical process to that followed in (30) - (32) for the plate bending case, the expression for the strip stiffness matrix and load vectors which have the following form

$$[K_{ij}^{\ell m}] = \begin{cases} \frac{\alpha}{2} \int_0^a e^{i(\ell - m)s} [\underline{B}_i^\ell]^T \underline{D} \underline{B}_j^\ell r ds & \text{for } \ell = m \\ 0 & \text{for } \ell \neq m \end{cases} \quad (60)$$

and

$$\underline{f}_i^\ell = \iint_A (\underline{N}_i^\ell)^T \underline{b} dA + \iint_A (\underline{N}_i^\ell)^T \underline{t} dA + \int_\Gamma (\underline{N}_i^\ell)^T \underline{p} d\Gamma \quad (61)$$

Further details on the load vector for different loading cases are given in Section 8. Matrix  $\underline{B}_i^\ell$  of (60) can be obtained from (57) by simply making  $S_\ell = C_\ell = 1$ .

The discretised equilibrium equations for the whole structure are obtained by minimising the Total Potential Energy. This process leads to a set of uncoupled systems of equations which are similar to those of (3) and which can be solved separately for each harmonic term.

#### 4.3 Assembly of the stiffness matrices and coordinate transformation

One of the main differences between the plate and folded plate strip formulations is that in the plate bending case the strips are all in the same plane, which coincides with the plate middle surface, whereas in the folded plate case the strips usually meet at different angles. Thus, to assemble the complete stiffness matrix of the structure from the individual strip stiffness matrices all nodal forces and displacements must be expressed in a common, and uniquely defined, coordinate system. The nodal displacements defined in the local strip coordinate system, shown in Figure 12, contain only two rotation components  $\theta_s$  and  $\theta_t$ . The third rotation,  $\theta_n$ , about the  $n$  axis does not appear in the strain definition and is therefore not required to model the structural behaviour of each individual strip. However, when several strips meeting at a common node lie in different planes it is necessary to include  $\theta_z$ , the rotation about the global  $\bar{z}$  axis, for a consistent transformation of displacements and forces from the local to the global coordinate system.

Thus, it is possible to write that

$$\bar{a}_i^l = \bar{T}^{(e)} a_i^l \quad (62)$$

$$\text{and } \bar{f}_i^l = \bar{T}^{(e)} f_i^l \quad (63)$$

where

$$\bar{a}_i^l = [\bar{u}_i^l, \bar{v}_i^l, \bar{w}_i^l, \theta_{\bar{x}i}^l, \theta_{\bar{y}i}^l, \theta_{\bar{z}i}^l]^T \quad (64)$$

$$\bar{f}_i^l = [F_{\bar{x}i}^l, F_{\bar{y}i}^l, F_{\bar{z}i}^l, M_{\theta_{\bar{x}i}^l}^l, M_{\theta_{\bar{y}i}^l}^l, M_{\theta_{\bar{z}i}^l}^l]^T$$

are the displacement and force vectors at node  $i$  of element  $e$  in the global coordinate system  $\bar{x}, \bar{y}, \bar{z}$  where  $\bar{y}$  is parallel to  $t$  and  $\bar{z}$  is the vertical axis as shown in Figure 12. Note also that

$$\bar{a}_i^l = [u_i^l, v_i^l, w_i^l, \theta_{si}^l, \theta_{ti}^l, 0]^T \quad (65)$$

$$\bar{f}_i^l = [F_{si}^l, F_{ti}^l, F_{ni}^l, M_{\theta_{si}^l}^l, M_{\theta_{ti}^l}^l, 0]^T \quad (66)$$

are the same vectors in the local strip coordinate system. The matrix

$$\bar{T}^{(e)} = \begin{bmatrix} \sin \phi & 0 & -\cos \phi & 0 & 0 & 0 \\ 0 & 1 & 0 & 0 & 0 & 0 \\ \cos \phi & 0 & \sin \phi & 0 & 0 & 0 \\ 1 & 0 & 0 & 1 & 0 & 0 \\ 0 & 0 & 0 & 0 & \sin \phi & \cos \phi \\ 0 & 0 & 0 & 0 & -\cos \phi & \sin \phi \end{bmatrix} \quad (67)$$

is the coordinate transformation matrix of element  $e$ , and  $\phi$  is the angle between axes  $s$  and  $\bar{z}$ , as shown in Figure 12.

The strip stiffness matrix in the global system can be written in the standard form as

$$[\bar{K}_{ij}^{ll}]^e = \bar{T}^{(e)} K_{ij}^{ll} [\bar{T}^e]^T \quad (68)$$

with

$$K_{ij}^{ll} = \begin{bmatrix} K_{ij}^{ll} & 0 \\ (5 \times 5) & \\ 0 & 0 \end{bmatrix} \quad (69)$$

The sixth row and column of  $K_{ij}^{ll}$  contains only zeros. This is done in (69) to facilitate the transformation from the local to the global system. Equation (69) can be written in a more practical form as

$$[\bar{K}_{ij}^{ll}]^e = \frac{\alpha}{2} \int [B_i^*]^T D B_j^* r ds \quad (70)$$

with

$$\tilde{B}_i^* = \tilde{B}_i T^T \quad (71)$$

Matrix  $\tilde{B}_i^*$  allows the direct evaluation of the local stress resultants from the global displacements using (55) and (49).

Thus, the local stress resultants can be written as

$$\sigma = \sum_{\ell=1}^n \sum_{i=1}^K \tilde{D} \tilde{B}_i^{*\ell} a_i^\ell \quad (72)$$

In general, matrix  $\tilde{K}_{ij}^{\ell\ell}$  will be fully populated and thus  $\theta_z$  will be an independent degree of freedom. A problem, however, arises if all strips associated with a particular node happen to lie in the same plane because the resultant diagonal stiffness coefficient corresponding to  $\theta_z$ , after assembly, will be zero. Such a node is termed a coplanar node and examples can be seen in Figure 14. This singularity of the global stiffness matrix has been avoided, in practice, by assembling the equations corresponding to the three rotations at a coplanar node, in the local system  $s, t, n$  in which  $s, n$  lie in the same common plane containing all the adjacent strips. Any arbitrary number is then put in the sixth leading diagonal location of matrix  $\tilde{K}_{ij}^{\ell\ell}$ . This implies that the sixth equation is a pseudo-equation. However, this does not affect the solution process since such an equation is uncoupled from the rest of the stiffness equations. This artifice, first suggested by Clough and Wilson[23] implies that all coplanar and non-coplanar nodes have six degrees of freedom. This is very convenient if the equation solution system does not allow for varying numbers of degrees of freedom at different nodes.

## 5. CURVED PLATES

The Mindlin strip formulation for the analysis of curved plates can be derived directly from the formulation given for curved folded plates presented in the previous section by simply neglecting the membrane behaviour of the structure in all equations. Details of the formulation follow precisely

the same steps as those explained previously and they will not be repeated here. The stiffness and load vectors for each harmonic term are obtained from (60) and (61) resp. However,  $B_i^\ell$  and  $\tilde{D}$  are now written as

$$B_i^\ell = \begin{bmatrix} 0 & \frac{\partial N_i}{\partial s} S_\ell & 0 \\ 0 & \frac{N_i}{r} \sin \phi S_\ell & -\frac{N_i \ell \pi}{b'} S_\ell \\ 0 & \frac{N_i \ell \pi}{b'} C_\ell & \left( \frac{\partial N_i}{\partial s} - \frac{N_i}{r} \sin \phi \right) C_\ell \\ \frac{\partial N_i}{\partial s} S_\ell & N_i S_\ell & 0 \\ \frac{N_i \ell \pi}{b'} C_\ell & 0 & N_i C_\ell \end{bmatrix} \quad (73)$$

and

$$\tilde{D} = \begin{bmatrix} \tilde{D}_b & 0 \\ 0 & \tilde{D}_s \end{bmatrix} \quad (74)$$

in which  $b' = r\alpha$  and  $a_i^\ell$  of (54) is now expressed as

$$a_i^\ell = [w_i^\ell, \theta_{si}^\ell, \theta_{ti}^\ell]^T$$

By making  $r$  very large so that  $\frac{1}{r} \sim 0$  and by letting  $b' = b$  it is possible to obtain the strain-displacement matrix for a straight (or right) plate given in (27).

## 6. FOLDED PLATES WITH RECTANGULAR PLANFORM

The formulation for folded plates with rectangular planform can be easily derived from the formulation for their curved counterparts presented in Section 4. Thus, only details of the main differences will be given here.

### 6.1 Displacement field

For a plane "shell" element the three displacements of a point across the thickness can be expressed in terms of the displacements of the middle surface as

$$\begin{aligned} u(x,y,z) &= u_o(x,y) + z \theta_x(x,y) \\ v(x,y,z) &= v_o(x,y) + z \theta_y(x,y) \\ w(x,y,z) &= w_o(x,y) \end{aligned} \quad (75)$$

where all terms have the same meaning of those of (38) except that the fixed local axes  $x, y, z$  replace the curvilinear ones  $s, t, n$  (see Figure 14(b)).

### 6.2 Strain field

From standard elasticity theory the strain vector can be written as

$$\epsilon = \begin{Bmatrix} \epsilon_m \\ 0 \\ \epsilon_s \end{Bmatrix} + \begin{Bmatrix} z \epsilon_b \\ \epsilon_s \end{Bmatrix} \quad (76)$$

where

$$\epsilon_m = \begin{Bmatrix} \frac{\partial u_o}{\partial x} \\ \frac{\partial v_o}{\partial y} \\ \frac{\partial u_o}{\partial y} + \frac{\partial v_o}{\partial x} \end{Bmatrix} \quad \epsilon_b = \begin{Bmatrix} \frac{\partial \theta_x}{\partial x} \\ \frac{\partial \theta_y}{\partial y} \\ \frac{\partial \theta_x}{\partial y} + \frac{\partial \theta_y}{\partial x} \end{Bmatrix} \quad \epsilon_s = \begin{Bmatrix} \theta_x + \frac{\partial w_o}{\partial x} \\ \theta_y + \frac{\partial w_o}{\partial y} \end{Bmatrix} \quad (77)$$

are the corresponding generalised strain vectors for membrane, bending and shear. It is worth noting the decoupling between membrane and flexural effects at element level, which did not occur in the curved bridge formulation (see (43)).

### 6.3 Stresses

The expressions for the stress resultant vectors are identical to those for curved bridges (see (47)) with indices  $x, y$  and  $s$  replacing  $s, \theta$  and  $n$  resp. The sign convention given in Figure 13 is also followed. The stress/strain relationship is identical to the one given in (48).

### 6.4 Finite strip formulation for folded plates with rectangular planform

The displacement and strain fields are expressed in exactly the same way as for curved bridges (see (52) and (56)) with the bridge length  $b$  and the coordinate  $y$  replacing the angles  $\alpha$  and  $\epsilon$  resp. (see Figure 14). The strain matrix  $B_i^\ell$  is obtained from (77) and (56), and it now takes the form

$$B_i^\ell = [B_{mi}^\ell, B_{bi}^\ell, B_{si}^\ell]^T \quad (78)$$

where

$$B_{mi}^\ell = \begin{bmatrix} \frac{\partial N_i}{\partial x} S_\ell & 0 & 0 & 0 & 0 \\ 0 & -N_i \frac{\ell \pi}{b} S_\ell & 0 & 0 & 0 \\ N_i \frac{\ell \pi}{b} C_\ell & \frac{\partial N_i}{\partial x} C_\ell & 0 & 0 & 0 \end{bmatrix}$$

$$B_{bi}^\ell = \begin{bmatrix} 0 & 0 & 0 & \frac{\partial N_i}{\partial x} S_\ell & 0 \\ 0 & 0 & 0 & 0 & -N_i \frac{\ell \pi}{b} S_\ell \\ 0 & 0 & 0 & N_i \frac{\ell \pi}{b} C_\ell & \frac{\partial N_i}{\partial x} C_\ell \end{bmatrix} \quad (79)$$

$$B_{si}^\ell = \begin{bmatrix} 0 & 0 & \frac{\partial N_i}{\partial x} S_\ell & N_i S_\ell & 0 \\ 0 & 0 & N_i \frac{\ell \pi}{b} C_\ell & 0 & N_i C_\ell \end{bmatrix}$$

are resp. the membrane, bending and shear strain matrix for node  $i$  and the  $\ell$ th harmonic term.

It is worth noting that matrix  $B_i^\ell$  for rectangular folded plates can be directly obtained from the expression for curved folded plates by simply making  $r$  very large so that  $1/r \rightarrow 0$  and by setting  $b' = b$  in (57).

These useful analogies allow all of the relevant matrices for rectangular folded plates to be derived from the corres-

ponding expressions for their curved counterparts[17].

## 7. AXISYMMETRIC SHELLS

The Mindlin formulation for axisymmetric shells closely follows the steps of the formulation for folded plates with curved planforms. In fact, for axisymmetric shells under arbitrary loading the expressions for the displacement, strain and stress fields are identical to those of (38) - (50). Moreover, the Total Potential Energy of the shell can be written in a form which is almost identical to that of (51) - the only difference being that all integrals are taken now over a whole circumference.

Thus, the Mindlin finite strip formulation for axisymmetric shell problems can be considered as another particular case of the curved folded plate formulation (as was the case for rectangular and folded plates) and the basic steps in both formulations are essentially the same.

### 7.1 Mindlin finite strip formulation for axisymmetric shells under arbitrary loading

The shell is divided into circular strips as shown in Figure 1. For axisymmetric shells under arbitrary loading the displacement vector can be expressed within each strip in terms of the symmetrical and non-symmetrical contribution

$$\underline{u} = \sum_{\ell=0}^n \sum_{i=1}^k (N_i^{\ell} \underline{a}_i^{\ell} + \bar{N}_i^{\ell} \bar{\underline{a}}_i^{\ell}) \quad (80)$$

where the displacement vector,  $\underline{u}$ , and nodal parameter vectors  $\underline{a}_i^{\ell}$  and  $\bar{\underline{a}}_i^{\ell}$  are defined by (40) and (54) resp., and

$$N_i^{\ell} = \begin{bmatrix} N_i C_{\ell} & 0 & 0 & 0 & 0 \\ 0 & N_i S_{\ell} & 0 & 0 & 0 \\ 0 & 0 & N_i C_{\ell} & 0 & 0 \\ 0 & 0 & 0 & N_i C_{\ell} & 0 \\ 0 & 0 & 0 & 0 & N_i S_{\ell} \end{bmatrix} \quad (81a)$$

$$\bar{N}_i^{\ell} = \begin{bmatrix} N_i S_{\ell} & 0 & 0 & 0 & 0 \\ 0 & N_i C_{\ell} & 0 & 0 & 0 \\ 0 & 0 & N_i S_{\ell} & 0 & 0 \\ 0 & 0 & 0 & N_i S_{\ell} & 0 \\ 0 & 0 & 0 & 0 & N_i C_{\ell} \end{bmatrix} \quad (81b)$$

are the shape function matrices corresponding to symmetrical and non-symmetrical displacement fields resp. Furthermore,  $S_{\ell} = \sin \ell\theta$  and  $C_{\ell} = \cos \ell\theta$ .

Note that in (80) the harmonic 'zero' has been included. This term has a clear physical meaning and it corresponds to an axisymmetrical deformation.

To simplify the computation it is usual to evaluate the response of the shell to an arbitrary loading as an independent sum of the symmetric and non-symmetric part of the deformation. Thus, for the case in which all loads are symmetric with respect to a plane (which we will take here as that of  $\theta = 0$  for simplicity) only matrix  $N_i^{\ell}$  of (80) will be used.

The study of the non-symmetric part will be identical taking  $\bar{N}_i^{\ell}$  instead of  $N_i^{\ell}$ .

Following precisely the same steps as those explained in Section 4.2 for the curved folded plate case, the decoupled system of stiffness equations for each harmonic term with the stiffness matrix may be obtained and written as

$$[K_{ij}^{\ell}]^e = 2\pi \int_0^{a^e} (\bar{B}_i^{\ell})^T \underline{D} \bar{B}_j^{\ell} r ds \quad \text{for } \ell = 0 \quad (82)$$

$$[K_{ij}^{\ell}]^e = \pi \int_0^{a^e} (B_i^{\ell})^T \underline{D} B_j^{\ell} r ds \quad \text{for } \ell \neq 0$$

where matrix  $\underline{D}$  is given by (49) and matrix  $B_i^{\ell}$  can be written in a general form for the axisymmetric and non-symmetric cases

$$\underline{B}_i^{\ell} = \left[ [\bar{B}_{mi}^{\ell}]^T, [\bar{B}_{bi}^{\ell}]^T, [B_{si}^{\ell}]^T \right]^T \quad (83)$$

where

$$\begin{aligned}
 \tilde{B}_{mi}^{\ell} &= \begin{bmatrix} \frac{\partial N_i}{\partial s} & 0 & 0 & 0 & 0 \\ N_i \frac{\sin \phi}{r} & \frac{N_i}{r} \bar{\ell} & -\frac{N_i}{r} \cos \phi & 0 & 0 \\ -\frac{N_i}{r} \bar{\ell} & \frac{\partial N_i}{\partial s} - \frac{N_i}{r} \sin \phi & 0 & 0 & 0 \end{bmatrix} \\
 \tilde{B}_{bi}^{\ell} &= \begin{bmatrix} 0 & 0 & 0 & \frac{\partial N_i}{\partial s} & 0 \\ 0 & 0 & 0 & \frac{N_i}{r} \sin \phi & \frac{N_i}{r} \bar{\ell} \\ 0 & -\frac{\partial N_i}{\partial r} \frac{\cos \phi}{r} & 0 & -\frac{N_i}{r} \bar{\ell} & \frac{\partial N_i}{\partial s} - \frac{N_i}{r} \sin \phi \end{bmatrix} \quad (84) \\
 \tilde{B}_{si}^{\ell} &= \begin{bmatrix} 0 & 0 & \frac{\partial N_i}{\partial s} & N_i & 0 \\ 0 & \frac{N_i}{r} \cos \phi & -\frac{N_i}{r} \bar{\ell} & 0 & N_i \end{bmatrix}
 \end{aligned}$$

are the membrane bending and shear strain matrices for the  $\ell$ th harmonic with

$$\begin{aligned}
 \bar{\ell} &= \ell && \text{for the symmetric case} \\
 \bar{\ell} &= -\ell && \text{for the non-symmetric case}
 \end{aligned}$$

It is worth pointing out that matrix  $\tilde{B}_i^{\ell}$  can be directly obtained from its analogous expression for curved folded plates by simply substituting in (57) the value of  $\frac{\ell\pi}{\alpha}$  by  $\bar{\ell}$  and making  $S_{\ell} = C_{\ell} = 1$ .

This shows again the versatility of the general formulation of Section 4 and how it allows folded plates, plates and axisymmetric shells to be treated in a unified manner.

The transformation of the strip stiffness matrix into a global coordinate system follows precisely the steps presented in Section 4.3 for curved folded plates with the transformation matrix being identical to that of (67). The transformation will not be repeated here.

The loads are obtained using the method described in Section 4.2 with the following expansions

$$[b, t, p] = \sum_{\ell=0}^n [S_{\ell} b^{\ell}, S_{\ell} t^{\ell}, S_{\ell} p^{\ell}] \quad (85)$$

where

$$S_{\ell} = \begin{bmatrix} C_{\ell} & 0 & 0 & 0 & 0 \\ 0 & S_{\ell} & 0 & 0 & 0 \\ 0 & 0 & C_{\ell} & 0 & 0 \\ 0 & 0 & 0 & C_{\ell} & 0 \\ 0 & 0 & 0 & 0 & S_{\ell} \end{bmatrix} \quad (86)$$

for the symmetric loading case. For the non-symmetric case

$$S_{\ell} = \begin{bmatrix} S_{\ell} & 0 & 0 & 0 & 0 \\ 0 & C_{\ell} & 0 & 0 & 0 \\ 0 & 0 & S_{\ell} & 0 & 0 \\ 0 & 0 & 0 & S_{\ell} & 0 \\ 0 & 0 & 0 & 0 & C_{\ell} \end{bmatrix} \quad (87)$$

Details of the load vector for different loading cases are given in the next section.

If the loading is also axisymmetric the same formulation is directly applicable by simply evaluating the contribution of the zero harmonic term only (i.e.  $\bar{\ell} = 0$  in (84)). However, a simpler formulation can be automatically derived taking into account the contribution of the non-zero displacements  $u$ ,  $w$  and  $\theta_s$  only in matrix  $\tilde{B}_i^0$ . Details of this formulation can be found in reference [24].

## 8. COMPUTATION OF THE EQUIVALENT NODAL FORCE VECTOR

As already mentioned in Section 4.2, the external loads acting over the structure are expanded in the same way as the

displacements, that is as the sum of the harmonic series along the longitudinal/circumferential direction of the structure. Moreover, the form of the Fourier expansions for the loads is the same as that chosen for the corresponding displacements, i.e.

$$\begin{array}{ccc} \text{Displacements} & & \text{Loads} \\ \underline{u} = \sum_{\ell=1}^n \underline{S}^{\ell} \underline{u}^{\ell} & & \underline{f} = \sum_{\ell=1}^n \underline{S}^{\ell} \underline{f}^{\ell} \end{array} \quad (88)$$

where  $\underline{f}^{\ell}$  and  $\underline{S}^{\ell}$  are the load amplitudes vector and the matrix of the harmonic functions for the  $\ell$ th harmonic term resp.

Thus, for the case of a rectangular plate

$$\begin{aligned} \underline{P} &= [P_w, M_{\theta x}, M_{\theta y}]^T = \sum_{\ell=1}^n \underline{S}^{\ell} [P_w^{\ell}, M_{\theta x}^{\ell}, M_{\theta y}^{\ell}]^T = \sum_{\ell=1}^n \underline{S}^{\ell} \underline{P}^{\ell} \\ \underline{t} &= [t_w, M_{\theta x}, M_{\theta y}]^T = \sum_{\ell=1}^n \underline{S}^{\ell} [t_w^{\ell}, M_{\theta x}^{\ell}, M_{\theta y}^{\ell}]^T = \sum_{\ell=1}^n \underline{S}^{\ell} \underline{t}^{\ell} \\ \underline{b} &= [b_w, 0, 0]^T = \sum_{\ell=1}^n \underline{S}^{\ell} [b_w^{\ell}, 0, 0]^T = \sum_{\ell=1}^n \underline{S}^{\ell} \underline{b}^{\ell} \end{aligned} \quad (89)$$

Matrix  $\underline{S}^{\ell}$  can be easily deduced from (59) as

$$\underline{S}^{\ell} = \begin{bmatrix} S_{\ell} & 0 & 0 \\ 0 & S_{\ell} & 0 \\ 0 & 0 & C_{\ell} \end{bmatrix} \quad (90)$$

In (89)  $\underline{P}$ ,  $\underline{t}$  and  $\underline{b}$  are the vectors of point loads, surface loads and body forces loads, resp. The three components of such vectors correspond to the loads associated with the vertical deflection and the two rotations, resp. For the body forces case only the vertical component,  $b_w$ , corresponding to the self weight of the structure per unit area, has been considered.

The load amplitudes are calculated individually using

Euler's formula. For instance for a uniformly distributed vertical load we can write  $q_w^{\ell}$  as

$$q_w^{\ell} = \frac{\int_0^b \sin \frac{\ell\pi}{b} y \, dy}{\int_0^b \sin^2 \frac{\ell\pi}{b} y \, dy} = \frac{2q_w}{\ell\pi} (\ell - \cos \ell\pi) \quad (91)$$

An identical process will be followed for the evaluation of the rest of the loading amplitude terms.

The vector of nodal forces for each strip for the  $\ell$ th harmonic term can be written in a general form for the different structures studied in this chapter using (61) and the property of the orthogonal function  $S_{\ell}$  and  $C_{\ell}$  as

$$\underline{f}_i^{\ell} = C \int_0^{a^e} N_i \underline{b}^{\ell} r \, ds + C \int_0^{a^e} N_i \underline{t}^{\ell} r \, ds + C q_i^{\ell} \quad (92)$$

For plates and folded plates  $C = \frac{L}{2}$  where  $L$  is the length or angle of the structure for the rectangular or curved case, resp. For axisymmetric shells,  $C = 2\pi$  and  $\pi$  for  $\ell = 0$  and  $\ell \neq 0$ , resp. For right structures  $r = 1$  in (92).

In Table 2, the expressions of  $\underline{f}_i^{\ell}$  for three typical loading cases of point load, uniform load and self weight, for plates, folded plates and axisymmetric shells (under symmetric loading) are given. The evaluation of the formulae of Table 2 for different strip elements mentioned in this chapter is simple and only involves the appropriate evaluation of the corresponding integrals for the strip shape functions over the strip length. This can be easily performed using the shape functions expressions of Figure 4, and it is left as an exercise for the reader. More details can be found in references [17] and [25].

LOADING CASE	PLATE	FOLDED PLATE	AXISYMMETRIC SHELL
POINT LOAD acting at node i at y = c	$\begin{Bmatrix} P_x \sin \frac{\pi c}{L} \\ M_{tx} \sin \frac{\pi c}{L} \\ M_{ty} \cos \frac{\pi c}{L} \end{Bmatrix}$ $f_1^i =$	$\begin{Bmatrix} P_x \sin \frac{\pi c}{L} \\ P_y \cos \frac{\pi c}{L} \\ P_z \sin \frac{\pi c}{L} \\ M_{tx} \sin \frac{\pi c}{L} \\ M_{ty} \cos \frac{\pi c}{L} \end{Bmatrix}$ $f_1^i =$	$\begin{Bmatrix} P_{z1} \cos \pi r \\ 0 \\ P_{z1} \cos \pi r \\ M_{ts1} \cos \pi r \\ 0 \end{Bmatrix}$ $f_1^i =$ $r \neq 0$
UNIFORM LOAD acting over the whole element between limits $b_0 \leq y \leq b_1$ ( $b_0 < c < b_1$ for axisymmetric shells)	$\begin{Bmatrix} q_x (\cos \frac{\pi b_1}{L} \cos \frac{\pi b_0}{L} - \cos \frac{\pi b_1}{L}) \\ q_y (\sin \frac{\pi b_1}{L}) \\ q_z (\cos \frac{\pi b_1}{L} - \cos \frac{\pi b_0}{L}) \\ m_{tx} (\cos \frac{\pi b_1}{L} - \cos \frac{\pi b_0}{L}) \\ m_{ty} (\sin \frac{\pi b_1}{L} - \sin \frac{\pi b_0}{L}) \end{Bmatrix}$ $f_1^i = C_1$ $C_1 = \frac{L}{\pi} \int_0^a r N_1(x) dx$	$\begin{Bmatrix} q_x (\cos \frac{\pi b_1}{L} \cos \frac{\pi b_0}{L} - \cos \frac{\pi b_1}{L}) \\ q_y (\sin \frac{\pi b_1}{L}) \\ q_z (\cos \frac{\pi b_1}{L} - \cos \frac{\pi b_0}{L}) \\ m_{tx} (\cos \frac{\pi b_1}{L} - \cos \frac{\pi b_0}{L}) \\ m_{ty} (\sin \frac{\pi b_1}{L} - \sin \frac{\pi b_0}{L}) \end{Bmatrix}$ $f_1^i = C_1$ $C_1 = \frac{L}{\pi} \int_0^a r N_1(x) dx$	$\begin{Bmatrix} q_r \sin \alpha_0 \cos \pi r \\ 0 \\ q_z \sin \alpha_0 \cos \pi r \\ m_{ts} \sin \alpha_0 \cos \pi r \\ 0 \end{Bmatrix}$ $f_1^i = C_1$ $C_1 = \frac{2}{\pi} \int_0^a r N_1 r dr$
SELF WEIGHT $\rho$ = density $E$ = gravity	$\begin{Bmatrix} 1 \\ r N_1(x) dx \\ 0 \\ 0 \end{Bmatrix}$ $f_1^i = \frac{2L \rho g t}{\pi} \int_0^a r N_1(x) dx$ $f_1^i =$ $f_1^e = 0$	$\begin{Bmatrix} 0 \\ 0 \\ 1 \\ 0 \\ 0 \end{Bmatrix}$ $f_1^i = \frac{2L \rho g t}{\pi} \int_0^a r N_1(x) dx$ $f_1^e =$ $f_1^s =$	$\begin{Bmatrix} 0 \\ 0 \\ 1 \\ 0 \\ 0 \end{Bmatrix}$ $f_1^i = 2 \rho g t \int_0^a r N_1 r dr$ $f_1^e = 0$

TABLE 2 EXPRESSIONS FOR THE LOAD FORCE VECTOR FOR NODE i FOR THE NTH HARMONIC TERM

9. THE REDUCED INTEGRATION FAMILY OF MINDLIN STRIP ELEMENTS FOR FOLDED PLATE AND AXISYMMETRIC SHELL ANALYSIS

The behaviour of Mindlin strip elements for folded plate or axisymmetric shell analysis is analogous to that explained in Section 3.4 for the plate case, i.e. the optimum performance of all strip elements occurs when selective or reduced integration is used. The Gaussian quadratures for the different integration rules for the linear, quadratic and cubic elements for the folded plate formulation presented in the last section are identical to those presented in Table 1. Moreover, it has been shown by Suarez[25] and Onate and Suarez[17,18] that the linear strip with reduced integration (one single Gaussian point for all integrals) has an excellent performance in practical folded plate and axisymmetric shell problems. Indeed, useful 'explicit' expressions for all element matrices can be obtained by simply evaluating all integrals at the strip mid-point[17]. The accuracy of the reduced integration linear strip will be shown in the examples which are now presented.

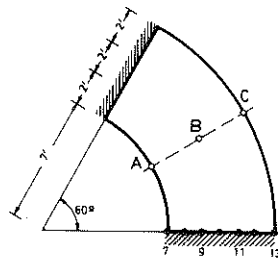
10. EXAMPLES

10.1 Example 1: Curved simply supported plate

In this example a curved thin plate simply supported at the two ends is subjected to a point load. Both experimental and numerical results are available for the plate.

The geometry of the plate, material properties, loading position and finite strip mesh used in the analysis are given in Figure 15. Results for the mid-span deflections obtained with the reduced integration linear element using six non-zero harmonic terms can be seen in the same figure where experimental and theoretical results obtained by Coull and Das[26], finite strip solutions based on Kirchhoff's theory obtained by Thorpe[27] and Cheung[12], and finite element solutions reported by Sawko and Meriman[28] and Fam and Turkstra[29] for the same problem are also shown for comparison. The solution obtained using the linear strip element is accurate.





12 Elements

6 Non zero harmonics

 $E = 42,460 \text{ lb/inch}^2$  $\nu = 0.3$  $t = 0.172'$ 

Loading : Point load of 1 lb acting in A,B,y C

		VERTICAL DEFLECTION (IN.)							
Loading Position	Rad.	COULL & DAS		FINITE STRIP			FINITE ELEMENT		
	inc.	Experi.	Theor.	Thorpe	Cheung	*	Sawko	Fam & Turkstra	
A	13	0.876	0.752	0.882	0.995	0.874	0.851	0.880	0.881
	11	0.578	0.500	0.582	0.624	0.581	0.559	0.577	0.578
	9	0.353	0.300	0.356	0.388	0.357	0.344	0.359	0.354
	7	0.194	0.180	0.195	0.206	0.194	0.192	0.193	0.194
B	13	0.457	0.470	0.459	0.441	0.460	0.445	0.446	0.457
	11	0.342	0.370	0.343	0.329	0.348	0.333	0.342	0.343
	9	0.241	0.250	0.242	0.222	0.247	0.236	0.241	0.241
	7	0.155	0.170	0.155	0.147	0.158	0.154	0.154	0.158
C	13	0.195	0.150	0.195	0.180	0.195	0.192	0.193	0.194
	11	0.163	0.135	0.165	0.152	0.167	0.162	0.163	0.164
	9	0.157	0.125	0.153	0.149	0.155	0.151	0.151	0.151
	7	0.169	0.145	0.170	0.173	0.170	0.170	0.169	0.169
Reference		26		27	12		28		29

\* LINEAR MINDLIN STRIP ELEMENT

REDUCED INTEGRATION

Fig 15 Slab model of Coull and Das : Results for the deflection along ABC obtained by several authors.

### 10.2 Example 2: Right bridge - Simple supported concrete slab/beam bridge over the motorway - Nueve de Julio (Buenos Aires)

This example shows the adequacy of the linear strip element for practical bridge deck analysis. The example chosen is one of the bridges of the urban motorway, Nueve de Julio actually under construction in the city of Buenos Aires (Argentina). The geometry of the structure, loading position, material properties and finite strip discretisation used in the analysis can be seen in Figure 16. Numerical results for the vertical deflection, transverse bending moment and longitudinal resultant stress in the slab at the mid section obtained with 15 non-zero harmonic terms are plotted in Figure 17. The corresponding diagrams shown in the same figure are extrapolated from the finite strip results which are marked with a circle. To assess the validity of the numerical solution, an equilibrium check was performed comparing the total longitudinal bending moment in the mid-span section with the value obtained using simple beam theory. The percentage of error obtained is less than 5%, which can be considered as good for practical design purposes.

### 10.3 Example 3: Simply supported curved box girder bridge

The geometry of the structure, material properties and finite strip mesh of 18 linear strip elements (with reduced integration) used in the analysis can be seen in Figure 18. This problem has also been analysed by Cheung[16] using a Kirchhoff strip formulation. Results for the horizontal and vertical displacements of the mid-span section for three different positions of the point load are shown in Figure 19. In Figure 20 the axial circumferential stress resultant and the radial and circumferential bending moments are plotted together with some of Cheung's results which are shown for comparison. A total of 15 non-zero harmonic terms were used in the analysis.

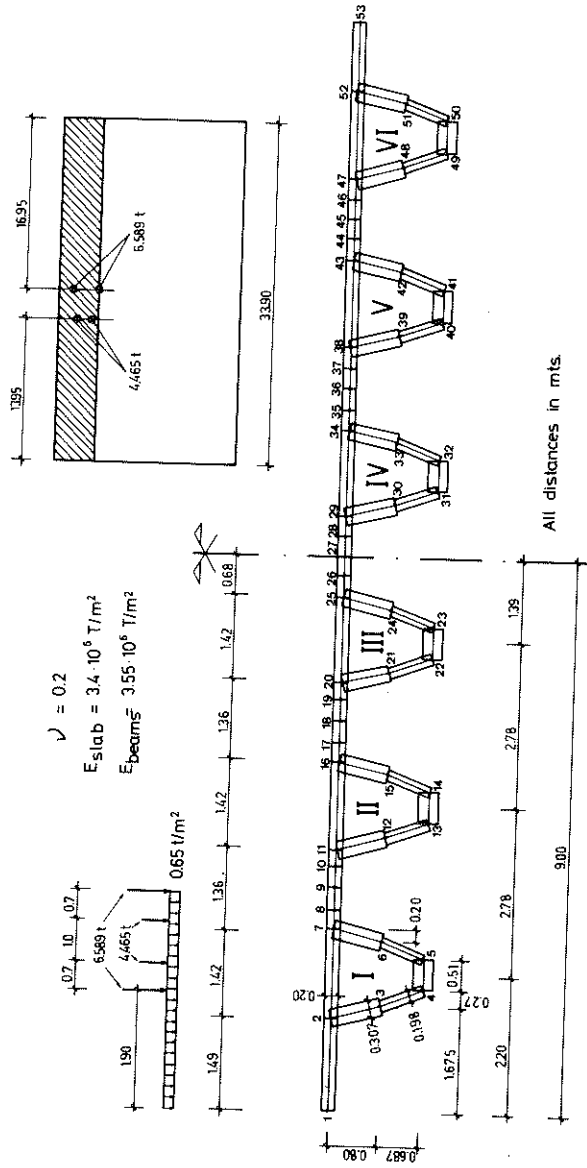


FIG. 16: Simple supported concrete bridge: Geometry of structure, loading position and idealisation into two noded finite strips.

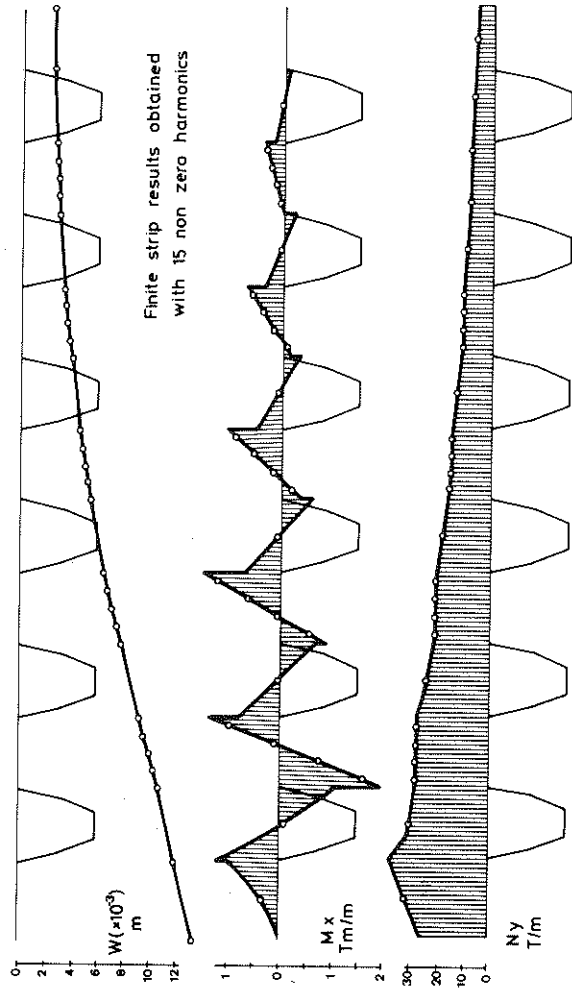


Fig. 17 Curves for the deflection,  $W$ , transverse bending moment,  $M_x$ , and longitudinal resultant stress,  $N_y$ , in the slab at the bridge mid section.

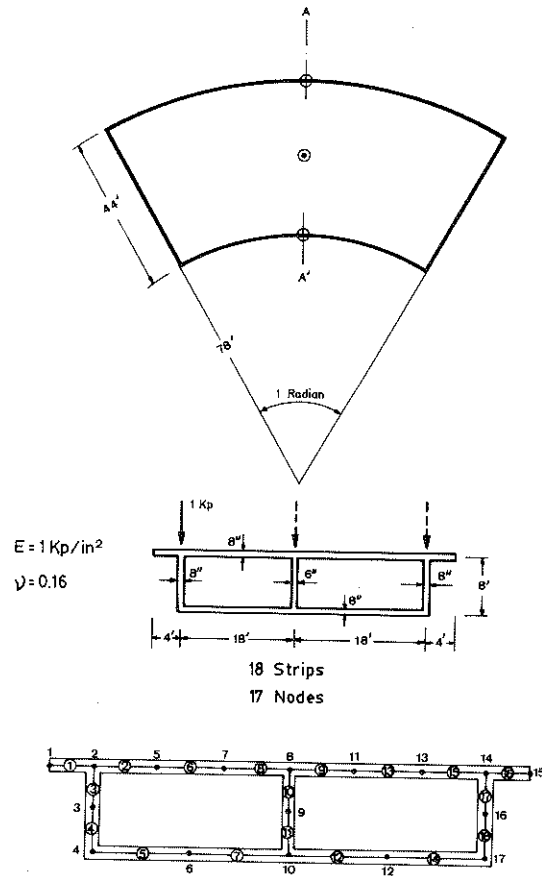


Fig 18 Curved box girder bridge. Geometry of the structure and finite strip idealisation into 18 strips.

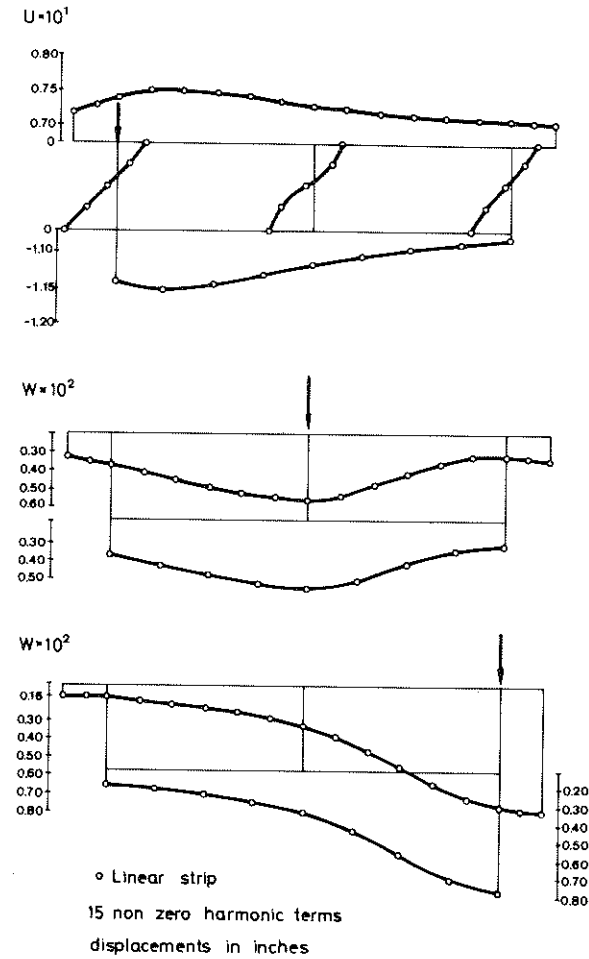


Fig. 19 Curved box girder bridge: Displacements at the mid section for several loading positions.

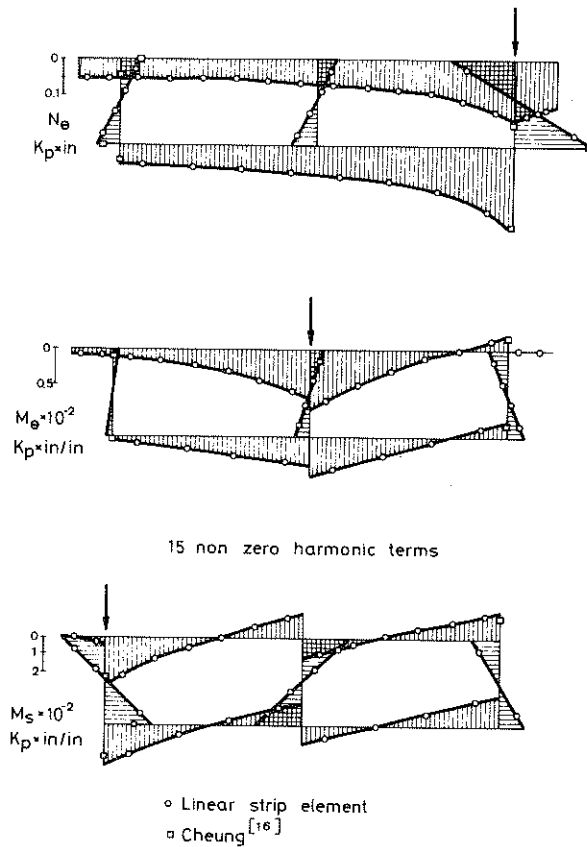


Fig. 20 Curved box girder bridge. Circumferential resultant stress,  $N_\theta$ , and bending moments  $M_s$  and  $M_\theta$  at the central section.

#### 10.4 Example 4: Circular plate under an eccentric point load

The fourth example is a thin circular plate subjected to a point load acting at a certain distance from the centre of the plate. The example is fully described in Figure 21 where results for the deflection and radial bending moment along several sections obtained with the linear axisymmetric element and with a mesh of 8-noded isoparametric reduced integrated Mindlin plate finite elements are shown for comparison. The Timoshenko[21] "exact" thin plate solution for the deflection under the load is also plotted. The accuracy of the linear element is again good.

#### 10.5 Example 5: Pinched cylindrical shell

The last example is the classical thin cylindrical shell under two diametrically opposed point loads. The cylinder has rigid diaphragms at the two end sections (see Figure 22). This example, well-known in the shell literature, has been solved by several authors. Amongst others, there is an "exact" analytical double series solution due to Flugge[32]. Finite element solutions have been reported by Oñate et. al.[31], Lindberg et. al.[32], Ahmad et. al.[33] and many others. The solution presented here is probably the simplest one using only 20 linear axisymmetric shell elements. Nevertheless, it is highly accurate as demonstrated in Figure 22 where results obtained with the linear element for the displacements and axial forces along several sections using 15 non-zero harmonic terms compare well with the more sophisticated analytical and finite element solutions.

### 11. COMPUTER IMPLEMENTATION OF THE FINITE STRIP METHOD

In this section the general lay-out of a computer program for analysis of prismatic structures by the finite strip method will be presented. Also, a detailed computer listing of a finite strip program for the analysis of right or curved Mindlin

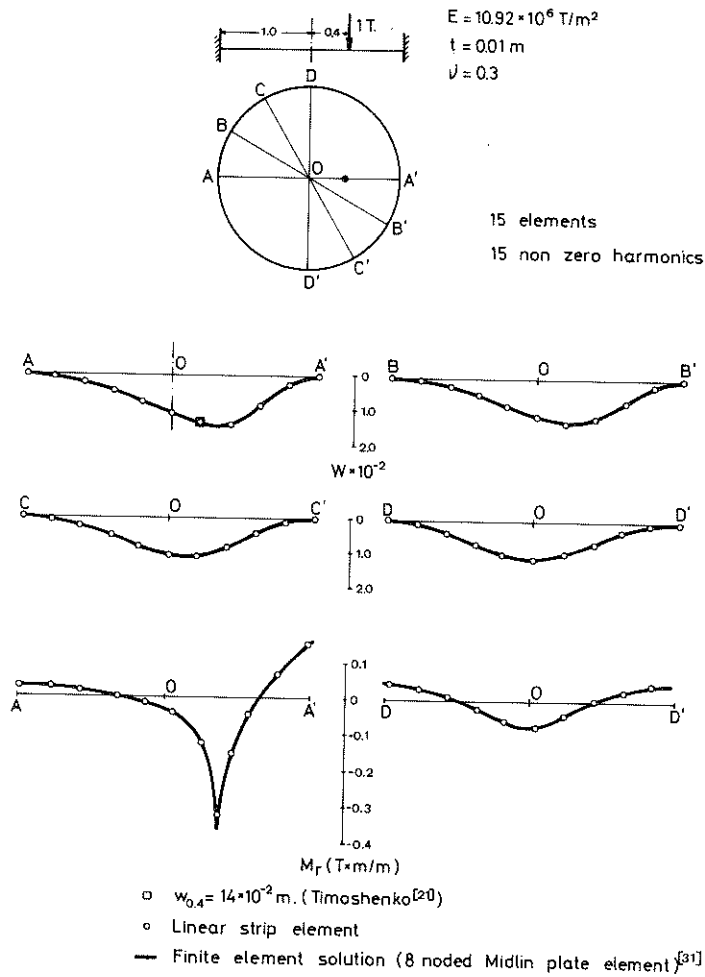


Fig. 21 Circular thin plate under point load. Vertical deflections  $w$ , and radial bending moment,  $M_r$ , distributions along several sections.

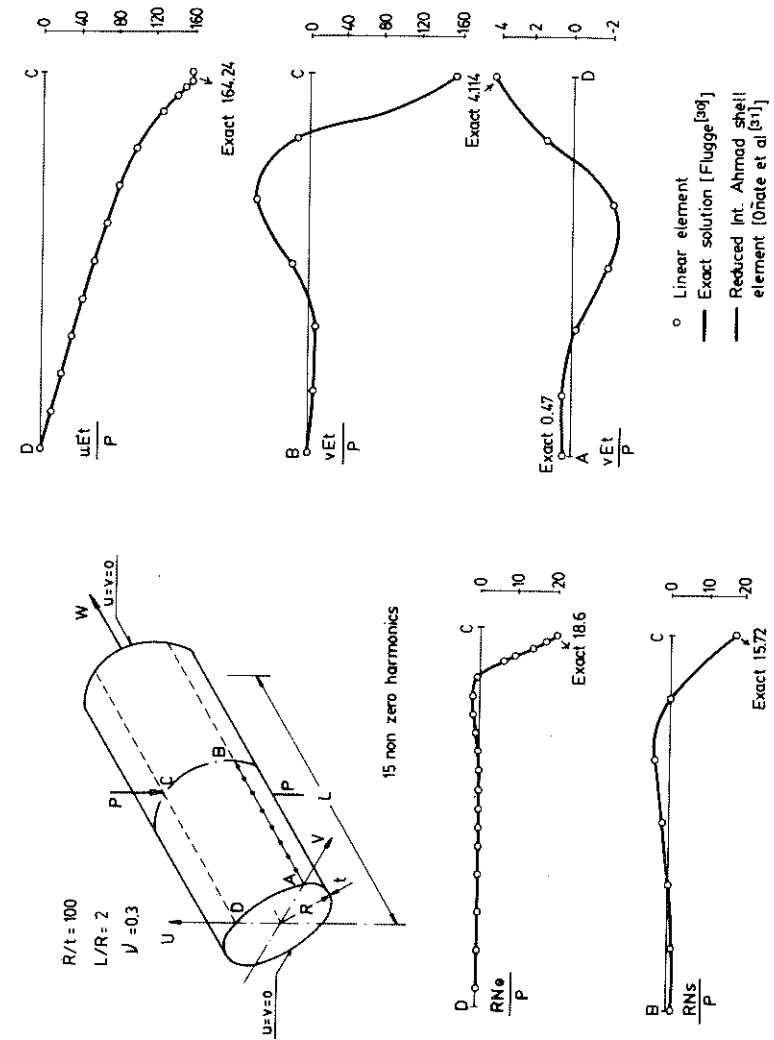


Fig. 22 Pinched cylindrical shell. Displacements and axial forces along several sections.

plates will be provided together with some examples and user's instructions.

We will adopt here the notation used by Hinton and Owen [34] for the definition of the program variables and sub-routines. Details of such a notation can be found in reference [34] and will not be given here. Also, details of standard subroutines, like that of solution of the system of linear equations by the frontal method which can also be found in references [34] and [35], will be omitted.

#### Program lay-out

Figure 23 shows the flow chart of a standard finite strip program. It can be seen that the construction of a finite strip program falls into four well-defined phases.

#### Phase 1 - Definition of data input

One of the advantages of the finite strip method is that relatively little data is needed compared with that required with the finite element method. Input data for a finite strip program is equivalent to that needed for a standard computer program for the analysis of framed structures. The subroutine controlling the input data is named INPUT.

#### Phase 2 - Stiffness and stress matrices and applied load vector generation for each harmonic term

The strip stiffness and stress matrices are calculated in subroutine STIFFS. The load vector is evaluated in subroutine LOADFS. Both subroutines are within a loop which implies that the calculations are performed for each harmonic term of the series used in the definition for the displacement field.

[Note that after subsequent solution for the nodal displacement amplitudes for each harmonic term, the strip stress matrices are employed in the evaluation of the stress resultants for that harmonic. This task is performed in subroutine STREFS.]

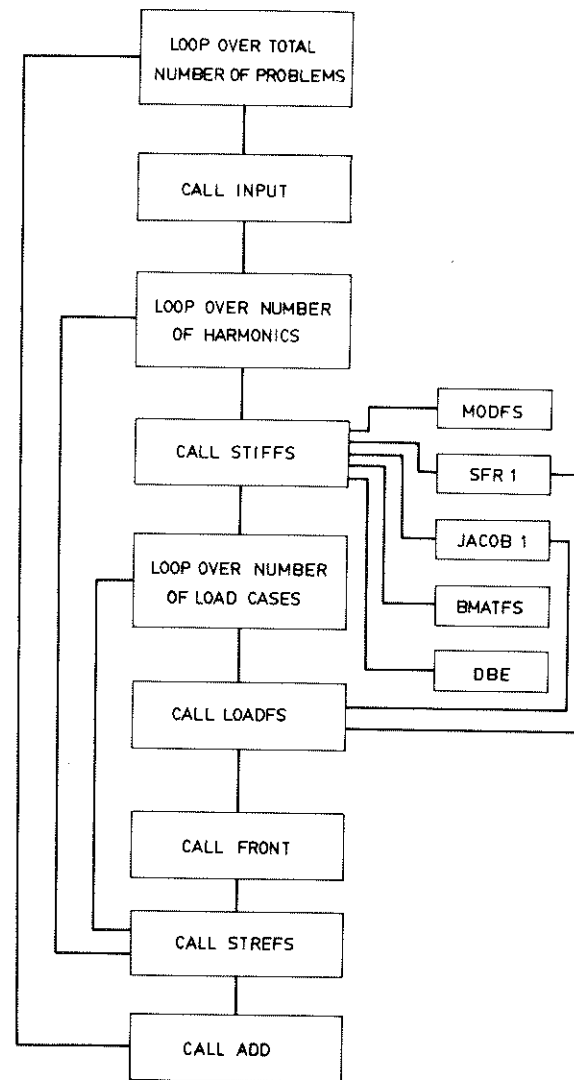


FIG. 23 FLOW CHART OF PROGRAM PBSTRIP

### Phase 3 - Solution of the stiffness equations for each

#### harmonic term

Subroutine FRONT is the equation solution subroutine which assembles the strip stiffness equations for each harmonic term and solves the unknown displacement amplitudes for the current harmonic using the frontal elimination technique [34,35].

### Phase 4 - Summation of displacement and stresses for all

#### harmonics

Subroutine ADD sums the contribution of all harmonic terms to evaluate the nodal displacements and stress resultants at any point in the structure.

The different phases of the program will be detailed in the following sections. As an example, and for the sake of clarity, all phases will be described for a plate bending finite strip program. The FORTRAN computer listing is also given. However, most steps in such a program are completely general and applicable to the different structures studied in this chapter.

## 12. PROGRAM PBSTRIP FOR THE ANALYSIS OF RIGHT OR CURVED PLATES BY THE FINITE STRIP METHOD

In this section the different phases of the finite strip program introduced earlier will be described for the particular case of a program for analysis of right and curved plates using any of the reduced integration family of Mindlin plate strip elements studied in Section 3. Most subroutines of the program are equally valid for direct use in more general finite strip programs for analysis of folded plates or axisymmetric shell structures. This point will be stressed throughout the following sections.

### 12.1 Main segment

A listing of the master segment of the program is now given. This is followed in Table 2 with a Nassi-Schneiderman (NS)-chart which describes the main segment.

```

C MASTER PBSTRIP
DIMENSION ADISP(3,40),AFORC(5,4,20),ASDIS(120),COORD(40,1),
.DISP(120),DIZPL(120),EFORC(400),ELOAD(20,12),FORCE(400),
.IFPRE(2,3),LNODS(20,4),MATNO(20),NOFIX(2),POSGP(4),PRESC(2,3),
.PROPS(20,5),TITLE(18),WEIGP(4)
MAIN 1
MAIN 2
MAIN 3
MAIN 4
MAIN 5
MAIN 6
C DIMENSION STATEMENTS ASSOCIATED WITH FRONTAL SOLUTION
MAIN 7
C
C DIMENSION EQRHS(1),EQUAT(12,1),FIXED(120),GLOAD(12),
.GSTIF(72),IFFIX(120),NACVA(12),NAMEV(1),NPIVO(1),VECRV(12)
MAIN 8
MAIN 9
MAIN 10
DATA MELEM/20/,MFACT/400/,MMATS/20/,MPOIN/40/,MTOTV/120/
MAIN 11
C
C DATA STATEMENT ASSOCIATED WITH FRONTAL SOLUTION ARRAYS
MAIN 12
MAIN 13
MAIN 14
DATA MBUFA/1/,MFRON/12/,MSTIF/72/,MVFIX/2/
MAIN 15
C *****
MAIN 16
C
C PROGRAM FOR THE ANALYSIS OF RIGHT AND CURVED PLATES
MAIN 17
C BY THE MINDLIN FINITE STRIP METHOD USING LINEAR, *
C QUADRATIC OR CUBIC STRIP ELEMENTS WITH FULL, REDUCED OR *
C SELECTIVE INTEGRATION *
MAIN 18
MAIN 19
MAIN 20
MAIN 21
C *****
MAIN 22
C
C READ(5,900) NPROB
MAIN 23
900 FORMAT(I5)
MAIN 24
WRITE(6,905) NPROB
MAIN 25
905 FORMAT(// 5X,'NUMBER OF PROBLEMS TO BE SOLVED=' ,I3)
MAIN 26
DO 40 IPROB=1,NPROB
MAIN 27
REWIND 7
MAIN 28
REWIND 8
MAIN 29
READ(5,910) TITLE
MAIN 30
910 FORMAT(18A4)
MAIN 31
WRITE(6,915) IPROB,TITLE
MAIN 32
915 FORMAT(//,,, 6X,12HPROBLEM NO. ,I3,10X,18A4)
MAIN 33
READ(5,920) NHARM,NSYME
MAIN 34
920 FORMAT(2I5)
MAIN 35
WRITE(6,925) NHARM,NSYME
MAIN 36
925 FORMAT(//, ' NUMBER OF HARMONIC TERMS TO BE USED =' ,I5,
MAIN 37
MAIN 38
MAIN 39
MAIN 40
C
C *****
C *** CALL THE SUBROUTINE WHICH READS MOST OF THE PROBLEM DATA.
MAIN 41
C
C CALL INPUT(COORD,IFPRE,LNODS,MATNO,MELEM,MMATS,MPOIN,MVFIX,
MAIN 42
MAIN 43
MAIN 44
MAIN 45
MAIN 46
MAIN 47
C
C *****
C *** LOOP OVER ALL THE HARMONICS
MAIN 48
C
C DO 30 IHARM=1,NHARM,NSYME
MAIN 49
REWIND 1
MAIN 50
REWIND 2
MAIN 51
REWIND 3
MAIN 52
REWIND 4
MAIN 53
REWIND 5
MAIN 54
REWIND 6
MAIN 55
C
C *****
C *** NEXT CREATE THE STRIP ELEMENT STIFFNESS FILE FOR EACH
MAIN 56
C *** HARMONIC
MAIN 57
C
C CALL STIFFS(COORD,IHARM,LNODS,MATNO,MELEM,MMATS,MPOIN,MELEM,
MAIN 58
MAIN 59
MAIN 60
MAIN 61
MAIN 62
DO 20 ICASE=1,NCASE
MAIN 63
C
C *****
C *** COMPUTE LOADS, FOR EACH HARMONIC, AFTER READING THE RELEVANT
MAIN 64
C *** EXTRA DATA
MAIN 65
C
C CALL LOADFS(COORD,ELOAD,ICASE,IHARM,LNODS,MATNO,MELEM,MMATS,
MAIN 66
MAIN 67
MAIN 68
MAIN 69
MAIN 70
MAIN 71
C *****
C *** MERGE AND SOLVE THE RESULTING EQUATIONS BY THE FRONTAL SOLVER
MAIN 72
C *** FOR EACH HARMONIC
MAIN 73
C
C CALL FRONT(ASDIS,ELOAD,EQRHS,EQUAT,FIXED,GLOAD,GSTIF,ICASE,
MAIN 74
MAIN 75
MAIN 76
MAIN 77
MAIN 78
MAIN 79
MAIN 80

```

```

C
C*** WRITE IN DISC DISPLACEMENTS FOR EACH HARMONIC
C
      WRITE(7) (ASDIS(IGASH),IGASH=NGISH,NGASH)
10 CONTINUE
C
C*** COMPUTE THE STRESSES IN ALL THE STRIPS FOR EACH HARMONIC
C
      CALL STREFS(ASDIS, LNODS, MELEM, MTOTV, NDOFN, NELEM, NGAUS, NNODE,
      .NSTRE)
20 CONTINUE
30 CONTINUE
C
C*** SUM DISPLACEMENTS AND STRESSES FOR ALL HARMONICS
C
      CALL ADD (ADISP, AFORC, DISPL, DIZPL, EFORC, FORCE, MELEM, MFACT, MPOIN,
      .MTOTV, NCASE, NDOFN, NELEM, NGAUS, NHARM, NPOIN, NSTRE, NSYME, TLENG)
40 CONTINUE
      STOP
      END
      MAIN 81
      MAIN 82
      MAIN 83
      MAIN 84
      MAIN 85
      MAIN 86
      MAIN 87
      MAIN 88
      MAIN 89
      MAIN 90
      MAIN 91
      MAIN 92
      MAIN 93
      MAIN 94
      MAIN 95
      MAIN 96
      MAIN 97
      MAIN 98
      MAIN 99
      MAIN 100

```

Set of maximum dimensions and read and write number of problems. MAIN 11-27	1
Loop over number of problems. MAIN 28	2
Rewind tapes for displacements and stresses. MAIN 29-30	3
Read and write problem title and data. MAIN 31-40	4
Call INPUT to read input data. MAIN 44-46	5
Loop over number of harmonics. MAIN 50	6
Rewind tapes 1-4,9. MAIN 51-55	7
Call STIFFS to evaluate element stiffness. MAIN 60-61	8

A

Table 2 Nassi-Schneiderman (NS) chart for main segment of PBSTRIP

Loop over each load case. MAIN 62	9
Evaluate load vector by calling LOADFS. MAIN 67-69	10
Call FRONT to solve for unknowns. MAIN 74-77	11
Write displacements to peripheral storage device 7. MAIN 78-85	12
Call STREFS to evaluate stress resultants for current harmonic. MAIN 89-90	13
Call ADD to sum displacements and stress resultants for all harmonics and then write our results. MAIN 96-97	14

Table 2 Nassi-Schneiderman (NS) chart for main segment of PBSTRIP

## 12.2 Input data subroutine INPUT

The input data for a finite strip program can be subdivided into three main classifications. Firstly, the data required to define the geometry of the structure and the support conditions must be supplied. Secondly, the properties of the constituent materials must be specified and finally, the applied loading must be defined.

The input data subroutine presented in this section is concerned with the geometrical and constitutive properties only. All the loading data is supplied in subroutine LOADFS. Subroutine INPUT, as presented here, can be used for any of the





Read and write the control parameters and define some further parameters. INPU 12-34	1.
Read and write the strip number, NUMEL, nodal connection numbers LNODS (NUMEL, INODE), and material identification number MATNO (NUMEL) for each strip. INPU 38-44	2.
Initialise nodal coordinates array COORD and then read and write node number IPOIN and coordinates COORD (IPOIN,1) for each node. INPU 48-63	3.
For prescribed nodes, read and write the prescribed node number, NVFIX (IVFIX), the prescribed degree of freedom indicator IFPRE (IVFIX, IDOFN) and the prescribed values PRESC (IVFIX, IDOFN) for each degree of freedom IDOFN. INPU 64-79	4.
Read and write the material properties PROPS (NUMAT, IPROP) for each individual material NUMAT. INPU 83-91	5.

Table 3 NS chart for subroutine INPUT

### 12.3 Stiffness matrix subroutine STIFFS

The purpose of this subroutine is to evaluate the stiffness and stress matrices for each strip and for each harmonic terms of the series. Both matrices are stored on disc file for subsequent use in the equation solution subroutine FRONT, and in the subroutine STREFS to compute the stress resultants resp. A NS chart describing STIFFS is provided in Table 4.

```

SUBROUTINE STIFFS (COORD, IHARM, LNODS, MATNO, MELEM, MMATS, MPOIN,
.NELEM, NEVAB, NGAUB, NGAUS, NNODE, NSTRE, NTYPE, POSGP, PROPS, TLENG,
.WEIGP)
STIF 1
.NELEM, NEVAB, NGAUB, NGAUS, NNODE, NSTRE, NTYPE, POSGP, PROPS, TLENG,
STIF 2
.WEIGP)
STIF 3
DIMENSION BMATX(5,12), CARTD(1,4), COORD(MPOIN,1), DBMAT(5,12),
STIF 4
.DERIV(1,4), DMATX(5,5), ELCOD(1,4), ESTIF(12,12), GPCOD(1,4),
STIF 5
.LNODS(MELEM,4), MATNO(MELEM), POSGP(4), PROPS(MMATS,5), SHAPE(4),
STIF 6
.SMATX(5,12,4), WEIGP(4)
STIF 7
C
STIF 8
C*** EVALUATION OF THE STIFFNESS MATRIX FOR THE
STIF 9
C*** LINEAR, QUADRATIC OR CUBIC STRIP ELEMENT
STIF 10
C
STIF 11
C
STIF 12
C*** LOOP OVER EACH ELEMENT
STIF 13
C
STIF 14
DO 55 IELEM=1, NELEM
STIF 15
LPROP=MATNO(IELEM)
STIF 16
DO 5 INODE=1, NNODE
STIF 17
LNODE=LNODS(IELEM, INODE)
STIF 18
ELCOD(1, INODE)=COORD(LNODE,1)
STIF 19
5 CONTINUE
STIF 20
C
STIF 21
C*** EVALUATE THE D-MATRIX
STIF 22
C
STIF 23
CALL MODPB(DMATX, LPROP, MMATS, NSTRE, PROPS)
STIF 24
C
STIF 25
C*** INITIALIZE THE ELEMENT STIFFNESS MATRIX
STIF 26
C
STIF 27
DO 10 IEVAB=1, NEVAB
STIF 28
DO 10 JEVAB=1, NEVAB
STIF 29
10 ESTIF(IEVAB, JEVAB)=0.0
STIF 30
KGASP=0
STIF 31
CALL GAUSSQ(NGAUB, POSGP, WEIGP)
STIF 32
C
STIF 33
C*** FULL OR SELECTIVE INTEGRATION FOR BENDING (NO. GAUSS POINTS=NGAUB)
STIF 34
C
STIF 35
DO 25 IGAUS=1, NGAUB
STIF 36
KGASP=KGASP+1
STIF 37
EXISP=POSGP(IGAUS)
STIF 38
CALL SFR1(DERIV, EXISP, NNODE, SHAPE)
STIF 39
CALL JACOB1(CARTD, DERIV, DJACB, ELCOD, GPCOD, IELEM, KGASP,
STIF 40
.NNODE, SHAPE)
STIF 41
DLENG=DJACB*WEIGP(IGAUS)
STIF 42
CALL BMATFS(BMATX, CARTD, GPCOD, IGAUS, IHARM, NEVAB, NNODE, NSTRE,
STIF 43
.NTYPE, SHAPE, TLENG)
STIF 44
CALL DBE(BMATX, DBMAT, DMATX, NEVAB, NSTRE)
STIF 45
KSTRE=NSTRE-2
STIF 46
DO 20 IEVAB=1, NEVAB
STIF 47
DO 20 JEVAB=IEVAB, NEVAB
STIF 48
DO 20 ISTRE=1, KSTRE
STIF 49
IF(NTYPE.EQ.2) GO TO 15
STIF 50
ESTIF(IEVAB, JEVAB)=ESTIF(IEVAB, JEVAB)+BMATX(ISTRE, IEVAB)*
STIF 51
.DBMAT(ISTRE, JEVAB)*DLENG*TLENG/2.0
STIF 52
GO TO 20
STIF 53
15 ESTIF(IEVAB, JEVAB)=ESTIF(IEVAB, JEVAB)+GPCOD(1, IGAUS)
STIF 54
.*BMATX(ISTRE, IEVAB)*DBMAT(ISTRE, JEVAB)*DLENG*TLENG/2.0
STIF 55
20 CONTINUE
STIF 56
25 CONTINUE
STIF 57
C
STIF 58
C*** REDUCED INTEGRATION FOR SHEAR TERMS (NO. GAUSS POINTS=NGAUS)
STIF 59
C
STIF 60
CALL GAUSSQ(NGAUS, POSGP, WEIGP)
STIF 61
C
STIF 62
C*** ENTER LOOPS FOR AREA NUMERICAL INTEGRATION
STIF 63
C
STIF 64
KGASP=0
STIF 65
DO 45 IGAUS=1, NGAUS
STIF 66
KGASP=KGASP+1
STIF 67
EXISP=POSGP(IGAUS)
STIF 68
CALL SFR1(DERIV, EXISP, NNODE, SHAPE)
STIF 69
CALL JACOB1(CARTD, DERIV, DJACB, ELCOD, GPCOD, IELEM, KGASP,
STIF 70
.NNODE, SHAPE)
STIF 71
DLENG=DJACB*WEIGP(IGAUS)
STIF 72
CALL BMATFS(BMATX, CARTD, GPCOD, IGAUS, IHARM, NEVAB, NNODE, NSTRE,
STIF 73
.NTYPE, SHAPE, TLENG)
STIF 74
CALL DBE(BMATX, DBMAT, DMATX, NEVAB, NSTRE)
STIF 75
LSTRE=NSTRE-1
STIF 76
DO 35 IEVAB=1, NEVAB
STIF 77
DO 35 JEVAB=IEVAB, NEVAB
STIF 78
DO 35 ISTRE=LSTRE, NSTRE
STIF 79
IF(NTYPE.EQ.2) GO TO 30
STIF 80

```

```

C
C*** STRAIGHT PLATE
C
ESTIF(IEVAB,JEVAB)=ESTIF(IEVAB,JEVAB)+BMATX(ISTRE,IEVAB)*DBMAT
.(ISTRE,IEVAB)*DLENG*TLENG/2.0
GO TO 35
C
C*** CURVED PLATE
C
30 ESTIF(IEVAB,JEVAB)=ESTIF(IEVAB,JEVAB)+GPCOD(1,IGAUS)*BMATX(
.ISTRE,IEVAB)*DBMAT(ISTRE,JEVAB)*DLENG*TLENG/2.0
35 CONTINUE
C
C*** STORE THE COMPONENTS OF THE DB MATRIX FOR THE ELEMENT
C
DO 40 ISTRE=1,NSTRE
DO 40 IEVAB=1,NEVAB
40 SMATX(ISTRE,IEVAB,KGASP)=DBMAT(ISTRE,IEVAB)
45 CONTINUE
C
C*** CONSTRUCT THE LOWER TRIANGLE OF THE STIFFNESS MATRIX
C
DO 50 IEVAB=1,NEVAB
DO 50 JEVAB=1,NEVAB
50 ESTIF(JEVAB,IEVAB)=ESTIF(IEVAB,JEVAB)
C
C*** STORE THE STIFFNESS MATRIX,STRESS MATRIX AND SAMPLING
C*** POINT COORDINATES FOR EACH ELEMENT ON DISC FILE
C
WRITE(1) ESTIF
WRITE(3) SMATX,GPCOD
55 CONTINUE
RETURN
END
STIF 81
STIF 82
STIF 83
STIF 84
STIF 85
STIF 86
STIF 87
STIF 88
STIF 89
STIF 90
STIF 91
STIF 92
STIF 93
STIF 94
STIF 95
STIF 96
STIF 97
STIF 98
STIF 99
STIF 100
STIF 101
STIF 102
STIF 103
STIF 104
STIF 105
STIF 106
STIF 107
STIF 108
STIF 109
STIF 110
STIF 111
STIF 112
STIF 113
STIF 114

```

Loop over each strip IELEM. STIF 15	1
Identify the material set number for current strip. STIF 16	2
Extract nodal coordinates for current strip. STIF 17-20	3
Call MODPB to evaluate matrix $\underline{D}$ for the strip. STIF 24	4
Initialise (zero) stiffness matrix array and Gauss point counter. STIF 28-31	5
Call GAUSSQ to set the Gauss-Legendre quadrature parameters for bending. STIF 32	6

A

Table 4 NS chart for subroutine STIFFS

Loop over bending Gauss points. STIF 36	7
Increment Gauss point counter, extract sampling position and call SFR1 to evaluate shape function $N_i$ and local derivatives $\partial N_i / \partial \xi$ . STIF 37-39	8
Call JACOBI to evaluate $\partial N_i / \partial x$ and then dx. STIF 40-42	9
Call BMATFS to evaluate strain matrix. STIF 43-44	10
Call DBE to evaluate stress matrix. STIF 45	11
Accumulate contributions to the strip stiffness matrix for either right or curved plates. STIF 47-57	12
Call GAUSSQ to set the Gauss-Legendre quadrature parameters for shear. STIF 61	13
Zero Gauss point counter. STIF 65	14
Loop over shear Gauss points. STIF 66	15
Increment Gauss point counter, extract sampling coordinate and call SFR1 to evaluate shape function $N_i$ and local derivatives $\partial N_i / \partial \xi$ . STIF 67-69	16

B

Table 4 NS chart for subroutine STIFFS

B	
Call JACOBI to evaluate $\partial N_i / \partial x$ and then dx. STIF 70-72	17
Call BMATFS to evaluate strain matrix. STIF 73-74	18
Call DBE to evaluate stress matrix. STIF 75	19
Accumulate contributions to the strip stiffness matrix for either right or curved plates. STIF 76-92	20
Extract components of the stress matrix for later use. STIF 96-99	21
Construct lower triangular part of strip stiffness matrix. STIF 103-105	22
Store on peripheral storage devices stiffness matrix, stress matrix and sampling point coordinates for each strip. STIF 110-112	23

Table 4 NS chart for subroutine STIFFS

The computer listing of STIFFS, provided above for the plate case, can be of direct use for folded plate of axisymmetric shell programs with the only (conceptual) difference being that for the axisymmetric shell case matrix  $B_i^{*l}$  of (57), relating local strains with global displacements, should be used instead of matrix  $B_i^l$  of (26). Also, the matrix  $D$  of (49) would substitute  $\underline{D}$  of (18), used in the plate program.

## 12.4 Subroutines used by STIFFS

## 12.4.1 Subroutine MODFS

This subroutine calculates the matrix of plate rigidities  $\underline{D}$  given in (18) and (19)

```

SUBROUTINE MODPB(DMATX,LPROP,MHATS,NSTRE,PROPS)
DIMENSION DMATX(5,5),PROPS(MHATS,5)
C
C*** EVALUATE D MATRIX
C
DO 5 ISTR=1,NSTRE
DO 5 JSTR=1,NSTRE
DMATX(ISTR,JSTR)=0.0
5 CONTINUE
YOUNG=PROPS(LPROP,1)
POISS=PROPS(LPROP,2)
THICK=PROPS(LPROP,3)
DMATX(1,1)=YOUNG*THICK*THICK/((12.0*(1.0-POISS*POISS))
DMATX(1,2)=POISS*DMATX(1,1)
DMATX(2,2)=DMATX(1,1)
DMATX(2,1)=DMATX(1,2)
DMATX(3,3)=(1.0-POISS)*DMATX(1,1)/2.0
DMATX(4,4)=YOUNG*THICK/(2.4*(1.0+POISS))
DMATX(5,5)=DMATX(4,4)
RETURN
END
MODP 1
MODP 2
MODP 3
MODP 4
MODP 5
MODP 6
MODP 7
MODP 8
MODP 9
MODP 10
MODP 11
MODP 12
MODP 13
MODP 14
MODP 15
MODP 16
MODP 17
MODP 18
MODP 19
MODP 20
MODP 21

```

The NS chart is now given in Table 5.

Initialise (zero) $\underline{D}$ matrix. MODP 5-8	1.
Extract Young's modulus, E, Poisson's ratio $\nu$ and strip thickness $t$ . MODPB 9-12	2.
Compute $\underline{D}$ matrix. MODPB 13-19	3.

Table 5 NS chart for MODFS

For folded plate and axisymmetric shell programs, matrix  $\underline{D}$  should be extended to include membrane effects according to (49).

## 12.4.2 Subroutine GAUSSQ

This subroutine sets up the local Gauss point coordinates with a strip and their resp. weights.

```

SUBROUTINE GAUSS(NGAUT,POSGP,WEIGP)
DIMENSION POSGP(4),WEIGP(4)
C
C*** SET UP GAUSS POINT COORDINATES AND WEIGHTS
C
IF(NGAUT.GT.3) GO TO 30
IF(NGAUT.GT.2) GO TO 20
IF(NGAUT.GT.1) GO TO 10
POSGP(1)=0.0
WEIGP(1)=2.0
GO TO 50
10 POSGP(1)=-0.577350269189626
WEIGP(1)=1.0
GO TO 40
20 POSGP(1)=-0.774596669241483
POSGP(2)=0.0
WEIGP(1)=0.555555555555556
WEIGP(2)=0.888888888888889
GO TO 40
30 POSGP(1)=-0.8611363115
POSGP(2)=-0.3399810435
WEIGP(1)=0.3478548452
WEIGP(2)=0.6521451548
40 KGAUT=NGAUT/2
DO 50 IGASH=1,KGAUT
JGASH=NGAUT+1-IGASH
POSGP(JGASH)=-POSGP(IGASH)
WEIGP(JGASH)=WEIGP(IGASH)
50 CONTINUE
RETURN
END
GAUS 1
GAUS 2
GAUS 3
GAUS 4
GAUS 5
GAUS 6
GAUS 7
GAUS 8
GAUS 9
GAUS 10
GAUS 11
GAUS 12
GAUS 13
GAUS 14
GAUS 15
GAUS 16
GAUS 17
GAUS 18
GAUS 19
GAUS 20
GAUS 21
GAUS 22
GAUS 23
GAUS 24
GAUS 25
GAUS 26
GAUS 27
GAUS 28
GAUS 29
GAUS 30
GAUS 31

```

Note that NGAUT may take values from 1 to 4 for the resp. Gauss-Legendre rule. This routine is valid for folded plate and axisymmetric shell programs.

#### 12.4.3 Subroutine SFR1

This subroutine calculates the shape functions SHAPE and their derivatives DERIV of a specified sampling point with coordinate S.

```

SUBROUTINE SFR1(DERIV,S,NNODE,SHAPE)
DIMENSION DERIV(1,4),SHAPE(4)
C
C*** CALCULATES SHAPE FUNCTIONS AND THEIR DERIVATIVES
C
C*** SHAPE FUNCTIONS
C
IF(NNODE.EQ.4) GO TO 10
IF(NNODE.EQ.3) GO TO 5
C*** TWO NODED STRIP
C
SHAPE(1)=(1.0-S)/2.0
SHAPE(2)=(1.0+S)/2.0
DERIV(1,1)=-1.0/2.0
DERIV(1,2)=1.0/2.0
GO TO 15
C
C*** THREE NODED STRIP
C
SFR1 1
SFR1 2
SFR1 3
SFR1 4
SFR1 5
SFR1 6
SFR1 7
SFR1 8
SFR1 9
SFR1 10
SFR1 11
SFR1 12
SFR1 13
SFR1 14
SFR1 15
SFR1 16
SFR1 17
SFR1 18
SFR1 19
SFR1 20
SFR1 21

```

```

5 SHAPE(1)=(S*S-S)/2.0
SHAPE(2)=1.0-S*S
SHAPE(3)=(S+S*S)/2.0
DERIV(1,1)=(2.0*S-1.0)/2.0
DERIV(1,2)=-2.0*S
DERIV(1,3)=(1.0+2.0*S)/2.0
GO TO 15
C
C*** FOUR NODED STRIP
C
10 SHAPE(1)=-9.0/16.0*(S*S*S-S/9.0-S*S+1.0/9.0)
SHAPE(2)=27.0/16.0*(S*S*S-S-S*S/3.0+1.0/3.0)
SHAPE(3)=-27.0/16.0*(S*S*S-S+S*S/3.0-1.0/3.0)
SHAPE(4)=9.0/16.0*(S*S*S-S/9.0+S*S-1.0/9.0)
DERIV(1,1)=-9.0/16.0*(3.0*S*S-1.0/9.0-2.0*S)
DERIV(1,2)=27.0/16.0*(3.0*S*S-1.0-2.0/3.0*S)
DERIV(1,3)=-27.0/16.0*(3.0*S*S-1.0+2.0/3.0*S)
DERIV(1,4)=9.0/16.0*(3.0*S*S-1.0/9.0+2.0*S)
15 CONTINUE
RETURN
END
SFR1 22
SFR1 23
SFR1 24
SFR1 25
SFR1 26
SFR1 27
SFR1 28
SFR1 29
SFR1 30
SFR1 31
SFR1 32
SFR1 33
SFR1 34
SFR1 35
SFR1 36
SFR1 37
SFR1 38
SFR1 39
SFR1 40
SFR1 41
SFR1 42

```

The NS chart is now given in Table 6

Evaluate shape functions and their local derivatives for a linear, 2-node strip.	SFR1 14-17	1.
Evaluate shape functions and their local derivatives for a quadratic, 3-node strip.	SFR1 22-27	2.
Evaluate shape functions and their local derivatives for a cubic, 4-node strip.	SFR1 32-39	3.

Table 6 NS chart for subroutine SFR1

#### 12.4.4 Subroutine JACOB1

This subroutine calculates the Gauss point coordinates, the Cartesian shape function derivatives  $dN_i/dx$  and an elemental length dx.

```

SUBROUTINE JACOBI(CARTD,DERIV,DJACB,ELCOD,GPCOD,I,ELEM,KGASP, JACO 1
.NNODE,SHAPE) JACO 2
DIMENSION CARTD(1,4),DERIV(1,4),ELCOD(1,4),GPCOD(1,4),SHAPE(4) JACO 3
C JACO 4
C*** CALCULATES COORDINATES OF GAUSS POINTS AND THE JACOBIAN JACO 5
C*** MATRIX AND ITS DETERMINANT AND THE INVERSE JACO 6
C JACO 7
C DJACB=0.0 JACO 8
GPCOD(1,KGASP)=0.0 JACO 9
C JACO 10
C*** CALCULATE COORDINATES OF SAMPLING POINT JACO 11
C JACO 12
DO 5 INODE=1,NNODE JACO 13
GPCOD(1,KGASP)=GPCOD(1,KGASP)+SHAPE(INODE)*ELCOD(1,INODE) JACO 14
5 CONTINUE JACO 15
C JACO 16
C*** CALCULATE DETERMINANT OF JACOBIAN MATRIX JACO 17
C JACO 18
DO 10 INODE=1,NNODE JACO 19
DJACB=DJACB+DERIV(1,INODE)*ELCOD(1,INODE) JACO 20
10 CONTINUE JACO 21
IF(DJACB) 15,15,20 JACO 22
15 WRITE(6,900) I,ELEM JACO 23
STOP JACO 24
C JACO 25
C*** CALCULATE CARTESIAN DERIVATIVES JACO 26
C JACO 27
DO 20 INODE=1,NNODE JACO 28
CARTD(1,INODE)=DERIV(1,INODE)/DJACB JACO 29
20 CONTINUE JACO 30
900 FORMAT(//,10X,36H PROGRAM HALTED IN SUBROUTINE JACOBI, //1X, JACO 31
.22H ZERO OR NEGATIVE AREA, // 10X,16H ELEMENT NUMBER ,15) JACO 32
RETURN JACO 33
END JACO 34

```

The NS chart is now given in Table 6. Note that JACOBI is valid for folded plate and axisymmetric shell programs.

Initialise (zero) Jacobian determinant and the Gauss point coordinate vector. JACO 8-9	1.
Calculate the coordinates of the sampling point. JACO 13-15	2.
Evaluate the Jacobian determinant and if it is zero or negative write a message and terminate run. JACO 19-24	3.
Evaluate Cartesian shape function derivatives $dN_i/dx$ . JACO 28-30	4.

Table 6 NS chart for subroutine JACOBI

### 12.4.5 Subroutine BMATFS

This subroutine calculates the strain matrix given by (27) at a sampling point.

```

SUBROUTINE BMATFS(BMATX,CARTD,GPCOD,IGAUS,IHARM,NEVAB,NNODE, BMAT 1
.NSTRE,NTYPE,SHAPE,TLENG) BMAT 2
DIMENSION BMATX(5,12),CARTD(1,4),GPCOD(1,4),SHAPE(4) BMAT 3
C BMAT 4
C*** EVALUATE B MATRIX BMAT 5
C BMAT 6
DO 5 ISTR=1,NSTRE BMAT 7
DO 5 IEVAB=1,NEVAB BMAT 8
BMATX(ISTR,IEVAB)=0.0 BMAT 9
5 CONTINUE BMAT 10
JGASH=0 BMAT 11
DO 15 INODE=1,NNODE BMAT 12
IGASH=JGASH+1 BMAT 13
IF(NTYPE.EQ.2) GO TO 10 BMAT 14
C BMAT 15
C*** STRAIGHT PLATE BMAT 16
C BMAT 17
BMATX(4,IGASH)=CARTD(1,INODE) BMAT 18
BMATX(5,IGASH)=SHAPE(INODE)*FLOAT(IHARM)*3.14159265/TLENG BMAT 19
IGASH=IGASH+1 BMAT 20
JGASH=IGASH+1 BMAT 21
BMATX(1,IGASH)=-CARTD(1,INODE) BMAT 22
BMATX(3,IGASH)=-SHAPE(INODE)*FLOAT(IHARM)*3.14159265/TLENG BMAT 23
BMATX(4,IGASH)=-SHAPE(INODE) BMAT 24
BMATX(2,JGASH)=SHAPE(INODE)*FLOAT(IHARM)*3.14159265/TLENG BMAT 25
BMATX(3,JGASH)=-CARTD(1,INODE) BMAT 26
BMATX(5,JGASH)=-SHAPE(INODE) BMAT 27
GO TO 15 BMAT 28
C BMAT 29
C*** CURVED PLATE BMAT 30
C BMAT 31
10 BMATX(4,IGASH)=CARTD(1,INODE) BMAT 32
BMATX(5,IGASH)=(SHAPE(INODE)/GPCOD(1,IGAUS))*FLOAT(IHARM)* BMAT 33
3.14159265/TLENG BMAT 34
IGASH=IGASH+1 BMAT 35
JGASH=IGASH+1 BMAT 36
BMATX(1,IGASH)=-CARTD(1,INODE) BMAT 37
BMATX(2,IGASH)=-SHAPE(INODE)/GPCOD(1,IGAUS) BMAT 38
BMATX(3,IGASH)=-SHAPE(INODE)/GPCOD(1,IGAUS))*FLOAT(IHARM)* BMAT 39
3.14159265/TLENG BMAT 40
BMATX(4,IGASH)=-SHAPE(INODE) BMAT 41
BMATX(2,JGASH)=(SHAPE(INODE)/GPCOD(1,IGAUS))*FLOAT(IHARM)* BMAT 42
3.14159265/TLENG BMAT 43
BMATX(3,JGASH)=-CARTD(1,INODE)+SHAPE(INODE)/GPCOD(1,IGAUS) BMAT 44
BMATX(5,JGASH)=-SHAPE(INODE) BMAT 45
15 CONTINUE BMAT 46
RETURN BMAT 47
END BMAT 48

```

For folded plate and axisymmetric shell programs, subroutine BMATFS should evaluate the strain matrix according to (56) - (57). The NS chart for NMATFS is now given in Table 8.

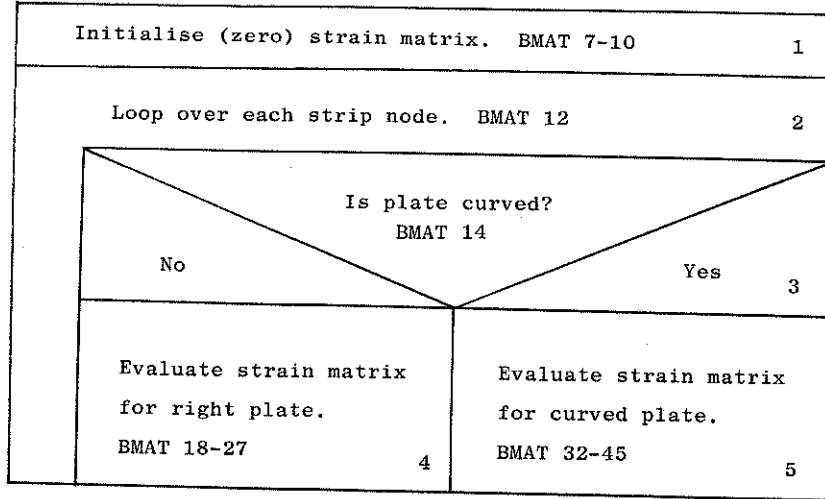


Table 8 NS chart for subroutine BMATFS

## 12.4.6 Subroutine DBE

This subroutine simply calculates the stress matrix  $\underline{DB}^l$  at any sampling point.

```

SUBROUTINE DBE(BMATX,DBMAT,DMATX,NEVAB,NSTRE)
DIMENSION BMATX(5,12),DBMAT(5,12),DMATX(5,5)
C
C*** CALCULATE D X B
C
DO 5 ISTR=1,NSTRE
DO 5 IEVAB=1,NEVAB
DBMAT(ISTR,IEVAB)=0.0
DO 5 JSTRE=1,NSTRE
DBMAT(ISTR,IEVAB)=DBMAT(ISTR,IEVAB)+
.DMATX(ISTR,JSTRE)*BMATX(JSTRE,IEVAB)
5 CONTINUE
RETURN
END
DBE 1
DBE 2
DBE 3
DBE 4
DBE 5
DBE 6
DBE 7
DBE 8
DBE 9
DBE 10
DBE 11
DBE 12
DBE 13
DBE 14

```

## 12.5 Evaluation of equivalent nodal load vector for each harmonic term: Subroutine LOADFS

Only two loading cases will be considered in the plate program presented here: a) a vertical point load acting at a node at a certain distance from the simply supported end and b) a uniformly distributed load acting over a certain number of strips. Extensions of the program for the consideration of other loading situations is easy once the basic steps for the two cases presented here are fully understood, and can be

attempted by the reader,

A FORTRAN listing of the subroutine is now presented.

```

SUBROUTINE LOADFS(COORD,ELoad,ICASE,IHARM,LNODS,MATNO,MELEM,
.MMAT,MPOIN,NDOFN,NELEM,NEVAB,NGAUS,NNODE,NPOIN,NFYPE,POSGP,
.PROPS,TLENG,WEIGP)
DIMENSION CARTD(1,4),COORD(MPOIN,1),DERIV(1,4),ELCOD(1,4),
.ELOAD(MELEM,12),GPCOD(1,4),LNODS(MELEM,4),MATNO(MELEM),POINT(3),
.POSGP(4),PROPS(MMAT,5),SHAPE(4),TITLE(18),WEIGP(4)
LOAD 1
LOAD 2
LOAD 3
LOAD 4
LOAD 5
LOAD 6
LOAD 7
C
C*** EVALUATE NODAL FORCE VECTOR
LOAD 8
C
IF(IHARM.GT.1) GO TO 5
LOAD 9
LOAD 10
C
C*** READ AND WRITE TITLE OF LOAD CASE
LOAD 11
LOAD 12
C
READ(5,900) TITLE
LOAD 13
900 FORMAT(18A4)
LOAD 14
C
C*** READ AND WRITE INDICATORS FOR TYPE OF LOAD
LOAD 15
LOAD 16
C
READ(5,905) IPLD,IUNIF
LOAD 17
905 FORMAT(2I5)
LOAD 18
WRITE(9) IPLD,IUNIF
LOAD 19
WRITE(6,910) ICASE
LOAD 20
910 FORMAT(/10X,'LOAD CASE NUMBER ',1X,I2)
LOAD 21
WRITE(6,900) TITLE
LOAD 22
WRITE(6,905) IPLD,IUNIF
LOAD 23
GO TO 10
LOAD 24
5 READ(9) IPLD,IUNIF
LOAD 25
10 CONTINUE
LOAD 26
DO 15 IELEM=1,NELEM
LOAD 27
DO 15 IEVAB=1,NEVAB
LOAD 28
15 ELOAD(IELEM,IEVAB)=0.0
LOAD 29
LOAD 30
C
C*** POINT LOAD
LOAD 31
C
IF(IPLD.EQ.0) GO TO 50
LOAD 32
IF(IHARM.EQ.1) WRITE(6,915)
LOAD 33
20 CONTINUE
LOAD 34
IF(IHARM.GT.1) GO TO 25
LOAD 35
READ(5,920) LODPT,POINT(1),YLOAD
LOAD 36
WRITE(9) LODPT,(POINT(IDOFN),IDOFN=1,NDOFN),YLOAD
LOAD 37
915 FORMAT(/10X,'POINT LOAD')
LOAD 38
WRITE(6,920) LODPT,(POINT(IDOFN),IDOFN=1,NDOFN),YLOAD
LOAD 39
920 FORMAT(15,4F10.5)
LOAD 40
GO TO 30
LOAD 41
25 READ(9) LODPT,(POINT(IDOFN),IDOFN=1,NDOFN),YLOAD
LOAD 42
30 CONTINUE
LOAD 43
C
C*** CALCULATE LOADS AND ASSOCIATE WITH NODAL POINTS
LOAD 44
C
FPLD=FLOAT(IHARM)*3.14159265*YLOAD/TLENG
LOAD 45
DO 35 IELEM=1,NELEM
LOAD 46
DO 35 INODE=1,NNODE
LOAD 47
NLCCA=LNODS(IELEM,INODE)
LOAD 48
IF(LODPT.EQ.NLCCA) GO TO 40
LOAD 49
35 CONTINUE
LOAD 50
40 DO 45 IDOFN=1,NDOFN
LOAD 51
IF(IDOFN.EQ.1.OR.IDOFN.EQ.2) SINCO=SIN(FPLD)
LOAD 52
IF(IDOFN.EQ.3) SINCO=COS(FPLD)
LOAD 53
NGASH=(INODE-1)*NDOFN+IDOFN
LOAD 54
ELOAD(IELEM,NGASH)=ELOAD(IELEM,NGASH)+POINT(IDOFN)*SINCO
LOAD 55
45 CONTINUE
LOAD 56
LOAD 57
LOAD 58
LOAD 59
LOAD 60
LOAD 61

```

```

IF (LOADPT.LT.NPOINT) GO TO 20
50 CONTINUE
C
C*** UNIFORM DISTRIBUTED LOAD
C
VLEPI=3.14159265*FLOAT(IHARM)
COEFL=2.0*YLENG/VLEPI
C
C*** LOOP OVER EACH STRIP
C
CALL GAUSSQ(NGAUS, POSGP, WEIGP)
DO 75 IELEM=1, NELEM
LPROP=MATNO(IELEM)
VDLDD=COEFL*PROPS(LPROP,4)
IF (VDLDD.EQ.0.0) GO TO 75
KGASP=0
C
C*** EXTRACT ELEMENT NODAL COORDINATES
C
DO 55 INODE=1, NNODE
LNODE=LNODES(IELEM, INODE)
ELCOD(1, INODE)=COORD(LNODE, 1)
55 CONTINUE
C
C*** ENTER LOOPS FOR NUMERICAL INTEGRATION
C
DO 70 IGAUS=1, NGAUS
KGASP=KGASP+1
EXISP=POSGP(IGAUS)
C
C*** EVALUATE THE SHAPE FUNCTIONS AT THE SAMPLING POINTS AND
C*** ELEMENTAL LENGTH
C
CALL SFR1(DERIV, EXISP, NNODE, SHAPE)
CALL JACOB1(CARTD, DERIV, DJACB, ELCOD, GPCOD, IELEM, KGASP, NNODE,
.SHAPE)
C
C*** CALCULATE LOADS AND ASSOCIATE WITH ELEMENT NODAL POINTS
C
DO 65 INODE=1, NNODE
NPOSN=(INODE-1)*NDGFN+1
IF (NTYPE.EQ.2) GO TO 60
C
C*** STRAIGHT PLATE
C
ELOAD(IELEM, NPOSN)=ELOAD(IELEM, NPOSN)+
.SHAPE(INODE)*VDLDD*DJACB*WEIGP(IGAUS)
GO TO 65
C
C*** CURVED PLATE
C
60 ELOAD(IELEM, NPOSN)=ELOAD(IELEM, NPOSN)+GPCOD(1, IGAUS)*
.SHAPE(INODE)*VDLDD*DJACB*WEIGP(IGAUS)
65 CONTINUE
70 CONTINUE
75 CONTINUE
RETURN
END

```

- LOAD 82
- LOAD 83
- LOAD 84
- LOAD 85
- LOAD 86
- LOAD 87
- LOAD 88
- LOAD 89
- LOAD 70
- LOAD 71
- LOAD 72
- LOAD 73
- LOAD 74
- LOAD 75
- LOAD 76
- LOAD 77
- LOAD 78
- LOAD 79
- LOAD 80
- LOAD 81
- LOAD 82
- LOAD 83
- LOAD 84
- LOAD 85
- LOAD 86
- LOAD 87
- LOAD 88
- LOAD 89
- LOAD 90
- LOAD 91
- LOAD 92
- LOAD 93
- LOAD 94
- LOAD 95
- LOAD 96
- LOAD 97
- LOAD 98
- LOAD 99
- LOAD 100
- LOAD 101
- LOAD 102
- LOAD 103
- LOAD 104
- LOAD 105
- LOAD 106
- LOAD 107
- LOAD 108
- LOAD 109
- LOAD 110
- LOAD 111
- LOAD 112
- LOAD 113
- LOAD 114
- LOAD 115
- LOAD 116
- LOAD 117
- LOAD 118
- LOAD 119

The NS chart for LOADFS is presented in Table 9

For the first harmonic only read and write the load case title and the load type code. LOAD 10-28		1
Initialise (zero) the load vector. LOAD 29-31		2
If there are point loads continue, otherwise jump to 10. LOAD 35		3
Is this the first harmonic? Yes <span style="margin-left: 150px;">LOAD 38</span> <span style="float: right;">No</span>		
Read and write nodal load data and then write on file 9. LOAD 39-43	Read load data from file 9. LOAD 45	4
		5
Identify loaded node with a strip. LOAD 52-55		7
Compute nodal forces for either a right or curved strip. LOAD 56-61		8
If all nodes have been considered continue; otherwise jump back to 4. LOAD 62		9
Set loading parameters for right and curved strip plate cases. LOAD 67-68		10
Call GAUSSQ to obtain Gauss point weights and sampling positions. LOAD 72		11
Loop over each strip. LOAD 73		12

A

Table 9 NS chart for subroutine LOADFS



A	
Identify strip material set number and extract strip load intensity parameter PROPS (LPROP,4). LOAD 74-75	13
If load intensity is zero, jump to next strip. LOAD 76	14
Zero Gauss point counter and extract element nodal coordinates. LOAD 77-84	15
Loop over each Gauss point. LOAD 88	16
Increment Gauss point counter and identify local coordinate of Gauss point. LOAD 89-90	17
Call SFR1 to evaluate shape functions and their local derivatives. LOAD 95	18
Call JACOBI to evaluate elemental length dx, etc. LOAD 96-97	19
Accumulate contributions to the consistent load vector for either right or curved strips. LOAD 101-115	20

Table 9 NS chart for subroutine LOADFS

### 12.6 Computation of the strip stress resultants for each harmonic term: Subroutine STREFS

This subroutine evaluates the stress resultants at the shear Gauss points for each strip and for each harmonic term accordingly to (25) making use of the stress matrix (see Section 12.3) and the strip nodal displacements computed in subroutine FRONT. The strip stress resultants for each harmonic are stored on a disc file for subsequent use in subroutine ADD

```

SUBROUTINE STREFS(ASDIS, LNODS, MELEM, MTOTV, NDOFN, NELEM, NGAUS,
.NNODE, NSTRE)
DIMENSION ASDIS(MTOTV), ELDIS(3,4), LNODS(MELEM,4), GPCOD(1,4),
.SMATX(5,12,4), STRSG(5)
C
C*** EVALUATE STRESSES AT THE SHEAR GAUSS POINTS FOR
C*** EACH STRIP
C
C*** LOOP OVER EACH STRIP ELEMENT
C
DO 20 IELEM=1, NELEM
C
C*** READ THE STRESS MATRIX ,SAMPLING POINT COORDINATES
C*** FOR THE STRIP
C
READ(3) SMATX, GPCOD
C
C*** IDENTIFY THE DISPLACEMENTS OF THE ELEMENT NODAL POINTS
C
DO 5 INODE=1, NNODE
LNODE=LNODS(IELEM, INODE)
NPOSN=(LNODE-1)*NDOFN
DO 5 IDOFN=1, NDOFN
NPOSN=NPOSN+1
ELDIS(IDOFN, INODE)=ASDIS(NPOSN)
5 CONTINUE
KGASP=0
C
C*** ENTER LOOPS OVER EACH SHEAR SAMPLING POINT
C
DO 15 IGAUS=1, NGAUS
KGASP=KGASP+1
DO 10 ISTR=1, NSTRE
STRSG(ISTR)=0.0
KGASH=0
C
C*** COMPUTE THE STRESS RESULTANTS
C
DO 10 INODE=1, NNODE
DO 10 IDOFN=1, NDOFN
KGASH=KGASH+1
STRSG(ISTR)=STRSG(ISTR)+SMATX(ISTR, KGASH, KGASP)*ELDIS(IDOFN,
.INODE)
10 CONTINUE
C
C*** WRITE STRESSES IN DISC FOR EACH HARMONIC
C
WRITE(8) (STRSG(ISTR), ISTR=1, NSTRE)
15 CONTINUE
20 CONTINUE
RETURN
END

```

The NS chart for STREFS is now given in Table 10

Loop over each strip. STRE 12	1
Read from file 3 the stress resultant matrix and the sampling point coordinates. STRE 17	2
Extract the displacements of the strip nodal points from the global displacement vector ASDIS. STRE 21-27	3

A

Table 10 NS chart for Subroutine STREFS

A	
Zero Gauss point counter. STRE 28	4
Loop over Gauss points. STRE 32	5
Increment Gauss point counter. STRE 33	6
Compute stress resultants at each Gauss point. STRE 34-45	7
Write in disc file 8 the Gauss point stress resultants. STRE 49	8

Table 10 NS chart for subroutine STREFS

This routine is identical for all of the different structural applications given in this chapter.

12.7 Subroutine for summing the contributions from all harmonics: Subroutine ADD

This subroutine evaluates the displacements and stress resultants at a given longitudinal section of the structure by summing the nodal displacements and Gauss point stress resultants obtained for all harmonic terms chosen for the analysis.

SUBROUTINE ADD (ADISP, AFORC, DISPL, DIZPL, EFORC, FORCE, MELEM, MFACT,	ADD	1
.MPOIN, MTOTV, NCASE, NDOFN, NELEM, NGAUS, NHARM, NPOIN, NSTRE, NSYME,	ADD	2
.TLENG)	ADD	3
DIMENSION ADISP(3, MPOIN), AFORC(5, 4, MELEM), DISPL(MTOTV),	ADD	4
.DIZPL(MTOTV), EFORC(MFACT), FORCE(MFACT), GPCOD(1, 4), SMATX(5, 12, 4),	ADD	5
.YSECT(5)	ADD	6
C	ADD	7
C*** SUM DISPLACEMENTS AND STRESSES FOR ALL HARMONICS	ADD	8
C	ADD	9
C*** READ AND WRITE SECTION ANALYSIS DATA	ADD	10
C	ADD	11
READ(5, 900) NSECT	ADD	12
900 FORMAT(15)	ADD	13
WRITE(6, 950) NSECT	ADD	14
READ(5, 905) YSECT(ISECT), ISECT=1, NSECT)	ADD	15
905 FORMAT(BF10, 3)	ADD	16
VARAD=3.14159265/TLENG	ADD	17
DO 105 ICASE=1, NCASE	ADD	18
DO 100 ISECT=1, NSECT	ADD	19
WRITE(6, 915) YSECT(ISECT)	ADD	20
RADIO=VARAD*YSECT(ISECT)	ADD	21
WRITE(6, 910) ICASE	ADD	22
910 FORMAT(//, 5X, 14H LOAD CASE NO=, I3, //)	ADD	23
REWIND 7	ADD	24
REWIND 8	ADD	25

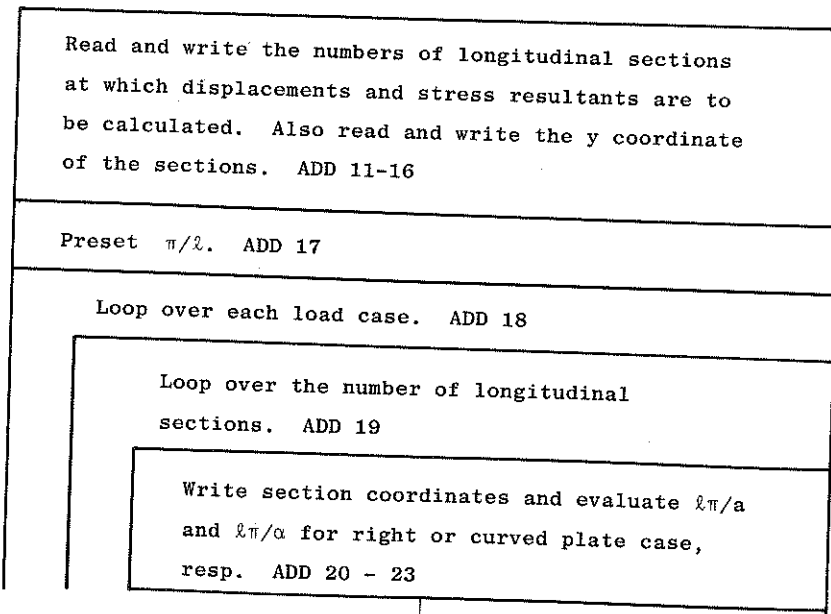
NUMOR=NPOIN	ADD	26
DO 5 IDOFN=1, NDOFN	ADD	27
DO 5 IUMDR=1, NUMDR	ADD	28
5 ADISP(IDOFN, IUMDR)=0.0	ADD	29
DO 10 IELEM=1, NELEM	ADD	30
DO 10 ISTR=1, NSTRE	ADD	31
DO 10 IGAUS=1, NGAUS	ADD	32
10 AFORC(ISTR, IGAUS, IELEM)=0.0	ADD	33
WRITE(6, 920)	ADD	34
WRITE(6, 925)	ADD	35
LDDIS=NUMOR*NDOFN	ADD	36
C	ADD	37
C*** READ BACK DISPLACEMENTS	ADD	38
C	ADD	39
DO 95 IHARM=1, NHARM, NSYME	ADD	40
DO 30 ICASO=1, NCASE	ADD	41
DO 15 IPOIN=1, NPOIN	ADD	42
NGASH=IPOIN*NDOFN	ADD	43
NGISH=NGASH-NDOFN+1	ADD	44
15 READ(7) (DIZPL(IDDIS), IDDIS=NGISH, NGASH)	ADD	45
IF(ICASO.NE.ICASE) GO TO 25	ADD	46
DO 20 IDDIS=1, LDDIS	ADD	47
20 DISPL(IDDIS)=DIZPL(IDDIS)	ADD	48
25 CONTINUE	ADD	49
30 CONTINUE	ADD	50
HARMO=FLOAT(IHARM)	ADD	51
FCTOR=HARMO*RADIO	ADD	52
C	ADD	53
C*** SUM DISPLACEMENTS FOR ALL HARMONICS	ADD	54
C	ADD	55
DO 35 IUMDR=1, NUMDR	ADD	56
IWDIS=(IUMDR-1)*3+1	ADD	57
IROTX=IWDIS+1	ADD	58
IROTY=IWDIS+2	ADD	59
ADISP(1, IUMDR)=ADISP(1, IUMDR)+DISPL(IWDIS)*SIN(FCTOR)	ADD	60
ADISP(2, IUMDR)=ADISP(2, IUMDR)+DISPL(IROTX)*SIN(FCTOR)	ADD	61
ADISP(3, IUMDR)=ADISP(3, IUMDR)+DISPL(IROTY)*COS(FCTOR)	ADD	62
35 CONTINUE	ADD	63
C	ADD	64
C*** PRINT DISPLACEMENTS	ADD	65
C	ADD	66
IF(IHARM.LT.NHARM) GO TO 45	ADD	67
DO 40 IPOIN=1, NPOIN	ADD	68
WRITE(6, 930) IPOIN, (ADISP(IDOFN, IPOIN), IDOFN=1, NDOFN)	ADD	69
40 CONTINUE	ADD	70
45 CONTINUE	ADD	71
C	ADD	72
C*** STRESSES AT SHEAR GAUSS POINTS	ADD	73
C	ADD	74
LDSTR=NELEM*NSTRE*NGAUS	ADD	75
C	ADD	76
C*** READ BACK STRESSES AT SHEAR GAUSS POINTS	ADD	77
C	ADD	78
DO 70 ICASO=1, NCASE	ADD	79
DO 55 IELEM=1, NELEM	ADD	80
KSTEG=NSTRE*NGAUS	ADD	81
LSTEG=(IELEM-1)*KSTEG	ADD	82
DO 50 IGAUS=1, NGAUS	ADD	83
NGEST=IGAUS*NSTRE+LSTEG	ADD	84
NGIST=NGEST-NSTRE+1	ADD	85
50 READ(8) (EFORC(IDSTR), IDSTR=NGIST, NGEST)	ADD	86
55 CONTINUE	ADD	87
IF(ICASO.NE.ICASE) GO TO 65	ADD	88
DO 60 IDSTR=1, LDSTR	ADD	89
60 FORCE(IDSTR)=EFORC(IDSTR)	ADD	90
65 CONTINUE	ADD	91
70 CONTINUE	ADD	92
REWIND 3	ADD	93
C	ADD	94
C*** SUM SHEAR GAUSS POINT STRESSES FOR ALL HARMONICS	ADD	95
C	ADD	96
DO 90 IELEM=1, NELEM	ADD	97
MSTEG=NSTRE*NGAUS	ADD	98
NSTEG=(IELEM-1)*MSTEG	ADD	99
READ(3) SMATX, GPCDD	ADD	100
DO 85 IGAUS=1, NGAUS	ADD	101
ISXDI=(IGAUS-1)*NSTRE+1+NSTEG	ADD	102
ISYDI=ISXDI+1	ADD	103
ISXYD=ISXDI+2	ADD	104
ISXZD=ISXDI+3	ADD	105

```

ISYZD=ISXDI+4
AFORC(1,IGAUS,IELEM)=AFORC(1,IGAUS,IELEM)+FORCE(ISXDI)*SIN(FCOR) ADD 106
AFORC(2,IGAUS,IELEM)=AFORC(2,IGAUS,IELEM)+FORCE(1SYDI)*SIN(FCOR) ADD 107
AFORC(3,IGAUS,IELEM)=AFORC(3,IGAUS,IELEM)+FORCE(1SYDI)*SIN(FCOR) ADD 108
AFORC(4,IGAUS,IELEM)=AFORC(4,IGAUS,IELEM)+FORCE(1SYDI)*COS(FCOR) ADD 109
AFORC(5,IGAUS,IELEM)=AFORC(5,IGAUS,IELEM)+FORCE(1SYDI)*SIN(FCOR) ADD 110
IF(IHARM.LY.NHARM) GO TO 80 ADD 111
IF(IGAUS.GT.1) GO TO 75 ADD 112
WRITE(6,935) ADD 113
WRITE(6,940) ADD 114
WRITE(6,945) ADD 115
75 CONTINUE ADD 116
C ADD 117
C*** PRINT FINAL SHEAR GAUSS POINT STRESSES ADD 118
C ADD 119
WRITE(6,935) IELEM,IGAUS,(AFORC(1STRE,IGAUS,IELEM),1STRE=1, ADD 120
.NSTRE),GPCOD(1,IGAUS) ADD 121
80 CONTINUE ADD 122
85 CONTINUE ADD 123
90 CONTINUE ADD 124
95 CONTINUE ADD 125
100 CONTINUE ADD 126
105 CONTINUE ADD 127
915 FORMAT(1H0,'TOTAL DISPLACEMENTS AND STRESSES AT Z=',F8.3,/) ADD 128
920 FORMAT(1H0,5X,13HDISPLACEMENTS) ADD 129
925 FORMAT(1H0,5X,4HNODE,6X,5HDISP.,8X,9H XZ-ROT.,7X,8H YZ-ROT.) ADD 130
930 FORMAT(1I10,3E16.8) ADD 131
935 FORMAT(2I5,6E15.8,F10.4) ADD 132
940 FORMAT(/ / 1X,'STRESSES AT THE SHEAR GAUSS POINTS',/) ADD 133
945 FORMAT(/ 4X,'EL',3X,'GP.',13H XX-MOMENT ADD 134
.15H YY-MOMENT ,15H XY-MOMENT ,15H XZ-FORCE ADD 135
.15H YZ-FORCE ,1X,'X-CORD GAUS P.1) ADD 136
950 FORMAT(/ / 1X,'NUMBER OF SECTIONS TO BE ANALYSED=',I9) ADD 137
RETURN ADD 138
END ADD 139
ADD 140

```

The NS chart for subroutine ADD is now given in Table 11.



A

Table 11 NS chart for subroutine ADD

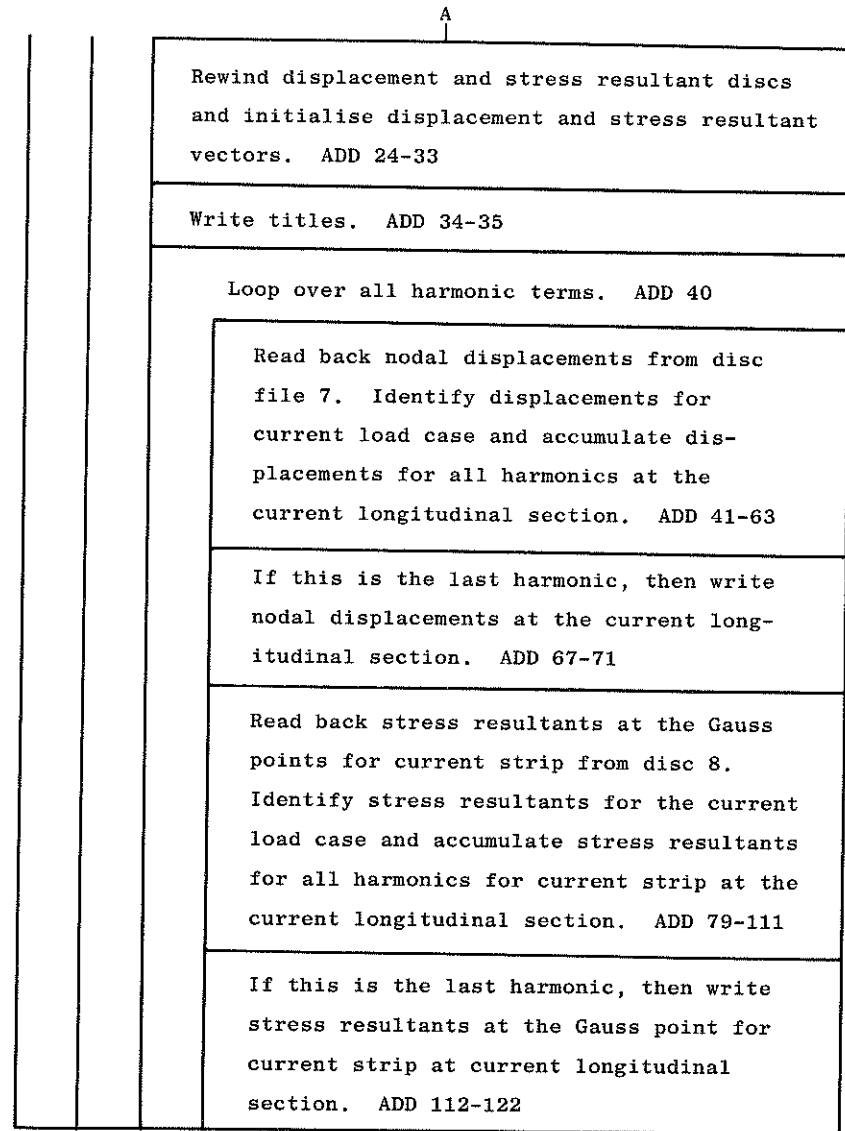


Table 11 NS chart for subroutine ADD

This subroutine is almost identical for all the different structures studied in this chapter. The only difference lays in the number of displacement and stress components and the type of expansions chosen for each particular problem.

### 12.9 Subroutine to solve the stiffness equations for each harmonic term: Subroutine FRONT

This subroutine solves the uncoupled system of stiffness equations for each harmonic term (see (35)) by the FRONTAL elimination technique [35]. Full descriptive comments of this subroutine, together with the corresponding comments can be found in reference [34] and they will not be given here.

```

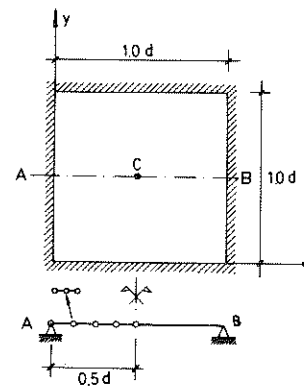
SUBROUTINE FRONT (ASDIS, ELOAD, EGRHS, EQUAT, FIXED, GLOAD, GSTIF,
. ICASE, IFFIX, IFPRE, LNODS, MBUFA, MELEM, MFRON, MSTIF, MTOTV, MVFIX,
. NACVA, NAMEV, NODFN, NELEM, NEVAB, NNODE, NOFIX, NPIVO, NPOIN, NVFIX,
. PRESC, VECRV)
DIMENSION ASDIS (MTOTV), ELOAD (MELEM, 12), EGRHS (MBUFA),
. EQUAT (MFRON, MBUFA), ESTIF (12, 12), FIXED (MTOTV), GLOAD (MFRON),
. GSTIF (MSTIF), IFFIX (MTOTV), IFPRE (MVFIX, 3), LNODS (MELEM, 4),
. LOCEL (12), NACVA (MFRON), NAMEV (MBUFA), NDEST (12), NOFIX (MVFIX),
. NPIVO (MBUFA), PRESC (MVFIX, 3), VECRV (MFRON)
C
C*** MERGE AND SOLVE THE RESULTING EQUATIONS
C*** BY THE FRONTAL METHOD FOR EACH HARMONIC
C
C*** FOR A COMPLETE DESCRIPTION OF THIS SUBROUTINE
C*** SEE THE BOOK "FINITE ELEMENTS IN PLASTICITY:
C*** THEORY AND PRACTICE" BY OWEN AND HINTON
C*** PINERIDGE PRESS, SWANSEA 1980
C
C RETURN
C END
FRON 1
FRON 2
FRON 3
FRON 4
FRON 5
FRON 6
FRON 7
FRON 8
FRON 9
FRON 10
FRON 11
FRON 12
FRON 13
FRON 14
FRON 15
FRON 16
FRON 17
FRON 18
FRON 19
FRON 20

```

## 13. EXAMPLES

### 13.1 Example 1: Simply supported square thick plate under uniformly distributed load

The geometry of the plate and the material properties are indicated in Figure 24. A mesh of five, three-noded strips with full integration has been used. This example has been discussed earlier in the chapter in Section 3.5. Figure 24 shows a plot of the numerical results obtained for the bending moment  $M_x$  along the central transverse section of the plate versus the theoretically exact values [32]. Accuracy of the numerical solution is noticeable. In section 14 computer listings of the data input and output results for this example are given.



Uniformly distributed load  $q$

$$q = 1.0 (F/d^2)$$

$$E = 10.920 (F/d^2)$$

$$\nu = 0.3$$

$$\text{thickness} = 0.1 d$$

5 three noded strips

Full integration

6 Non zero harmonics

$$W_C (\text{obtained}) = 0.4272 \times 10^{-2} (d)$$

$$W_C (\text{exact}) [21] = 0.4270 \times 10^{-2} (d)$$

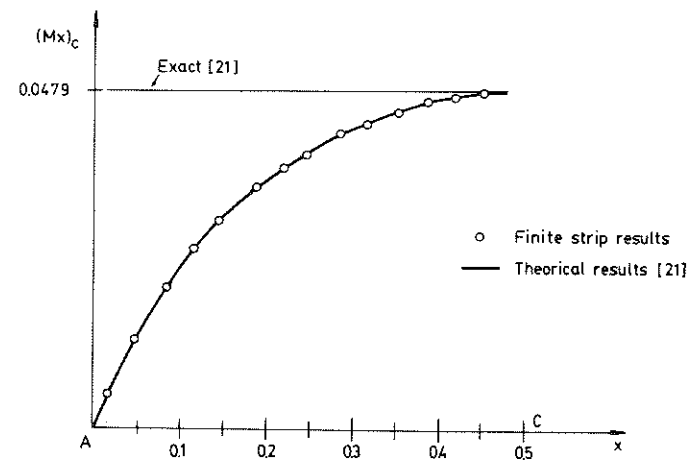
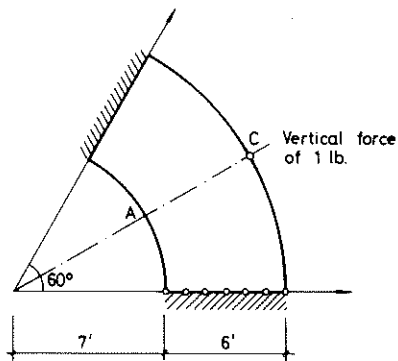


Fig. 24 Example 1. Thick square plate under uniformly distributed loading.



$E = 42460 \text{ lb/in}^2$       12 two noded strips  
 $\nu = 0.3$                       Reduced integration  
 thickness = 0.172 in      6 non zero harmonics

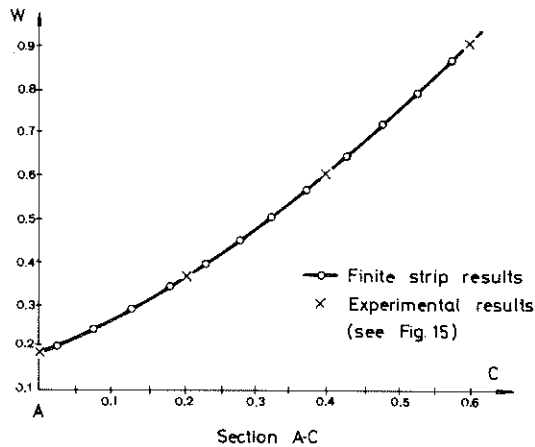


Fig. 25 Example 2: Circular slab simply supported at two ends under point load acting at the center of a free edge.

13.2 Example 2: Circular slab simply supported at two ends under point load acting at the center of a free edge

This example was discussed earlier in Section 10.1. The geometry and material properties are shown in Figure 25. A mesh of twelve, two-noded strips with reduced integration has been used for the analysis. In the same figure a plot of the numerical solution obtained by Coull and Das for the same problem [26] is also shown in the figure for comparison. Accuracy of the numerical results is again good. Data input for this problem is given in Section 15. A listing of the numerical results obtained is also presented in Section 15.

14. INPUT AND OUTPUT DATA FOR EXAMPLE 1

Input data for Example 1 is now listed.

1	SIMPLY SUPPORTED SQUARE PLATE. QUADRATIC STRIP WITH FULL INTEGRATION						
11	2						
11	5	2	1	1	3	1	3 3
1.							
1	1	1	2	3			
2	1	3	4	5			
3	1	5	6	7			
4	1	7	8	8			
5	1	9	10	11			
1	.0						
2	.05						
3	.1						
4	.15						
5	.2						
6	.25						
7	.30						
8	.35						
9	.40						
10	.45						
11	.5						
1	101						
11	010						
110920.		.3		.1		1.	
UNIFORM LOAD							
0	1						
1							
0.5							

Typical output data for Example 1 is now listed.

PROBLEM NO. 1 SIMPLY SUPPORTED SQUARE PLATE. QUADRATIC STRIP WITH FULL INTEGRATION

NUMBER OF HARMONIC TERMS TO BE USED = 11  
 INDICATOR FOR SYMMETRY OF LOADING ( 1 FOR NON SYMMETRY, 2 FOR SYMMETRY ) = 2  
 LENGTH OF THE PLATE= 1.00000

NPOIN = 11 NLELM = 5 NVPFX = 2 INCASE = 1 NTYPE = 1 NNODE = 3 NDOFN = 3  
 NMMATS = 1 NPROP = 5 NGAUB = 3 NGAUS = 3 NDIHE = 1 NSTRE = 5 NEVAB = 9

ELEMENT	PROPERTY	NODE NUMBERS
1	1	1 2 3
2	1	3 4 5
3	1	5 6 7
4	1	7 8 9
5	1	9 10 11

MODAL POINT COORDINATES

MODE	X
1	0.00000
2	0.05000
3	0.10000
4	0.15000
5	0.20000
6	0.25000
7	0.30000
8	0.35000
9	0.40000
10	0.45000
11	0.50000

RESTRAINED NODES

NODE CODE	FIXED VALUES
1 101	0.00000 0.00000 0.00000
11 010	0.00000 0.00000 0.00000

MATERIAL PROPERTIES

NUMBER	1
0.108200E+05	0.300000E+00 0.100000E+00 0.100000E+01 0.000000E+00

LOAD CASE NUMBER 1  
 UNIFORM LOAD  
 0 1

NUMBER OF SECTIONS TO BE ANALYSED= 1

TOTAL DISPLACEMENTS AND STRESSES AT Z. 0.500

LOAD CASE NO= 1

DISPLACEMENTS

NODE	DISP.	XZ-ROT.	YZ-ROT.
1	0.000000E+00	0.134854E-01	0.000000E+00
2	0.714032E-03	0.132200E-01	-0.923487E-10
3	0.139809E-02	0.125430E-01	-0.182944E-09
4	0.203262E-02	0.115109E-01	-0.267729E-09
5	0.260408E-02	0.102355E-01	-0.344004E-09
6	0.310131E-02	0.875822E-02	-0.410272E-09
7	0.351662E-02	0.714906E-02	-0.465529E-09
8	0.384477E-02	0.543559E-02	-0.509111E-09
9	0.408153E-02	0.365863E-02	-0.540538E-09
10	0.422445E-02	0.189859E-02	-0.559517E-09
11	0.427228E-02	0.000000E+00	-0.565858E-09

## STRESSES AT THE SHEAR GAUSS POINTS

EL	GP	XX-MOMENT	YY-MOMENT	XY-MOMENT	XZ-FORCE	YZ-FORCE	X-CORD GAUS P.
1	1	0.344624E-02	0.224752E-02	0.129786E-08	0.344417E+00	0.777929E-09	0.112702E+00
1	2	0.111826E-01	0.868759E-02	0.128385E-08	0.265092E+00	0.207174E-09	0.500000E-01
1	3	0.188927E-01	0.150398E-01	0.125730E-08	0.274231E+00	0.122838E-08	0.987296E-01

## STRESSES AT THE SHEAR GAUSS POINTS

EL	GP	XX-MOMENT	YY-MOMENT	XY-MOMENT	XZ-FORCE	YZ-FORCE	X-CORD GAUS P.
2	1	0.231534E-01	0.186229E-01	0.121808E-08	0.247447E+00	0.208295E-08	0.111270E+00
2	2	0.111826E-01	0.236994E-01	0.112975E-08	0.192381E+00	-0.100963E-08	0.150000E+00
2	3	0.330994E-01	0.288891E-01	0.103397E-08	0.186392E+00	-0.212736E-08	0.188730E+00

## STRESSES AT THE SHEAR GAUSS POINTS

EL	GP	XX-MOMENT	YY-MOMENT	XY-MOMENT	XZ-FORCE	YZ-FORCE	X-CORD GAUS P.
3	1	0.356971E-01	0.316057E-01	0.969291E-09	0.167887E+00	-0.270671E-08	0.211270E+00
3	2	0.387503E-01	0.355468E-01	0.851558E-09	0.129077E+00	-0.355219E-08	0.250000E+00
3	3	0.416819E-01	0.390826E-01	0.730621E-09	0.118339E+00	-0.425440E-08	0.288730E+00

## STRESSES AT THE SHEAR GAUSS POINTS

EL	GP	XX-MOMENT	YY-MOMENT	XY-MOMENT	XZ-FORCE	YZ-FORCE	X-CORD GAUS P.
4	1	0.431349E-01	0.408900E-01	0.656436E-09	0.102008E+00	-0.459466E-08	0.311270E+00
4	2	0.447815E-01	0.433852E-01	0.525483E-09	0.740215E-01	-0.507922E-08	0.350000E+00
4	3	0.462832E-01	0.454172E-01	0.393004E-09	0.593722E-01	-0.544764E-08	0.388730E+00

## STRESSES AT THE SHEAR GAUSS POINTS

EL	GP	XX-MOMENT	YY-MOMENT	XY-MOMENT	XZ-FORCE	YZ-FORCE	X-CORD GAUS P.
5	1	0.469292E-01	0.463202E-01	0.314104E-09	0.456623E-01	-0.560721E-08	0.411270E+00
5	2	0.474945E-01	0.473364E-01	0.177384E-09	0.240885E-01	-0.579543E-08	0.450000E+00
5	3	0.479053E-01	0.478943E-01	0.401654E-10	0.643182E-02	-0.588011E-08	0.488730E+00

## 15. INPUT AND OUTPUT DATA FOR EXAMPLE 2

Input data for Example 2 is now listed.

```

1
CIRCULAR PLATE SUPPORTED AT TWO ENDS.LINEAR ELEMENT WITH REDUCED INTEGRATION
11 2
13 12 0 1 2 2 1 1 1
1.04720
1 1 1 2
2 1 2 3
3 1 3 4
4 1 4 5
5 1 5 6
6 1 6 7
7 1 7 8
8 1 8 9
9 1 9 10
10 1 10 11
11 1 11 12
12 1 12 13
1 7.
2 7.5
3 8.
4 8.5
5 9.
6 9.5
7 10.
8 10.5
9 11.
10 11.5
11 12.
12 12.5
13 13.
142460.3 .3 .172
CIRCULAR PLATE UNDER EDGE POINT LOAD
1
13 1. .5236
1
.5236

```

Typical output data for Example 2 is now listed.

PROBLEM NO. 1 CIRCULAR PLATE SUPPORTED AT TWO ENDS-LINEAR ELEMENT

NUMBER OF HARMONIC TERMS TO BE USED = 11  
 INDICATOR FOR SYMMETRY OF LOADING ( 1 FOR NON SYMMETRY, 2 FOR SYMMETRY) = 2

ANGLE OF THE PLATE = 1.04720

NPOTN = 13 NLEMH = 12 NVPFX = 0 NCASE = 1 NTYPE = 2 NNOFN = 2  
 NMATS = 1 NPROP = 5 NGAUB = 1 NGAUS = 1 NDIHE = 1 NSTRE = 5 NEVAB = 6

ELEMENT	PROPERTY	NODE NUMBERS
1	1	1 2
2	1	2 3
3	1	3 4
4	1	4 5
5	1	5 6
6	1	6 7
7	1	7 8
8	1	8 9
9	1	9 10
10	1	10 11
11	1	11 12
12	1	12 13

NODAL POINT COORDINATES

NODE	X
1	7.00000
2	7.50000
3	8.00000
4	8.50000
5	9.00000
6	9.50000
7	10.00000
8	10.50000
9	11.00000
10	11.50000
11	12.00000
12	12.50000
13	13.00000

MATERIAL PROPERTIES  
 NUMBER

1 0.424689E+05 0.300000E+00 0.172000E+00 0.000000E+00 0.000000E+00

PROPERTIES

LOAD CASE NUMBER 1  
 CIRCULAR PLATE UNDER EDGE POINT LOAD

POINT LOAD

13 1.00000 0.00000 0.00000 0.52360

NUMBER OF SECTIONS TO BE ANALYSED= 1

TOTAL DISPLACEMENTS AND STRESSES AT Z= 0.524

LOAD CASE NO= 1

DISPLACEMENTS

NODE	DISP.	XZ-ROT.	YZ-ROT.
1	0.194096E+00	0.691507E-01	-0.370931E-08
2	0.228811E+00	0.737695E-01	-0.388639E-08
3	0.269167E+00	0.797079E-01	-0.441637E-08
4	0.309786E+00	0.867774E-01	-0.479069E-08
5	0.359095E+00	0.943980E-01	-0.517592E-08
6	0.404263E+00	0.102548E+00	-0.565801E-08
7	0.457688E+00	0.111042E+00	-0.602984E-08
8	0.515410E+00	0.119893E+00	-0.670909E-08
9	0.577619E+00	0.128821E+00	-0.709822E-08
10	0.644414E+00	0.138241E+00	-0.826672E-08
11	0.715932E+00	0.147683E+00	-0.885256E-08
12	0.792337E+00	0.157782E+00	-0.114704E-07
13	0.873764E+00	0.167534E+00	-0.130092E-07



## STRESSES AT THE SHEAR GAUSS POINTS

EL	GP	XX-MOMENT	YY-MOMENT	XY-MOMENT	XZ-FORCE	YZ-FORCE	X-CORD GAUS P.
1	1	-0.230874E-01	0.477447E+00	0.905515E-08	-0.682050E-01	0.286527E-07	0.725000E+01

## STRESSES AT THE SHEAR GAUSS POINTS

EL	GP	XX-MOMENT	YY-MOMENT	XY-MOMENT	XZ-FORCE	YZ-FORCE	X-CORD GAUS P.
2	1	-0.700295E-01	0.479293E+00	0.112182E-07	-0.531946E-01	-0.284223E-07	0.775000E+01

## STRESSES AT THE SHEAR GAUSS POINTS

EL	GP	XX-MOMENT	YY-MOMENT	XY-MOMENT	XZ-FORCE	YZ-FORCE	X-CORD GAUS P.
3	1	-0.105912E+00	0.488393E+00	0.105541E-07	-0.249140E-01	0.145402E-07	0.925000E+01

## STRESSES AT THE SHEAR GAUSS POINTS

EL	GP	XX-MOMENT	YY-MOMENT	XY-MOMENT	XZ-FORCE	YZ-FORCE	X-CORD GAUS P.
4	1	-0.126036E+00	0.496998E+00	0.109210E-07	-0.803868E-02	-0.227868E-07	0.875000E+01

## STRESSES AT THE SHEAR GAUSS POINTS

EL	GP	XX-MOMENT	YY-MOMENT	XY-MOMENT	XZ-FORCE	YZ-FORCE	X-CORD GAUS P.
5	1	-0.140992E+00	0.513161E+00	0.126238E-07	0.796940E-02	0.168662E-07	0.925000E+01

## STRESSES AT THE SHEAR GAUSS POINTS

EL	GP	XX-MOMENT	YY-MOMENT	XY-MOMENT	XZ-FORCE	YZ-FORCE	X-CORD GAUS P.
6	1	-0.148458E+00	0.531339E+00	0.115947E-07	0.336698E-01	-0.325593E-07	0.975000E+01

## STRESSES AT THE SHEAR GAUSS POINTS

EL	GP	XX-MOMENT	YY-MOMENT	XY-MOMENT	XZ-FORCE	YZ-FORCE	X-CORD GAUS P.
7	1	-0.150729E+00	0.559987E+00	0.167009E-07	0.370290E-01	0.346755E-07	0.102500E+02

## STRESSES AT THE SHEAR GAUSS POINTS

EL	GP	XX-MOMENT	YY-MOMENT	XY-MOMENT	XZ-FORCE	YZ-FORCE	X-CORD GAUS P.
8	1	-0.145828E+00	0.582086E+00	0.140238E-07	0.815597E-01	-0.661010E-07	0.107500E+02

## STRESSES AT THE SHEAR GAUSS POINTS

EL	GP	XX-MOMENT	YY-MOMENT	XY-MOMENT	XZ-FORCE	YZ-FORCE	X-CORD GAUS P.
9	1	-0.144149E+00	0.645892E+00	0.273290E-07	0.759511E-01	0.775997E-07	0.112500E+02

## STRESSES AT THE SHEAR GAUSS POINTS

EL	GP	XX-MOMENT	YY-MOMENT	XY-MOMENT	XZ-FORCE	YZ-FORCE	X-CORD GAUS P.
10	1	-0.128782E+00	0.704029E+00	0.237931E-07	0.169320E+00	-0.155864E-06	0.117500E+02

## STRESSES AT THE SHEAR GAUSS POINTS

EL	GP	XX-MOMENT	YY-MOMENT	XY-MOMENT	XZ-FORCE	YZ-FORCE	X-CORD GAUS P.
11	1	-0.120586E+00	0.811450E+00	0.607846E-07	0.169711E+00	0.155147E-06	0.122500E+02

## STRESSES AT THE SHEAR GAUSS POINTS

EL	GP	XX-MOMENT	YY-MOMENT	XY-MOMENT	XZ-FORCE	YZ-FORCE	X-CORD GAUS P.
12	1	-0.654474E-01	0.951187E+00	0.601473E-07	0.450070E+00	-0.445487E-06	0.127500E+02

## 16. DATA INPUT INSTRUCTIONS FOR PROGRAM PBSTRIP

<u>DATA SET 1</u>	PROBLEM DATA (I5). One record
Cols. 1-5 NPROB	Total number of problems to be solved in one run.
<u>DATA SET 2</u>	TITLE (12A6). One record
Cols. 1-72 TITLE	Title of the problem - limited to 72 alphanumeric characters.
<u>DATA SET 3</u>	NUMBER OF HARMONICS (2I5). One record
Cols. 1-5 NHARM	Total number of harmonics to be used for each problem.
Cols. 6-10 NSYME	Symmetry parameter = 0 non-symmetric loading = 1 symmetric loading (with respect to the axis $y = \frac{b}{2}$ ).
<u>DATA SET 4</u>	CONTROL DATA (9I5). One record
Cols. 1-5 NPOIN	Total number of nodal points.
" 6-10 NELEM	Total number of strips.
" 11-15 NVFIX	Total number of restrained points where one or more degrees of freedom are restrained along the longitudinal direction.
" 16-20 NCASE	Total number of load cases to be analysed.
" 21-25 NTYPE	Indicator for right or curved plate. = 1 right plate = 2 curved plate.
" 26-30 NNODE	Number of nodes per strip. = 2 linear strip = 3 quadratic strip = 4 cubic strip.
" 31-35 NMATS	Total number of different materials.

Cols. 36-40 NGAUB	Order of integration formulae for numerical integration of bending stiffness (see Table 1).
" 41-45 NGAUS	Order of integration formulae for numerical integration of shear stiffness (see Table 1).
<u>DATA SET 5</u>	PLATE LENGTH/ANGLE (F10.5). One record
Cols. 1-10 TLENG	Plate length (right plate) or angle (curved plate).
<u>DATA SET 6</u>	ELEMENT DATA (6I5). One record for each strip element. Total of NELEM cards.
Cols. 1-5 NUMEL	Strip element number.
" 6-10 MATNO(NUMEL)	Material property number.
" 11-15 LNODS(NUMEL,1)	1st nodal connection number.
" 16-20 LNODS(NUMEL,2)	2nd nodal connection number.
" 21-25 LNODS(NUMEL,3)	3rd nodal connection number (for quadratic or cubic strips only).
" 26-30 LNODS(NUMEL,4)	4th nodal connection number (for cubic strip only).
<u>DATA SET 7</u>	NODE CARDS (I5,2F10.5). One record for each nodal point. Total of NPOIN records.
Cols. 1-5 IPOIN	Nodal point number.
" 6-15 COORD(IPOIN,1)	The x coordinate of the node.
" 16-25 COORD(IPOIN,2)	The z coordinate of the node.
<u>DATA SET 8</u>	RESTRAINED NODE DATA (I5,2x,3I1,3F10.5). One record for each restrained node. Total of NVFIX records.
Cols. 1-5 NVFIX(IVFIX)	Restrained node number.
" 8 IFPRE(IVFIX,1)	Condition of longitudinal restraint on nodal displacement w.
" 9 IFPRE(IVFIX,2)	Condition of longitudinal restraint on nodal rotation $\theta_x$ .

Cols. 10 IFPRE(IVFIX,3) Condition of longitudinal restraint on nodal rotation  $\theta_y$ .

In Cols. 8-10:

IFPRE = 0 No displacement

= 1 Nodal displacement restrained.

" 11-20 PRESC(IVFIX,1) The prescribed value of nodal displacement  $w$ .

" 21-30 PRESC(IVFIX,2) The prescribed value of nodal rotation  $\theta_x$ .

" 31-40 PRESC(IVFIX,3) The prescribed value of nodal rotation  $\theta_y$ .

Note: The program is able to deal with only zero prescribed values. Other prescribed values, different from zero, should be input separately for each harmonic term accordingly to the contribution of the prescribed movement to each harmonic, which should be properly evaluated beforehand.

#### DATA SET 9

MATERIAL DATA (I5,4F10.5). One record for each different material. Total of NMATS records.

Cols. 1-5 NUMAT Material identification number.

" 6-15 PROPS(NUMAT,1) Young's modulus,  $E$ .

" 16-25 PROPS(NUMAT,2) Poisson's ratio,  $\nu$ .

" 26-35 PROPS(NUMAT,3) Element thickness.

" 36-45 PROPS(NUMAT,4) Distributed load intensity.

#### DATA SET 10

LOAD CASE TITLE DATA (12A6). One record.

Cols. 1-72 TITLE Title of the load case - limited to 72 alphanumeric characters.

#### DATA SET 11

LOAD CONTROL DATA (2I5). One record.

Cols. 1-5 IPLD Applied vertical point load control parameter  
= 0 no applied vertical nodal loads to be input.

= 1 applied vertical nodal loads to be input.

" 6-10 IUNIF Uniformly distributed load control parameter.

= 0 No distributed load case to be considered.

= 1 Distributed load case to be considered.

#### DATA SET 12

APPLIED VERTICAL POINT LOAD DATA (I5,2F10.5). One record for each loaded nodal point.

Cols. 1-5 LODPT Node number.

" 6-15 POINT(i) Value of the vertical point load acting at the node.

" 16-25 YLOAD The y coordinate of the point at which the load acts.

Notes: 1) The last record should be that for the highest numbered node whether it is loaded or not.

2) If IPLD = 0 in Data Set 9, omit this set.

DATA SETS 10 TO 12 TO BE REPEATED FOR EACH LOAD CASE IN ACCORDANCE WITH NCASE IN DATA SET 4.

DATA SETS 2 TO 12 TO BE REPEATED FOR EACH PROBLEM IN ACCORDANCE WITH NPROB IN DATA SET 1.

#### DATA SET 13

NUMBER OF OUTPUT SECTIONS DATA (I5). One record.

Cols. 1-5 NSECT Number of output section ( $\leq 5$ ).

#### DATA SET 14

SECTION COORDINATES DATA (8F10.5). One record.

Cols. 1-10 YSECT(1) The y (right plate) or  $\theta$  (curved plate) coordinate of the first output section.

" 11-20 YSECT(2) ditto for the second section

⋮

" 41-50 YSECT(5) ditto for the fifth section.

## 17. DICTIONARY OF MAIN VARIABLE NAMES

- ASDIS (NTOTV) - Vector of nodal displacement amplitudes for each harmonic.
- BMATX (NSTRE,NEVAB) - Matrix  $\underline{B}^{\ell}$  for each element.
- CARTD (1,INODE) - Cartesian shape function derivative  $\frac{\partial N_i}{\partial x} (e)$ .
- COORD (NPOIN,1) - Coordinates of nodal points.
- DBMAT (NSTRE,NEVAR) - Matrix  $\underline{D} \underline{B}^{\ell}$  for each element.
- DERIV (1 NODE) - Shape function derivative  $\frac{\partial N_i}{\partial \xi} (e)$ .
- DMATX (NSTRE,NSTRE) - Matrix  $\underline{D}$  for each element.
- ELOAD (NELEM,NEVAB) - Nodal forces for each element.
- ESTIF (NEVAB,NEVAB) - The element stiffness matrix  $[\underline{K}^e]^{\ell}$ .
- GPCOD (1,NGAUS) - Coordinate x of the shear integration points.
- IFPRE (2,NDOFN) - Integer code to specify prescribed degrees of freedom.
- LNODS (10,NNODE) - Element node number listed for each element.
- MATNO (NELEM) - Material set number for each element.
- NDIME - Number of coordinate components required to define each node (=1).
- NDOFN - Number of degrees of freedom per node.
- NELEM - Number of strip elements.
- NEVAB - Number of variables per element = NNODE \* NDOFN.
- NGAUB - Number of Gaussian integration points for the flexure terms.
- NGAUS - Number of Gaussian integration points for the shear terms.
- NHARM - Number of harmonic terms to be used in the analysis.

- NNODE - Number of nodes per strip element.
- NOFIX (2) - List of prescribed node numbers (maximum of two nodes to be prescribed).
- NPOIN - Total number of nodal points.
- NPROP - Number of material parameters required to define the characteristics of a material completely.
- NSTRE - Number of stress components per element.
- NSYME - Code for symmetric loading.
- NTYPE - Code for right (= 1), or curved (= 2) plate.
- POINT - Value of the vertical point load.
- POSGP (4) - Coordinates of integration points.
- PRESC (2,NDOFN) - Values of the prescribed degrees of freedom.
- PROPS (1,5) - Values of the material parameters.
- TLENG - Plate length (right) or angle (curved).
- YLOAD - y coordinate of the transverse section where the point load acts.
- WEIGP (4) - Weights of the integrating points.

## 18. REFERENCES

- GRAFTON, P.E. and STROME, D.R. - Analysis of axisymmetric shells by the direct stiffness method. J.A.I.A.A., 2342-7, 1963.
- AHMAD, S., IRONS, B.M. and ZIENKIEWICZ, O.C. - Curved thick shell and membrane elements with particular reference to axisymmetric shell problems. Proc. 2nd Conf. on Matrix Methods in Structural Mechanics. Wright-Patterson A.F. Base, Ohio, AFFDL-TR-68-150, 1968.
- WILSON, E.L. - Structural analysis of axisymmetric solids. J.A.I.A.A., 3, 2269-74, 1965.
- CHEUNG, Y.K. - Finite strip method analysis of elastic slabs. Proc. A.S.C.E., 94, 1365-1378, 1968.

5. CHEUNG, Y.K. - The finite strip method in the analysis of elastic plates with two opposite simply supported ends. Proc. I.C.E., 40, 1-7, 1968.
6. CHEUNG, Y.K. - Analysis of box girder bridges by finite strip method. A.C.I. Publications, SP 26, 357-378, 1969.
7. CHEUNG, Y.K. - Folded plate structures by finite strip method. Proc. A.S.C.E., 96, 2963-2979, 1969.
8. CHEUNG, Y.K. - The analysis of cylindrical orthotropic curved bridge decks. Pub. Int. Ass. Struct. Engrs. 29, 41-52, 1969.
9. WILLAM, K.J. and SCORDELIS, A.C. - Analysis of orthotropic folded plates with eccentric stiffeners. Report No. SESM 70-2. Dept. of Civil Engng., Univ. of California, Berkeley, 1970.
10. LOO, Y.C. and CUSENS, A.R. - A refined finite strip method for the analysis of orthotropic plates. Proc. I.C.E., 48, 85-91, 1970.
11. CUSENS, A.R. and LOO, Y.C. - Application of the finite strip method in the analysis of concrete box girders. Proc. I.C.E., 57-II, 251-273, 1974.
12. CHEUNG, Y.K. - The Finite Strip Method in Structural Analysis, p. 232, Pergamon Press, 1976.
13. BENSON, P.R. and HINTON, E. - A thick finite strip solution for static free vibration and stability problems. Int. J. Num. Meth. Engng., 10, 665-678, 1976.
14. OÑATE, E. - Comparisons of finite strip method for the analysis of box girder bridges. M.Sc. Thesis Dept. of Civil Engng., Univ. College of Swansea, 1976.
15. LOO, Y.C. and CUSENS, A.R. - The Finite Strip Method in Bridge Engineering, Viewpoint Public, 1978.
16. CHEUNG, M.S. and CHEUNG, Y.K. - Analysis of curved bridges by the finite strip method. Research Report Dept. of Civil Engng., Univ. of Calgary, Canada, 1970.
17. OÑATE, E. and SUAREZ, B. - A unified approach for the analysis of bridges, plates and axisymmetric shells using the linear Mindlin strip elements. Computers and Structures, 17, 407-426, 1983.

18. OÑATE, E. and SUAREZ, B. - A comparison of the linear quadratic and cubic Mindlin strip elements for the analysis of thick and thin plates. Computers and Structures, 17, 427-439, 1983.
19. TIMOSHENKO, S. - Strength of Materials, Van Nostrand, New York, 1955.
20. ZIENKIEWICZ, O.C. - The Finite Element Method, McGraw-Hill, New York, 1979.
21. TIMOSHENKO, S. and WOJNOWSKY-KRIEGER, S. - Theory of Plates and Shells, 2nd Edition McGraw-Hill, New York, 1959.
22. ALWAR, R.S. and RAMACHANDRAN, K.N. - Theoretical and photoelastic analysis of thick slabs subject to highly localised loads. Buid. Sci., 7, 159-166, Pergamon Press, 1972.
23. CLOUGH, R.W. and WILSON, E.L. - Dynamic finite element analysis of arbitrary thin shells. Computers and Structures, 1, 35, 1971.
24. ZIENKIEWICZ, O.C., BAUER, O.C., MORGAN, K. and ONATE, E. - A simple and efficient element for axisymmetric shells, Int. J. Num. Meth. Engng., 11, 1545-1558, 1977.
25. SUAREZ, B. - La formulación de Bandas finitas de Reissner Mindlin para análisis de placas, puentes y láminas de revolución, Ph.D. Thesis E.T.S. Ing. Caminos, Barcelona, 1982.
26. COULL, A. and DAS, Y.P.C. - Analysis of curved bridge decks. Proc. I.C.E., 37, 75-85, 1967.
27. THORPE, J. - Ph.D. Thesis, University of Dundee, 1976.
28. SAWKO, F. and MERRIMAN, Y.P.A. - An annular segment finite element for plate bending. Int. J. Num. Meth. Engng., 3, 119-129, 1971.
29. FAM, A. and TURKSTRA, Y.C. - A finite element method for box bridge analysis. Computers and Structures, 5, 179-186, 1975.
30. FLUGGE, W. - Stresses in Shells, p.525, Springer-Verlag, Berlin, 1973.
31. OÑATE, E., HINTON, E. and GLOVER, Y.N. - Techniques for improving the performance of Ahmad shell elements. Int. Conf. Appl. Num. Modelling, Edited by Pentech Press, Madrid, 1979.

32. LINDBERG, G.M., OLSEN, M.D. and COWPER, Y.G.R. - New Developments in the Finite Element Analysis of Shells. Struc. Material Laboratory, 1-38, 1969.
33. AHMAD, S., IRONS, B.M. and ZIENKIEWICZ, O.C. - Curved thick shell and membrane elements with particular reference to axisymmetric problems. Proc. 2nd Conference Matrix Methods in Struct. Mech., Wright-Patterson A.F. Base, Ohio, 1968.
34. HINTON, E. and OWEN, D.R.J. - Finite Element Programming. Academic Press, London, 1979.
35. IRONS, B.M. - A frontal solution program for finite element analysis. Int. J. Num. Meth. Engng., 2, 5-32, 1970.

## CHAPTER 3

### MINDLIN PLATE FINITE ELEMENTS

E. HINTON<sup>\*</sup> and H.H. ABDEL RAHMAN<sup>\*\*</sup>

\* University College of Swansea, U.K.

\*\* University of Petroleum and Minerals, Dhahran, Saudi Arabia

#### 1. INTRODUCTION

The main objectives of this chapter are as follows:

- a) to briefly review various plate elements based on Mindlin plate theory,
- b) to describe a hierarchical version of the heterosis plate element,
- c) to present a documented program called MINDLIN in which the heterosis element is implemented, and
- d) to provide a set of user instructions for MINDLIN and also examples demonstrating the use of the program and the performance of the heterosis plate element.

The main equations of Mindlin plate theory have already been presented in the chapter dealing with closed form solutions. However, for completeness, a brief resume is now provided.

#### 2. REVIEW OF MINDLIN PLATE THEORY

##### 2.1 Mindlin plate formulation - displacement approach

Mindlin plate theory [1] allows for transverse shear deformation effects and thus offers an attractive alternative to classical Kirchhoff thin plate theory. The main assumptions are that